

**ENABLING THE DEVELOPMENT OF FURAN-BASED  
BIOREFINERIES**

by

**Anurag S. Mandalika**

A thesis submitted in partial fulfillment of the requirements for the degree of

**Master of Science**

**(Biological Systems Engineering)**

at the

**UNIVERSITY OF WISCONSIN-MADISON**

**2012**

Approved by:

---

Professor Troy Runge

Biological Systems Engineering Department

University of Wisconsin–Madison

Date: \_\_\_\_\_

## **Acknowledgements**

I wish to express utmost gratitude to my advisor, Prof Troy Runge, without whose guidance and inspiration, I could not have accomplished this work and I will forever remain indebted to him for his generosity and helpfulness. The leeway I received under his tutelage helped me think like a researcher without being biased or afraid of trying out new things. His pleasing company and jovial nature put me at ease many times, and helped to make research an enjoyable experience. I also wish to extend my gratitude to the members of my committee, Prof Xuejun Pan and Prof Roger Rowell, who have kindly agreed to review my work.

I am also heavily indebted to former members of the SHARC lab, Pamella Wipperfurth and Prof Chunhui Zhang, who helped me learn the ropes in the lab, and for displaying enormous amounts of patience in answering my questions and guiding my early work. In this light, I also wish to extend my gratefulness to BSE graduate student Yi-Kai Su who kindly trained me on microbial methods, and whose help was instrumental in performing the research for Chapter 6. I also wish to thank my colleagues Jeff Muller, Dr Alberto Negri, Shengfei Zhou and Sarah Krantz, whose company was helpful in making the lab a lively place, and was also very inspirational for me while writing. Special thanks go to Dr JunYong Zhu and Doreen Mann of the Forest Products Laboratory for letting me use the rotating digester and getting me trained on the same. I would also like to thank Dr Hem Chandra Joshi for constant mentoring through my undergraduate years, and also for

kindly reviewing my thesis and suggesting changes to improve upon it during the draft stage.

I also wish to thank the entire BSE department, especially Debby Sumwalt, Patrick Litza, Sue Reinen and Hal Bohne, for being extremely helpful, inviting and accepting. I also thank my colleagues and friends in the department who have ensured that company was always friendly and educational at the same time.

Finally, I would like to thank my parents and my little sister, who are the most important part of my life, and whose support was indispensable towards the completion of this work.

## Abstract

Dilute aqueous solutions of furfural were produced in high yield from biomass hydrolysates using an acid-catalyzed batch reactive distillation (BRD) process that separated the vapor phase from the aqueous reactant medium. Hot water hydrolysates from hybrid poplar, miscanthus, switchgrass and corn stover were dehydrated using sulfuric acid in the BRD configuration to produce furfural in excess of 85% of the theoretical (molar) yield based on the total pentose content. Using xylose as the model compound, and temperature and acid concentration as the variables, the process conditions were optimized by the construction of a three-level statistical model. Hot water hydrolysis of biomass provided with a cellulose- rich solid fraction which has potential for conversion into pulp or cellulosic ethanol, while the liquid fraction, rich in hemicellulose sugars, was converted into furfural. Furfural was converted into furfuryl alcohol with yield in excess of 50% using *S cerevisiae* (Baker's yeast), and the organism was also capable of converting the furfural that was produced in the BRD reaction. Fractionating the biomass allows for exploration of the concept of the integrated biorefinery where the hemicellulose sugars are not underutilized or encountered as potential inhibitors during microbial conversions of the solid stream, but are converted into furfural, a valuable chemical precursor. Further conversion into furfuryl alcohol using the microbial method offers an environmentally-friendlier alternative to the conventional copper chromite-catalyzed hydrogenation reaction that is used in industry. In this manner, the basis for a biorefinery based on the production of furan-based compounds has been explored.

## Contents

Acknowledgements .....	i
Abstract .....	iii
List of Tables.....	viii
List of Figures .....	ix
List of Equations .....	xii
Chapter 1-Introduction and Objectives .....	1
Chapter 2- Review of Literature .....	4
2.1. The need for bio-based societies .....	4
2.1.1. Background.....	4
2.1.2. Why fossil resources cannot remain the backbone of modern, industrialized societies .....	5
2.2. Fulfilling the necessity for bio-based societies- Means and avenues.....	10
2.2.1. Platform Chemicals and the Integrated Biorefinery .....	10
2.2.2. The case for a furan-based biorefinery .....	13
2.3. Furfural as a platform chemical .....	14
2.3.1. Uses of furfural .....	15
2.3.2. Furfural Derivatives .....	17
2.4. Production of furfural .....	27
2.5. Pentose dehydration mechanism for furfural formation.....	29
2.6. Reaction losses during the production of furfural .....	34
2.7. Research towards improving furfural yields .....	35
2.8. Composition of lignocellulosic biomass.....	38
2.8.1. Cellulose .....	39
2.8.2. Hemicellulose .....	43
2.8.3. Lignin .....	44
2.8.4. Extractives .....	47
2.9. Pretreatment of biomass: Hot-water hydrolysis for hemicellulose extraction .....	48
Chapter 3- Materials, Chemicals, Experimental and Analytical Techniques .....	52
3.1. Introduction.....	52

3.2. Materials and Chemicals.....	52
3.2.1. Biomass feedstock: Harvest and treatment.....	52
3.2.2. Chemicals and Reagents .....	54
3.3. Experimental Techniques .....	54
3.3.1. Dehydration of aqueous xylose solutions using the batch process .....	54
3.3.2. Determination of biomass moisture content.....	57
3.3.3. Hot-water extraction/ hydrolysis of biomass.....	58
3.3.4. Determination of higher heating value (HHV) of biomass and extracted solids using oxygen bomb calorimetry .....	61
3.4. Analytical Techniques .....	64
3.4.1. Measurement of furfural .....	65
3.4.2. Measurement of sugars.....	68
3.4.3. Measurement of cell growth and estimation of furfural and furfuryl alcohol concentrations.....	69
Chapter 4- Model Compound Dehydration .....	73
4.1. Introduction.....	73
4.2. Materials and Methods .....	77
4.2.1. Chemicals and Reagents .....	77
4.2.2. Apparatus .....	78
4.2.3. Methodology .....	79
4.2.4. Analysis.....	80
4.3. Results and Discussion.....	80
4.3.1. Xylose dehydration in the batch configuration.....	80
4.3.2. Xylose dehydration using the BRD configuration.....	86
4.3.3. BRD dehydration using acid-injection.....	92
4.4. Conclusions.....	94
Chapter 5- Biomass Fractionation and BRD Dehydration of Biomass and Water-Extracted Hydrolysates.....	97
5.1. Introduction.....	97
5.2. Materials and Methods .....	98
5.2.1. Materials and Reagents .....	98

5.2.2. Apparatus .....	99
5.2.3. Methodology .....	99
5.2.4. Analysis.....	101
5.3. Results and Discussion.....	102
5.3.1. Hot-water extraction of biomass feedstock.....	102
5.3.2. BRD dehydration of untreated poplar .....	108
5.3.3. BRD dehydration of biomass hydrolysates .....	109
5.3.4. Heating value of water-extracted solids .....	113
5.4. Conclusions.....	117
Chapter 6- Microbial Conversion of Furfural into Furfuryl Alcohol.....	120
6.1. Introduction.....	120
6.2. Mechanism .....	121
6.3. Materials and Methods .....	124
6.3.1. Chemicals.....	124
6.3.2. Apparatus .....	125
6.3.3. Analysis.....	125
6.4. Results and Discussion.....	126
6.4.1. Preliminary experiments with pure furfural to find maximum furfural dosage .....	126
6.4.2. Transformation of hybrid poplar BRD product in the presence of active dry yeast..	133
6.5. Conclusions and next steps.....	138
Chapter 7-Conclusions and Future Work.....	141
7.1. Conclusions.....	141
7.2. Future research .....	144
References.....	146
Appendix A-Dehydration of xylose using different reactor schemes.....	156
A1. Batch dehydration results using xylose as the model compound.....	156
A2. BRD dehydration results using xylose as the model compound .....	156
A2.1. Initial Experiments.....	156
A2.2. BRD Statistical Model .....	157
A2.3. BRD Acid Injection .....	157

Appendix B-Characterization of hot-water hydrolysates.....	158
B1. Hydrolysate sugar and furfural concentrations .....	158
B2. Total Pentose and Total Hexose .....	158
Appendix C-Optical Density of Bakers' yeast during fermentation.....	159
C1. Optical density of control samples- fermentation in YPD lacking furfural .....	159
C2. Optical density of yeast- fermentation of BRD product.....	160

## List of Tables

2.1: Representative values of the functional groups present in hardwood and softwood lignins.....	47
3.1: Composition of the biomass feedstock used in this study as estimated by Wipperfurth.....	53
3.2: Moisture contents of the four untreated biomass feedstock used in this study with standard error (for triplicate measurements).....	58
5.1: Table showing the theoretical furfural yield (average for triplicate runs, based on three different hydrolysate characterization results) and the selectivity towards the dehydration reaction for all four biomass feedstock.....	113
5.2: Comparison of the higher heating values of all four biomass feedstock.....	113

## List of Figures

2.1: The catalytic decarbonylation reaction of furfural for the production of furan.....	17
2.2: The catalytic hydrogenation of furan for the production of THF.....	19
2.3: Copper chromite catalyzed conversion of furfural into furfuryl alcohol.....	21
2.4: Possible furan-based chemicals with furfural as a precursor.....	28
2.5: Scheme 1 proposed to explain the mechanism of xylose dehydration into furfural via the formation of open-chain intermediates.....	30
2.6: Schemes 2 and 3 hypothesizing intramolecular rearrangements within the pyran molecule for the formation of furfural via cyclic intermediates.....	31
2.7: Proposed mechanism for formation of furfural from D-xylose.....	33
2.8: The structure of lignocellulose showing the breakdown into its components of cellulose (glucose subunits), hemicellulose (pentoses and hexoses) and lignin (monolignol subunits).....	40
2.9: The structure of cellulose.....	41
2.10: Structures of the three monolignols that constitute lignin.....	46
3.1: A simplified (not-to-scale) schematic of the setup, control and sampling operation of the batch reactor for the dehydration of xylose solutions to produce furfural.....	55
3.2: Simplified schematic of the batch reactor.....	56
3.3: Simplified schematic of the rotating digester.....	60
3.4: Picture of the rotating digester in operation.....	60
3.5: Setup used for conducting the furfural reduction experiments using active dry yeast, showing the apparatus used for sampling with time.....	63
3.6: Standard curve generated for furfural using UV absorbance spectroscopy.....	66
3.7: Comparison of the ultraviolet absorption spectra of pure furfural and the BRD reaction product showing the furfural absorption maximum at 276 nm.....	67
3.8: Chromatogram showing the composition of the standards.....	68
3.9: Chromatogram showing the composition of the sugar standard.....	69

3.10: Calibration curve generated for a mixture of furfural and furfuryl alcohol at different concentrations using ultraviolet absorption spectroscopy.....	70
3.11: Absorption spectra generated for furfural, furfuryl alcohol, and a mixture of both chemicals.....	71
3.12: Plot of the ratio of absorbance values for furfural at 276 and 215 nm.....	72
4.1: Vapor-liquid equilibrium (VLE) data of furfural and water.....	74
4.2: Schematic of an ideal BRD device.....	76
4.3: Simplified schematic of the batch reactive distillation.....	78
4.4: Plot showing the dependence of furfural yield on the CSF, both in the presence and absence of salt.....	81
4.5: Plot showing the effect of CSF on furfural yield with time for four of the 20 minute runs, indicative of the subsequent transformation of furfural into loss products.....	83
4.6: Plot showing the concentration of xylose as it is being converted with time, for four different values of the CSF (both in the presence and absence of salt), beginning with the first sample (at 6 min for 60 min reactions).....	85
4.7: Plot showing a typical time-based furfural formation curve for one of the preliminary experiments.....	87
4.8: Plot showing the effect of CSF on furfural yield for the range of experiments conducted using BRD.....	88
4.9: Plot showing the time-based accumulation of furfural extracted from the vapor phase for a typical xylose BRD reaction.....	90
4.10: Plot showing the predicted versus observed theoretical furfural yields from MODDE fit for the xylose BRD experiments.....	91
4.11: Coefficient plot obtained for the statistical model constructed in MODDE.....	92
5.1: Schematic showing the strategy employed for the fractionation of the biomass and subsequent dehydration to produce furfural using the BRD process.....	100
5.2: Hybrid poplar sugar extracted from autohydrolysis with standard error.....	103
5.3: Miscanthus sugar extracted from autohydrolysis with standard error.....	103

5.4: Switchgrass sugar extracted from autohydrolysis with standard error.....	104
5.5: Corn stover sugar extracted from autohydrolysis with standard error.....	104
5.6: Total pentose and total hexose content obtained from the hot-water hydrolysis.....	108
5.7: Average furfural theoretical yields obtained from all four biomass hydrolysates with standard error.....	112
5.8: Plot showing the higher heating value (HHV, Btu/lb) of untreated, oven-dried and water-extracted, oven-dried biomass solids obtained using oxygen bomb calorimetry, performed in triplicates with standard error.....	115
5.9: Summary of the furfural yields obtained using various methods of acid-catalyzed dehydration.....	118
6.1: Proposed pathway for the transformation of furfural into furfuryl alcohol in conjunction with the fermentation of glucose.....	124
6.2: Plot showing the change in optical density of yeast with time for the control (no furfural added) and flasks with 10 and 30 g/l furfural added.....	128
6.3: Disappearance of furfural (solid lines) and appearance of furfuryl alcohol (dashed lines) shown with time.....	129
6.4: Plot showing the conversion of furfural and detection of furfuryl alcohol at much higher furfural dosages of 30 g/l and 40 g/l.....	130
6.5: Furfuryl alcohol yield obtained at different doses of furfural.....	132
6.6: Plot showing the optical density measured with time for the control with no furfural, one flask dosed with pure furfural, and flask containing the BRD product.....	134
Fig. 6.7: Plot showing the conversion of furfural for the samples at 0.083 hr and at 10 hr when the reaction was finished.....	136
6.8: Chromatograph showing the elution of peaks for the unknown compounds A and B, and for furoic acid for the 10 hour sample of a BRD product flask.....	138
7.1: Schematic of proposed biorefinery concept.....	142

## List of Equations

3.1. Calculation of biomass moisture content.....	58
3.2. Calculation of yeast Optical Density (OD).....	73
4.1. Calculation of Combined Severity Factor (CSF).....	80
4.2. Theoretical yield of furfural from xylose.....	83
5.1. Concentration of total pentose in biomass hydrolysates.....	106
5.2. Concentration of total hexose in biomass hydrolysates.....	106
6.1. Theoretical yield of furfuryl alcohol from furfural for microbial conversion.....	131

## Chapter 1-Introduction and Objectives

The concept of the integrated biorefinery has lately been upheld as key to chart the path towards independence from a fossil fuel-based economy, and for the implementation of a renewable, bio-based economy. A biorefinery has been defined as a ‘facility that integrates biomass conversion processes and equipment to produce fuels, power and chemicals from biomass’<sup>1</sup>, not unlike the concept of a petroleum refinery. While the petroleum refinery processes a single source (crude oil) to produce a range of fuels and chemicals, modern biorefineries are tasked with the need to process a myriad range of feedstock to produce a wide variety of possible biofuels and biochemicals.

To choose between the many potential bio-based products that an integrated biorefinery can be designed to produce, the concept of platform chemicals has been developed. These offer the flexibility of producing a range of chemicals based on the conversion strategy employed. These platform chemicals, or building blocks, have loosely been defined as ‘molecules with multiple functional groups that possess the potential to be transformed into new families of useful chemicals’<sup>2</sup>. This original DOE report that expounded on this idea was later revisited<sup>3</sup> with improved criteria to also include furan-derived chemicals such as furfural and hydroxymethylfurfural, identified as ‘new top chemical opportunities from biorefinery carbohydrates’.

Furfural, a furan-based product of the dehydration of pentoses, has received increased attention due to the position it inhabits as a precursor for the production of many industrially important compounds such as furan, furfuryl alcohol, tetrahydrofuran, 2-

methylfuran, furoic acid, etc<sup>4</sup>. The unique properties of furfural such as corrosion resistance, thermosetting abilities and solvent properties has enabled its use in the production of resins and industrial solvents<sup>4-6</sup> amidst less common applications as a nematicide and a fungicide<sup>7</sup>.

While global production of furfural, at 280,000 tons per year, is sizeable and the technology of production is mature, development of furfural-based biorefineries is hampered by factors such as low yield from the conversion and the absence of a strong economic incentive. Conventional furfural production typically results in yields of ~50% (based on pentose), and because the biomass is reacted as whole, other components of the plant matter degrade into a resinous sludge, without adding value to the process<sup>6, 8, 9</sup>.

Hexose sugars, representing a high-value carbohydrate source, are degraded during this process without being salvaged because the raw biomass (corn cobs, bagasse) is cheap and abundant. Also, recent research into improving furfural yields has typically focused on the use of expensive heterogeneous solid acid catalysts and solvent-recovery operations, which might prove to be cost and scale-prohibitive for implementation<sup>8, 10-12</sup>.

Primarily, the development of a biorefinery model should seek to (1) improve the yield of furfural from pentose sugars and (2) recover the hexose sugars that do not contribute towards the formation of furfural in a form that renders them suitable for further conversion.

Since the primary role of furfural has been that of a chemical precursor, the production of a higher value compound derived from furfural such as furfuryl alcohol will add further value to such a biorefinery. Industrial production of furfuryl alcohol is based on the

hydrogenation of furfural in the presence of copper chromite catalyst in high yields. The use of hydrogen and expensive heterogeneous catalysts may not be ideal for the development of an integrated biorefinery, and other ways of accomplishing the same reaction are desired. Research<sup>13-16</sup> from a biodetoxification standpoint has shown the conversion of furfural into furfuryl alcohol during fermentation. Both these compounds are inhibitory towards the growth and activity of microorganisms and the conversion occurs as a consequence of microbial metabolism of furfural to produce a slightly less inhibitory compound (furfuryl alcohol).

The overall objectives of this research study are outlined as:

1. Development of processes in order to produce furfural in higher yields without the requirement for expensive catalysts or solvent recovery operations.
2. Development of a process where the hexose sugars are separated from the pentoses and sourced in a form suitable for further conversion, thereby adding value and furthering the biorefinery concept.
3. Exploration of a microbial method for the conversion of furfural into furfuryl alcohol, with the goal of making the process more environmentally-friendly than the industrial hydrogenation process

## **Chapter 2- Review of Literature**

### **2.1. The need for bio-based societies**

#### **2.1.1. Background**

A steady rise in crude oil prices leading to a spurt in 2008<sup>17</sup> has intensified a recession that has choked world economies in its crushing grip. As of July 2012, major economies of the European Union were faced with the looming axe of austerity and the developing economies such as China<sup>18</sup> and India<sup>19</sup> began reporting growth figures that failed to meet expectations. The United States, having dealt with a downgrade of its credit rating, was precariously poised on the verge of slipping back into an extended recession after having made modest gains at improving growth and reducing unemployment.

Developing countries, armed with the task of driving the world economy out of the recession doldrums, are faced with the excruciating need for rapid industrialization and development. This has led to an increased demand for fossil fuel resources in these countries, whose burgeoning populations also aspire to better standards of living that emulate those currently enjoyed by populations in the Western hemisphere. The 2011 International Energy Outlook<sup>17</sup>, published by the United States Energy Information Administration (EIA), forecasts a global increase in energy consumption of 1.6% per year for the period 2008-2035. This increase, however, is not seen to be uniform across the globe: the more developed Organization for Economic Co-operation and Development (OECD) countries are expected to see increases in their energy consumption by 0.6%, while the developing, non-OECD nations are expected to consume 2.3% per year more energy (2.9% in Asia). In 2008, OECD nations consumed 244.5 quadrillion Btu of

energy, while the non-OECD nations registered a slightly higher consumption of 260.5 quadrillion Btu. By the end of 2035, non-OECD nations are expected to consume ~1.8 times the energy consumed by OECD nations at 481.6 quadrillion Btu<sup>17</sup>. These forecasts are for the Reference case, which assumes that existing laws and regulations concerning the energy sector remain unchanged.

All of the projected increases in energy demand and the exigent need to restore economic stability across the world have placed a significant burden on the world's fossil-fuel based societies. In order to jumpstart a sorely needed global economic recovery and sustain it over the long term, a steady, cheap supply of resources are needed to fuel the world's industries so that productivity can be increased and the world's populace may begin to embrace the standards of living they aspire to.

### **2.1.2. Why fossil resources cannot remain the backbone of modern, industrialized societies**

Beginning with the extensive use of coal to power the Industrial Revolution and large-scale use of oil since the end of the First World War, fossil fuels have revolutionized mankind from a predominantly rural pastoral society to an ever-expanding urban society propelled by factories and mechanized industry. Resources of fossil origin have fueled this tremendous transformation allowing for advances ranging from superfast computing to the first human steps on lunar surface. In 2008, fossil-based fuels accounted for ~67% of global primary energy consumption (excluding electricity)<sup>20</sup> and ~84.5% of US energy consumption<sup>17</sup>, indicating the extent to which our dependence on non-renewable fossil energy exists.

Unfortunately, fossil fuels present a bleak prospect for long-term global economic growth and sustenance, while assuring high standards of living all across the globe. Energy expenditures are inextricably tied into the intricate workings of the economy, and have shown to be accurate indicators of economic health. Historically, whenever the United States' expenditure on energy has been on the rise and has exceeded 10% of its GDP (gross domestic product), the country has either found itself in recession or the economic growth was retarded<sup>21</sup>. Hamilton<sup>22</sup> has found a statistically-significant correlation between dramatic increases in crude oil prices in the years since the Second World War, and an American recession three-quarters of a year later. Though sudden oil prices are not implicated as a causal agent of a recession in this study, it concluded that the correlations suggested a strong influence between both events.

Another aspect contriving to further augment the uncertainty associated with fossil fuel resources is the geopolitical one: as witnessed yet again during the smoldering months of the Arab Spring revolution that began in 2011, major oil-producing regions are politically very volatile, and cannot be relied upon to provide the stable supply that is needed to grow and sustain a recuperating world economy. As of July 2012, civilians in large numbers were being massacred by pro-government forces in Syria where the Arab Spring was in full bloom and threatening to spill over into neighboring countries. While this effort might stand as a testament of peoples' yearning for democracy, political volatility is not seen as boding well for a stable supply of oil. The pursuit of an opaque and aggressive nuclear policy by Iran have led to tensions between Iran and Israel (and the United States), leading to the imposition of tough sanctions on the former. This has

squelched oil supply to developing economies such as China and India (historically dependent on Iranian oil) and has slowed the pace of economic growth in these economies.

The 1973 Yom Kippur (Arab-Israeli) war that saw the OPEC (Oil and Petroleum Exporting Countries) place an embargo on crude oil exports to countries constituting the NATO (North Atlantic Treaty Organization), is a classic case in point<sup>23</sup>. This action was one of the main factors that dragged the world into the depression of 1973<sup>24</sup> when oil prices in the West skyrocketed and global economies slumped. The depression of the 1970s is a chilling reminder of the fragile nature of the crude oil supply chain, and the rather intricate political factors that influence it. The uninterrupted supply of fossil fuel resources from clustered hotspots of the world is not a given and has all the bearings of turning into a costly risk if it were assumed to be thus.

The countries of Nigeria and Libya have witnessed severe exploitation of land, resources and people by their governments and oil corporations in an effort to keep up with the demand for oil. Poor governance has led to endemic corruption in these places.

Government officials in these regions make decisions aiming to maximize profits while ensuring the systematic destruction of near-fragile habitats, endangering local industry, and often, the livelihood of people dependent on it. Such cases have paved the way for socio-economic debates which have called into question the true costs of producing oil with the environment and the quality of human life (often life itself) at stake<sup>25</sup>.

Perhaps the greatest opposition yet towards the continued dependence on fossil fuel resources is the environmental one, and the catastrophic effects of anthropogenic global warming. Indiscriminate use of traditional petroleum-based fossil fuels for transportation such as gasoline and diesel fuel has severely impacted our environment and has led to an increase in global warming due to the release of carbon dioxide and other greenhouse gases<sup>26</sup>. Dickinson and Cicerone<sup>27</sup> in 1986 predicted that future additions of trace gases (methane, ozone, nitrous oxides, CFCs, etc) over the next 39 years (corrected for the current year) have the potential to double, or even quadruple warming effects and corresponding temperature rise. Climatic change arising as a direct consequence of human activities has impacted the ecosystems of flora and fauna<sup>28</sup>, and has driven many of these species to extinction. Based on a species distribution model constructed to account for ~20% of the earth's terrestrial area, Thomas et al<sup>29</sup> have predicted that 15-37% of species inhabiting this area could be extinct by the year 2050, and this was shown to be directly affected by implementing climate warming scenarios.

The melting of ice at the poles caused primarily and accelerated by global climate change introduces the threat of a rising sea-level to coastal towns in cities in both the developing and developed worlds<sup>30</sup>, with a massive humanitarian crisis waiting to happen. In addition, continental glaciers that are the lifelines of many rivers that are essential for modern-day cities that adorn their shores have begun receding sharply, thinning the amount of freshwater available for human consumption. Glaciers such as Grinnell in the US, Solheimajokull in Iceland and Chacaltaya in Bolivia, among numerous others are merely feeble reminders of their past glory not very long ago<sup>31,32</sup>.

More recently, the controversial procedure of hydraulic fracturing (hydrofracking or fracking) has been the source of intense political and scientific debate internationally. The process, which makes use of tremendous volumes of water to fracture shale rock and release methane gas trapped in cavities within the rock. The process has been widely blamed for the contamination of well water close to the sites of fracking<sup>33</sup>, and also for the occurrence of earthquakes of small magnitudes (probably due to fluid injection)<sup>34, 35</sup>. One recent study<sup>36</sup> has estimated that the process of fracking might lead to increased GHG emissions into the atmosphere over the lifetime of a fracking well (due to methane emissions from drilling and flow-back return fluids compared to conventional natural gas drilling. It has also found that the footprint of a fracking well might be much larger than that of a coal-fired plant over a 20-year horizon. As natural gas (especially from fracking) is being touted as a cleaner fossil fuel alternative to coal and as a bridge till renewable energy comes of age, one needs to explore all of the environmental consequences of the process as well before passing verdict and adopting fracking as a viable means to generate power.

These economic, social and environmental scenarios beg the question of potential ways to turn around our petroleum- based economies into more sustainable and renewable societies. Biomass has been touted as a potential source for transportation fuels for over a decade now. In the United States, biomass as a resource has tremendous potential and can displace much of the petroleum that is being imported from outside her borders. The much-touted Billion Ton Study<sup>37</sup> conducted by the ORNL in 2005 has famously proclaimed that biomass production in the United States is capable of displacing 30% of

the country's petroleum needs within 25 years using conventional biofuels such as ethanol and biodiesel. More importantly, the study has identified 1.3 billion dry tons of biomass available annually for conversion into biofuels.

## **2.2. Fulfilling the necessity for bio-based societies- Means and avenues**

Having outlined the desperate need to gradually lessen modern society's dependence on non-renewable fossil resources and to realize the true potential of bio-based social and economic underpinnings, an exploration of the available avenues is both necessary and beneficial. The upcoming discourse identifies the biorefinery as a central tenet for such a transformation, and provides some background and comparisons to cement this idea.

### **2.2.1. Platform Chemicals and the Integrated Biorefinery**

It is envisioned that bio-based societies can become a reality when renewable substitutes, derived from biomass, have been found for the vast array of products derived from the processing of crude petroleum and other fossil fuels. The petroleum refinery, while mostly derided on for being the cause of much pollution and environmental degradation, is may be prudent to look up to them as a model for the development of biological refineries. Many fuels and chemicals such as gasoline, diesel fuel, kerosene, waxes, lubricating oils, greases, asphalts and plastics are valuable products obtained from the fractional distillation process. The design of modern-day biorefineries needs to emulate the petroleum refinery and they should be able to produce a variety of fuels and value-added chemicals by processing a wide array of biomass feedstock using physical, chemical or biological means (or various combinations of these). The integrated

biorefinery has been defined as ‘a facility that integrates biomass conversion processes and equipment to produce fuels, power, and chemicals from biomass’<sup>38</sup>.

The current status of integrated biorefineries in the United States is still in its infancy. As of November 2011, there were 25 such biorefineries funded by the Department of Energy across the US at the pilot, demonstration and commercial-scales<sup>39</sup>. The technologies employed by these facilities include algal, chemical and biochemical, thermochemical-gasification and pyrolysis, and hybrid versions of these. At present, Abengoa in Kansas (cellulosic ethanol from stover, switchgrass and woody biomass; 25 Mgal/yr), POET in Iowa (cellulosic ethanol from corn cobs; 25 Mgal/yr), Flambeau River Biofuels in Wisconsin (renewable diesel and Fisher-Tropsch waxes from paper mill residue and waste forest material; 9 Mgal/yr), Mascoma in Michigan (cellulosic ethanol from aspen; 40 Mgal/yr) and Bluefire, LLC in Mississippi (cellulosic ethanol from wood wastes and sorted municipal solid waste; 19 Mgal/yr) are the only DOE-funded biorefineries operating on a commercial scale. The smaller-scale facilities are involved in the production of cellulosic and algal ethanol, algal lipids, renewable diesel and gasoline, Fischer-Tropsch liquids, biobutanol, etc. using a variety of conversion technologies. The last point leads us to a new problem: one of too many.

One of the major hurdles in the way of the realization of biorefineries is the sheer number of potential feedstock, conversion processes and value-added products that can be implemented. This is in addition to difficulties encountered with biomass storage and logistics<sup>40</sup>, giving rise to costs associated with sorting, drying and transportation. Seasonal changes in the composition of biomass further compound the problem of

feedstock variability. While the petroleum refinery only processes crude oil using fractional distillation to generate a wide array of compounds, the issue is not so simple in the case of biorefineries. Owing to the inherent limitations of chemical and biological pathways, the production of certain biofuels and biochemicals can be accomplished only by converting certain feedstock in specific ways. So far, transportation fuels have been viewed as the main target of our efforts in this area, but there are various other chemicals of fossil fuel origin that need to be produced via the means of the biorefinery, if transformation into a bio-based society is desired.

For example, in 2010, 6.99 billion barrels of petroleum were consumed in the United States, of which 71% comprised of gasoline, diesel and jet fuels<sup>41</sup>. Of the remaining, 2% was used as petrochemical feedstock for the production of plastics, solvents, lubricants, specialty chemicals, etc. Of the 419.4 million barrels of Liquid petroleum gases (LPG) and Natural Gas Liquids (NGL) produced the US in 2010, which account for 6% of total petroleum refinery products, 79% was used in the production of plastic products, materials and resins (2006)<sup>42</sup>. While the replacement of fossil-origin fuel sources with biomass-derived fuel sources might seem like a tall order at this point, other products from the refining process can be replaced with renewable sources, and biomass is the only feedstock among all the renewables that can be used to accomplish this. This is because the production of synthetic organic materials such as fibers, rubbers, adhesives, coatings, plastics, etc. (currently produced primarily from petroleum and natural gas), requires a carbon source, and amongst all the renewable energy sources, biomass is the only feedstock that fulfills this requirement<sup>43</sup>. Therefore, the use of biomass feedstock to

account for the non-fuel applications of everyday life that are mostly derived from non-renewable fossil sources brings closer to fruition the realization of a bio-based society.

To identify the most valuable chemicals amidst a cornucopia of available candidates for production in the integrated biorefinery, the concept of the *platform chemical* has been introduced. Also referred to as building blocks, platform chemicals are defined as ‘molecules with multiple functional groups that possess the potential to be transformed into new families of useful chemicals’. In essence, these are compounds that serve as precursors for the evaluation of numerous pathways which lead to more specialized chemicals. Twelve such candidates were identified in a study conducted by the United States Department of Energy (US DOE) in 2004<sup>2</sup>, which included compounds such as levulinic acid, glycerol, sorbitol, etc. The study recommended that research into their production and implementation would be a promising first step towards the development of biorefineries. The study was revisited in 2010 by Bozell and Petersen<sup>3</sup>, in which they defined strict criteria for the identification of chemicals as ‘new top chemical opportunities’, and this included chemicals such as ethanol, lactic acid, and furfural, etc. The later study has outlined specific characteristics by which to define platform chemicals, which should aid in narrowing down research and development efforts, leading to a concerted pursuit of the yet-elusive bio-based society.

### **2.2.2. The case for a furan-based biorefinery**

Over 79% of the renewable, bio-based production capacity of the DOE-sponsored biorefineries is devoted towards the production of cellulosic ethanol to partially displace the consumption of crude oil used for transportation purposes<sup>39</sup>. Given the lethargy of the

state of technology, the ambitiousness of the DOE's goals and the urgency of the situation that demands its replacement, it might be worthwhile to explore other alternatives that may have been overlooked in the single-minded pursuit of fuel ethanol. In addition, as discussed before, significant quantities of non-fuel products currently derived from fossil sources need to be displaced, and biomass, being the only source of renewable carbon, will be the perfect candidate to cater to this need.

As the following sections will demonstrate, a huge untapped potential exists for the use of furfural (and derived compounds) to form the basis for biorefineries targeted towards the production of both fuel and non-fuel products that currently owe their origin to non-renewable fossil resources.

### **2.3. Furfural as a platform chemical**

Furfural, identified as one of the most promising chemicals by Bozell et al<sup>3</sup>, is the natural dehydration product of five-carbon sugars, arabinose and xylose. As of 2002, the market price of furfural was reported to be \$1,700 per ton<sup>44</sup>. Apart from being a valuable platform chemical derived from renewable biomass feedstocks, furfural is the precursor for many furan-based chemicals, and finds itself inextricably involved in largely catalytic transformations leading to higher-value chemicals and solvents.

As the following sections demonstrate, furfural offers enormous prospects for the development of a biorefinery geared towards the production of furfural and its derivatives. It promises to offer a whole new class of chemicals of the furan family that can be derived from biomass feedstock, with very well established chemistry that has been comprehensively researched since furfural was first produced in large quantities.

### 2.3.1. Uses of furfural

Ever since its discovery, furfural and the ensuing furan chemistry has fascinated researchers who set about finding applications for the chemical class. A peculiar review of some applications explored for furfural and its derivatives by early researchers, from being used as a candle odorant in churches to the treatment of athlete's foot for a Midwestern soccer team, was provided by Peters in 1946<sup>45</sup>, including the perceived importance of the chemical in those early days. A more conventional review of some of the more widespread applications for furfural is provided in this section.

Furfural has found applications as a selective solvent in the refining of petroleum, lubricating oils, diesel fuels and vegetable oils<sup>7, 46</sup>. Owing to a structure composed of conjugating double bonds, furfural is susceptible to the phenomenon of 'intermolecular conjugation', whereby furfural interacts with other unsaturated compounds (double bonds only) to form enlarged conjugated systems, which allow for their separation from mixtures containing saturated compounds. The first large-scale application of furfural was as a solvent for the purification of wood rosin<sup>47</sup>. In the refining of lubricating oils, petroleum and diesel fuel, furfural has been used to separate aromatics and retain paraffinic-type compounds from the mixture to improve the viscosity index, ignition characteristics, oxidation stability, color, flash point, and to lower the carbon-forming tendency<sup>48</sup>. By the same principle, furfural is also used to extract unsaturated compounds from vegetable oils for the preparation of 'drying oils', used to make paints and varnishes<sup>6, 7</sup>.

Furfural has also been touted as an effective agent to control soil nematodes (plant-parasitic roundworms). Along with benzaldehyde and thymol, furfural was found to control nematodes indirectly by changing the soil microflora in a way that the growth of bacteria which kill the nematodes is encouraged<sup>6</sup>. Rodriguez-Kabana et al<sup>49</sup> investigated the action of furfural on different species of parasitic and non-parasitic nematodes during three phases of growth: soil preplant, eight week-old soil, and eight week-old root growth. The efficacy of furfural was also compared with 1,3-Dichloropropene (1,3-D), a commercial nematicide, and the authors concluded that the effect of furfural in controlling nematodes was superior to that of 1,3-D during all the growth phases. Also, being relatively inexpensive and non-toxic towards humans, furfural could be considered with other commercial, broad-spectrum nematicides.

An application for furfural as a fungicide was identified as early as commercial production of furfural began at the Quaker Oats company in 1923. Miner<sup>50</sup> identified that furfural at lower concentrations was a much better fungicide than formaldehyde was at much higher concentrations. Research on the use of furfural to control the growth of *Rhizoctonia solani* was studied by Raeder et al<sup>51</sup> in 1925 and by Flor<sup>52</sup> in 1926. Canullo et al<sup>53</sup> treated soil with furfural to control southern blight (*Sclerotium rolfsii*) in lentil. Furfural also showed to stimulate the growth of bacteria antagonistic to the southern blight fungus, as well as of the beneficial fungi, *Trichoderma* spp. A much more recent study<sup>54</sup> investigated the effect of a commercial nematicide (MultiGuard Protect®) on controlling the population of *Meloidogyne incognita* (southern root-knot nematode) and galling on tomato and pepper, with effective management of galling observed on the

former. In addition, the treatment with the furfural-based nematicide did not seem to have phytotoxic effects on either plant.

The greatest application of furfural, however, is its conversion into derivatives such as furfuryl alcohol, furan, furoic acid, etc. and the potential applications for these chemicals. A brief review of the importance and production of some of these furan-based furfural derivatives is provided here.

### 2.3.2. Furfural Derivatives

#### 2.3.2.1. Conversion into furan

The catalytic decarbonylation of furfural at high temperatures leads to the production of furan, by the liberation of a molecule of carbon monoxide (figure 2.1).

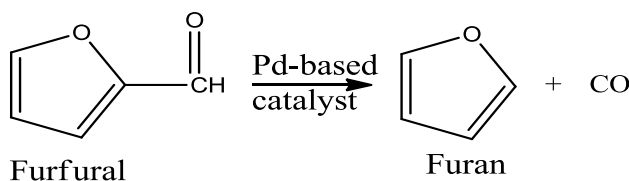


**Fig. 2.1:** The catalytic decarbonylation reaction of furfural for the production of furan.

The oldest-known method of producing furan from furfural involved the production of the intermediate furoic acid (through the Cannizzaro reaction), followed by decarboxylation to produce furan. Hurd et al<sup>55</sup> initiated efforts for the direct production of furan from furfural using reaction with fused alkali (yields up to 60%) and the pyrolysis of furfural (yields ~16.5%). Wilson<sup>56</sup> in 1945 reported the use of nickel gauze to catalyze the decarbonylation of furfural into furan with the beneficial effect of hydrogen to provide with yields in excess of 50%. The presence of hydrogen was thought to either

catalyze the reaction, or clean the active center of the catalyst by washing away materials that may be poisonous to the catalyst.

Lejemble et al<sup>57</sup> have reviewed that despite the availability of several metal oxide catalysts (iron, zinc, manganese, chromium, etc.), noble metals are mostly preferred to catalyze the decarbonylation reaction. The extreme conditions (300-500 °C) results in a breakdown of furan into heavy products, resulting in a short-term deactivation of the catalysts. In addition, even with the use of promoters, the metal oxide catalysts are known to lose activity soon, leading to the adoption of noble metals, especially palladium, as preferred catalysts. Palladium, supported on either alumina or activated carbon, was reviewed to be an efficient catalyst to convert furfural to furan<sup>57</sup>. Singh et al<sup>58</sup> have studied the kinetics of the decarbonylation with Pd supported over carbon and alumina, concluding that the former was a better support. In agreement with Wilson's observations, Singh et al found that the presence of hydrogen boosted furan yields by aiding the transport process of commuting the reactants and products to and from the catalyst active sites.

Zeitsch<sup>6</sup> has reviewed that today, furan is commercially produced by heating furfural to 158 °C in presence of 5% Pd catalyst supported on microporous carbon, with potassium carbonate used to promote the reaction. Furan yields from this reaction are reported to be in excess of 98%.

McKillip et al<sup>7</sup> have reviewed the uses of furans as mostly for the production of pharmaceuticals, agricultural chemicals, stabilizers, etc. The Diels-Alder reaction of

furan with maleic acid results in the production of a 1:1 furan-maleic anhydride copolymer, which finds use as a complex-forming agent for  $\text{Cu}^{2+}$  ions. Furan is also used in the synthesis of thiophene and pyrrole.

### 2.3.2.2. Conversion into Tetrahydrofuran

Perhaps the most promising use of furan lies in its conversion into tetrahydrofuran (THF), which presents attractive prospects for use as a solvent, especially as a dissolving agent for polyvinylchloride and vinylidenechloride copolymers<sup>59</sup>. It also finds applications as a raw material for spandex fibers and polyurethane elastomers<sup>59</sup>. THF is manufactured by the catalytic hydrogenation of maleic anhydride according to a process patented by du Pont<sup>60</sup>. Production of THF from furan (ultimately from furfural) provides with a selective industrial solvent from renewable means.

The hydrogenation reaction in the presence of nickel catalysts (Ni is preferred, while noble metals may also be used but lead to hydrogenolysis side products) has been called the most significant reaction of furan, commercially<sup>7</sup>. The hydrogenation of furan is catalyzed by the same catalyst used for the decarbonylation of furfural, Pd supported on carbon<sup>6</sup> (figure 2.2).

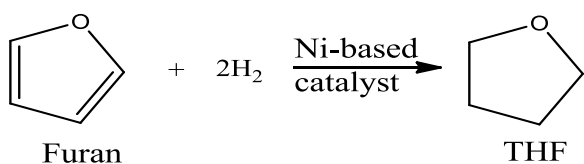


**Fig. 2.2:** The catalytic hydrogenation of furan for the production of THF<sup>6</sup>.

### **2.3.2.3. Conversion into furoic acid**

Furoic acid finds application for its conversion into furoyl chloride, which is used in the manufacture of pharmaceuticals (as an intermediate), fungicides and insecticides, hypolipidemic and anti-inflammatory agents<sup>6, 61</sup>.

The first step to producing furoic acid from furfural is by subjecting the latter to a Cannizzaro reaction with aqueous sodium hydroxide to produce furfuryl alcohol and sodium 2-furancarboxylate<sup>6</sup>. Upon separating the furfuryl alcohol, sodium 2-furancarboxylate is acidified with sulfuric acid to produce furoic acid and sodium hydrogen sulfate. Furoic acid yields from this process are reported to be quite low, amounting to only 45-53% of the theoretical yield, with furfuryl alcohol polymers and sodium hydrogen sulfate formed as the major side-products, apart from unwanted by-products.

### **2.3.2.4. Conversion into furfuryl alcohol**

Around 62% of the furfural produced globally each year is converted into furfuryl alcohol, which finds its largest application in the manufacture of foundry resins. Resins made from cross-linked polymers of furfuryl alcohol with itself and other products (furfural, formaldehyde, phenolic compounds, urea, etc.) were shown to possess excellent chemical, thermal and mechanical properties, in addition to withstanding corrosion and solvent action<sup>47</sup>. Furfuryl alcohol has also been used in the manufacture of furan fiber-reinforced plastics (FRP) for use in piping, and is recommended for use for high performance chemical processes when chlorinated aromatics, oxygenated organic

solvents, etc. are used owing to its anti-corrosion properties. Such corrosion-resistant off-the-shelf piping has been available since 1977<sup>7, 47</sup>.

The most common use of furfural is its conversion into furfuryl alcohol by hydrogenation over copper chromite catalysts. In the past, commercial production of furfuryl alcohol was carried out using 1-2% copper chromite catalyst at 1,000-1,500 psi by hydrogenating technical-grade furfural in 110-gallon autoclaves at 175 °C. Wojcik<sup>62</sup> has also reported that the hydrogenation reaction may be carried out in presence of other suitable catalysts, but that it was difficult to terminate the reaction once furfuryl alcohol was produced. Quantitative yields of 96-99% were reported for this reaction. Further hydrogenation of furfuryl alcohol (using copper chromite) at ~250 °C and slightly higher pressures produces 2-methylfuran (36%), pentanol (36%), 1,5-pentanediol (15%) and 1,2-pentanediol (14%) as products of hydrogenolysis of the alcohol.

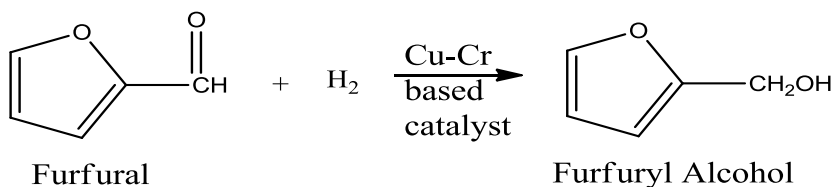


**Fig. 2.3:** Copper chromite catalyzed conversion of furfural into furfuryl alcohol (adapted from Wojcik<sup>62</sup>).

Brown and Hixon<sup>63</sup> first reported a continuous vapor-phase process for the production of furfuryl alcohol from furfural using a copper chromite catalyst stabilized with calcium (to sustain the activity and catalyst life). Yields up to 95% furfuryl alcohol were reported, with 2-methylfuran being the dominant byproduct.

The reaction is thought to occur by hydrogenation of the carbonyl group on furfural, first by the occurrence of an alkoxide intermediate (due to the formation of a C-H bond), followed by the subsequent addition of the second H atom, producing furfuryl alcohol<sup>64</sup>. Several catalysts have been evaluated for the hydrogenation of furfural into furfuryl alcohol. Copper is a highly selective catalyst for the hydrogenation reaction and is widely used in its chromite form, while decarbonylation becomes the dominant path when using palladium, leading to the production of 2-methylfuran in the latter case.

Today, the hydrogenation reaction is accomplished using either the vapor phase or the liquid phase reaction, but the former is more commonly employed.

In the vapor phase process, furfural is mixed with hydrogen in a countercurrent packed column, and then this mixture is passed into a tubular reactor (oil-heated, maintained at 135 °C) filled with pellets of copper chromite, which catalyze the reaction producing furfuryl alcohol vapor, which is liquefied using raw furfuryl alcohol circulated around the system using a pump. Purification of the product stream to produce furfuryl alcohol is achieved by means of distillation, and the impurities constitute 2-methylfuran (2-MF), unreacted furfural, products of polymerization and reaction water. The theoretical yield of furfuryl alcohol from this process is reported to be in excess of 92%, with 2-MF being the principal byproduct. An overview of the vapor and liquid phase industrial process and unit operations is provided by Zeitsch<sup>6</sup>.

While commercial procedures for preparation of furfuryl alcohol have relied on the use of copper chromite catalysts, the moderate activity and the toxicity associated with chromite

have generated interest in the evaluation of other possible candidates to catalyze the hydrogenation reaction. Research has been done on the use of highly selective heterogeneous catalysts such as carbon-supported copper<sup>65</sup>, Raney nickel<sup>66</sup>, Ni amorphous alloys, mixed copper- zinc alloys doped with Al, Mn and Fe, Cu/ MgO catalysts<sup>67</sup>.

#### ***2.3.2.5. Microbial Conversion of furfural into furfuryl alcohol***

A relatively understudied area of furfuryl alcohol production involves the microbial reduction of furfural to produce furfuryl alcohol. Most of the literature that has been published in this regard pertains to conversion of fermentation inhibitors into less toxic chemical products. Therefore, all the microorganisms that have been studied are involved in fermentation processes to produce ethanol.

Lignocellulose, by virtue of its structure arising out of the crystalline cellulose structure enclosed in a lignin shell bonded by the hemicellulose acting as glue, is notoriously resistant to chemical and biological attacks. This resistance of lignocellulosic biomass to breakdown is termed as biocalcitrance<sup>13, 68</sup>. Following the pretreatment of lignocellulosic biomass during the production of cellulosic ethanol to separate the sugars from the rest of the plant matrix, inhibitors such as furfural, 5-hydroxymethylfurfural (HMF), acetic acid, formic acid, vanillin, levulinic acid, 4-hydroxybenzaldehyde, etc. are produced<sup>13</sup>. Of these, the first two have been identified to be the most potent inhibitors to microbial growth and activity.

Conventional detoxification methods of biomass following pretreatment operations, such as steam explosion, dilute acid treatment or ammonia fiber explosion, involve water

washing and over-liming of the biomass. Despite being a fast process, this method of detoxification results in a significant loss in sugar yields (up to 30% of the pretreated solids) which translates into lost feedstock for conversion into ethanol, along with generating large amounts of wastewater that increases processing costs and dilutes the sugar stream for fermentation leading to increased costs during the distillation of ethanol<sup>13</sup>. The alternative is to employ microorganisms which degrade the inhibitors into less toxic compounds as part of their metabolism, but this strategy faces hurdles as it is a very slow process and not much is known about the genetic and metabolic pathways that are utilized to effect such conversions<sup>13</sup>. The advantages and shortcomings of both strategies for bi detoxification have led to the advocating of a hybrid process that involves the microbial transformation at a high reaction rate, the latter deriving impetus from insight into the genetic and metabolic knowledge of the biochemical pathways utilized.

The yeast strain *Saccharomyces cerevisiae* 354 has been reported to convert pure furfural to furfuryl alcohol, tolerating furfural concentrations up to 3%. Molasses were used as the sugar source for the yeast. Yields of 96% have been reported at much milder conditions of 30 °C, compared to the very high temperatures and pressures needed for the chemical reduction of furfural to furfuryl alcohol<sup>69</sup>.

De Villegas et al<sup>70</sup> investigated the effects of aeration and stirring on the production of furfuryl alcohol using *S cerevisiae* 354, and obtained a conversion of 70% with a final furfural concentration of 35%. They identified that anaerobic conditions with low stirring

gave the best results, when each of the conditions were run for 48 hours. As with the study by Villa et al, the sugar source was molasses.

Palmqvist et al<sup>14</sup> conducted similar studies by growing Baker's yeast grown on agar slants with glucose as the carbon source at 30 °C overnight. They report yields of ~97% with a furfural concentration of 29 mM. Higher concentrations of furfural in the reaction mixture were shown to have adverse effects on the specific growth rate of the organisms. Again, this study was conducted from the perspective of reducing the inhibitory effects of furfural on ethanol yields.

Belay et al<sup>71</sup> used the methanogen *Methanococcus deltae* ΔLH grown on CO-H<sub>2</sub> to study the conversion of furfural to furfuryl alcohol at slightly elevated temperatures. This investigation was conducted from an anaerobic digestion standpoint, especially in the case of pulp mill wastewater treatment. An interesting observation from this study was the slightly better growth in *M deltae* cultures that were grown in the presence of low concentrations of furfural (5- 10 mM). Cultures in the presence of higher furfural concentrations showed severely inhibited growth. A conversion of 97.5% was reported in this study for *M deltae* cultures inoculated with 10 mM furfural.

Nichols et al<sup>16</sup> studied the use of the fungus *Coniochaeta ligniaria* NRRL30616 grown on corn stover dilute- acid hydrolysate to convert furfural to furfuryl alcohol and furoic acid. Ammonium sulfate was used as a nitrogen source while inoculating the hydrolysate with the fungus at 30 °C for 18- 24 hr. Fermentations were run for up to 70 hours to study the conversion of furfural and HMF, both of which showed final concentrations of close

to zero ppm from initial values of ~200 and ~300 ppm, respectively. No mention of the yield is provided in this study, as the primary objective seems to have been the conversion/ removal of fermentation inhibitors.

In the study conducted by Gutierrez et al<sup>72</sup>, the effect of converting furfural on ethanol production from xylose using *Escherichia coli* (K011 and LY01) and *Klebsiella oxytoca* (P2) was investigated. The organisms were grown using tryptone and yeast extract as the sole carbon sources and complete conversion of furfural to furfuryl alcohol was observed. Both the *E coli* strains are derivatives of *E coli B* and are integrated with genes from *Zymomonas mobilis* to produce ethanol. All three strains were observed to reduce over 90% of the furfural into furfuryl alcohol within the first five hours.

Research has shown that furfural can be converted into furfuryl alcohol is very high yields by employing microbial processes, albeit from the perspective of detoxifying lignocellulosic hydrolysates. Exploration of this concept seems appealing towards developing a non-toxic and less energy-intensive way of producing furfuryl alcohol, with all aspects indicative of a truly green process that is in line with the goals of the integrated biorefinery.

Apart from the three chemicals discussed here, furfural plays the role of a precursor to many other chemicals of established and often under-utilized value. A good review of some of these is presented by Sain et al<sup>4</sup>, Zeitsch<sup>6</sup>, McKillip et al as a chapter in Ullmann's Encyclopedia of Industrial Chemistry<sup>7</sup> and by Kottke in the Kirk-Othmer Encyclopedia of Chemical Technology<sup>47</sup>. Figure 2.4 shows some of the pathways that are

available for the production of a wide variety of useful compounds with furfural as a precursor (adapted from Sain et al<sup>4</sup>). Exploration, and alternatives to most of these catalytic processes (expensive, toxic and hard to recycle) promises to open up an exciting new research area towards the development of environmentally-benign processes that can be integrated into modern integrated biorefineries.

#### **2.4. Production of furfural**

Furfural was first discovered by the German chemist Johann Wolfgang Dobereiner in 1832<sup>49</sup>, and research and commercial production of furfural began extensively in 1921<sup>4</sup>. In the absence of a synthetic route for preparing furfural, it has traditionally been produced from plant residues rich in pentosan, such as corn cobs, oat and rice hulls, cottonseed hull bran, etc (as of the late 1940s)<sup>73</sup>.

The first commercial production of furfural was performed at the Quaker Oats company in Cedar Rapids, Iowa, in the early 1920s<sup>6</sup>. Furfural production at the Quaker Oats company was accidental, arising out of a desire to improve the digestibility of the 50 to 60,000 lb. of oat hulls being processed per year at the plant for animal feed using acid treatment that would release the sugars and improve the palatability of the feed<sup>74</sup>. Since then, of the 400 tons of oat hulls generated per day at the Quaker Oats plant, 40 tons were used to produce over 5,400 lb. of furfural<sup>9</sup> as of 1932. Today, over 280,000 tons of furfural is produced per year, with the greatest amount produced in China (200,000 tons), followed by the Dominican Republic (32,000 tons) and South Africa (20,000 tons)<sup>5</sup>. Together, these three nations account for 90% of global furfural production.

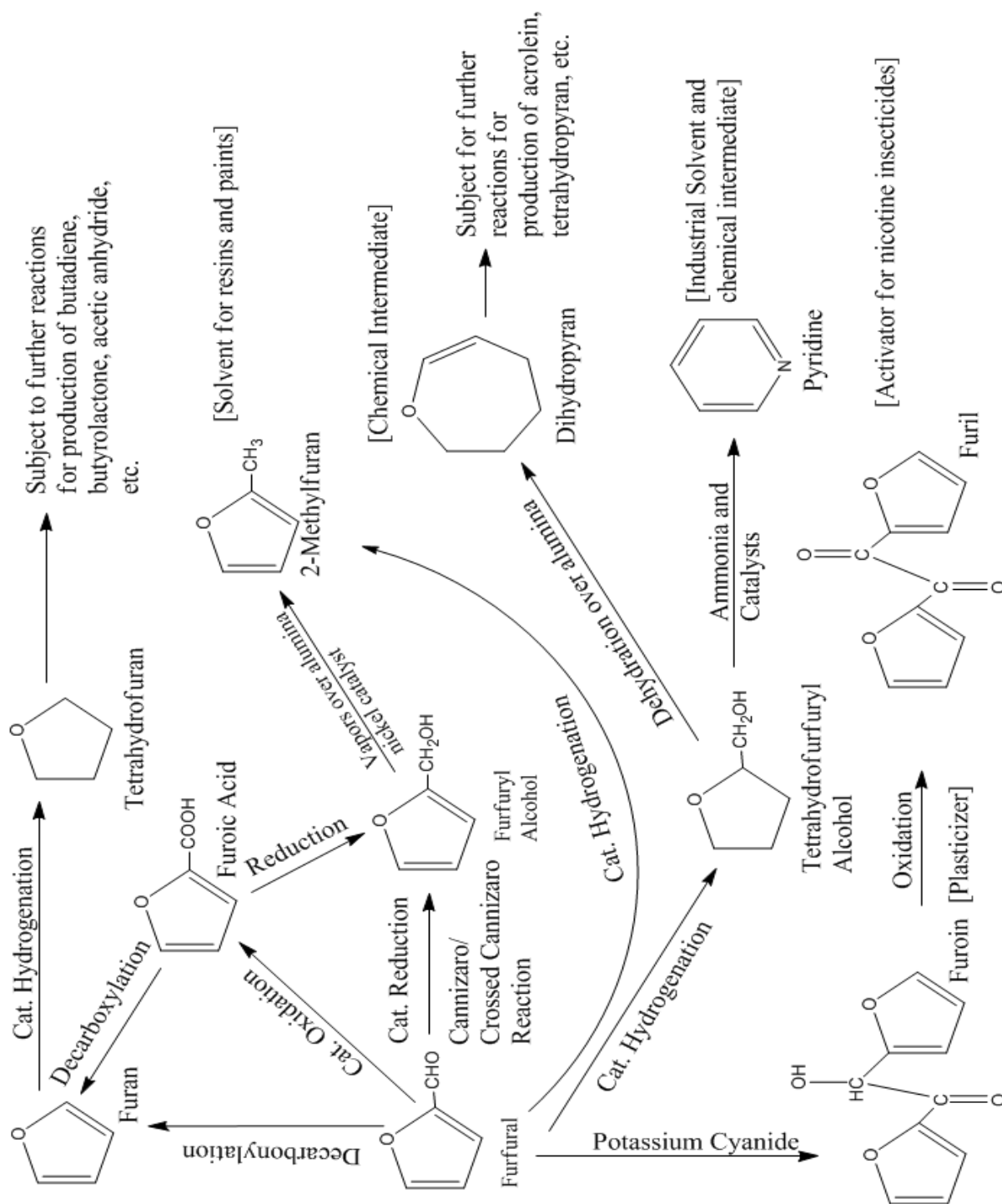


**Fig. 2.4:** Possible furan-based chemicals with furfural as a precursor. Uses of some of the chemicals are provided in the brackets (adapted from Sain et al<sup>4</sup>).

## 2.5. Pentose dehydration mechanism for furfural formation

Contradictory theories exist in literature to explain the mechanism of furfural formation from D-xylose, and evidence has been obtained in validation of both theories, making the true nature of the dehydration mechanism ambiguous. Three schemes seeking to explore the dehydration mechanism have been proposed and so far, there is no real consensus on the flawlessness of one scheme over the others.

Aldopentoses can assume three forms in aqueous solution: open-chain, furanose and pyranose<sup>75</sup>. Based on the finding that almost all of the glucose in equilibrium solution was of the pyranose form, this convention has been extended to the aldopentoses<sup>75, 76</sup>. Bishop and Cooper<sup>77</sup> estimated that ~100% of the D-xylose existed in the pyranose form in equilibrium solutions (65.1% as  $\alpha$ -Pyranoside and 29.8% as  $\beta$ -Pyranoside). The insignificant quantity of the aliphatic form of the aldopentose in aqueous solutions has led to the argument that they play a very minor role in the kinetics of furfural formation from xylose.

Nevertheless, Hurd and Isenhour<sup>78</sup> argued that an aliphatic intermediate was a necessary step towards the conversion of xylose into furfural, regardless of the prevalence of cyclic or acyclic form of the aldopentose. A second scheme involving an aliphatic intermediate was proposed by Wolfrom et al<sup>79</sup> in 1948 for the dehydration of D-glucose to produce 5-HMF via the formation of aliphatic intermediates, which was extended for the dehydration of D-xylose<sup>80</sup>. The validity of both these schemes was examined by Bonner and Roth<sup>80</sup> using <sup>14</sup>C radioactive assays, and it was observed that the aldehydic carbon (C1) was unaffected during the course of the mechanism, suggesting that both schemes

were plausible. Based on xylose dehydration experiments carried out in acidified, tritiated water, Feather et al<sup>81</sup> observed that the furfural produced contained no carbon-bound tritium, leading them to conclude that the dehydration proceeded via an acyclic reaction scheme (figure 2.5). The aldopentose structure was presumed to open up into the aldose form, which isomerizes to give an intermediate, which further dehydrates to give furfural<sup>81, 82</sup>.

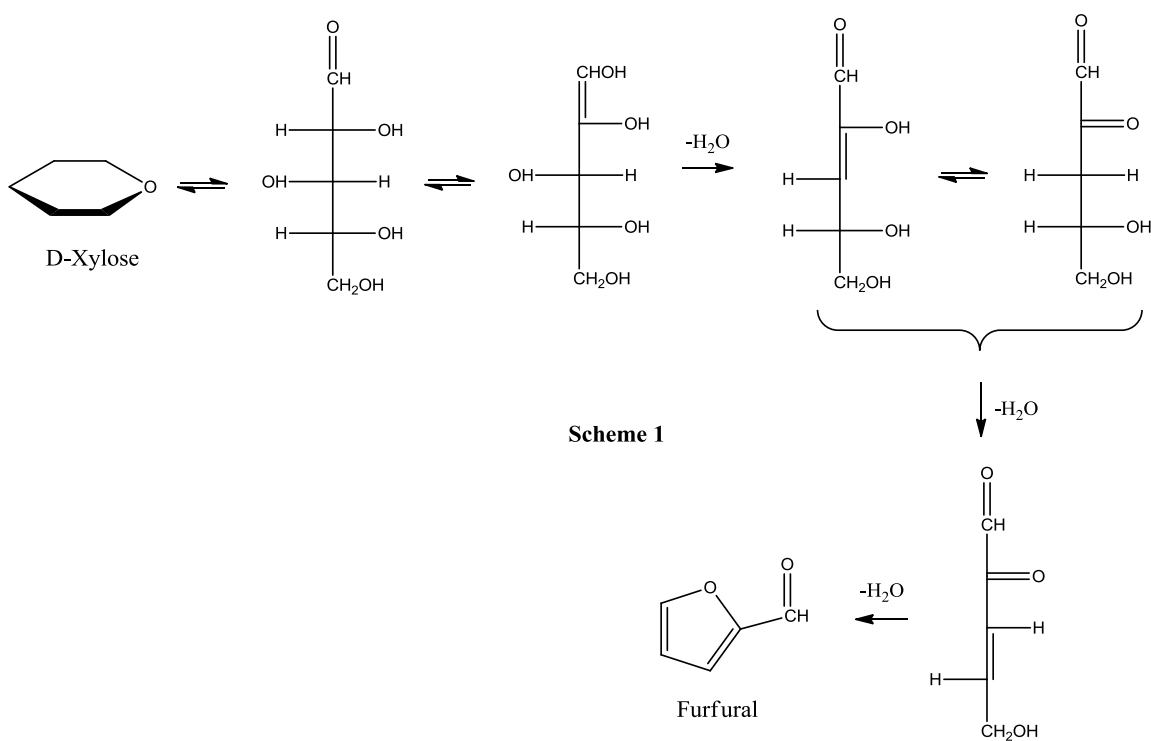
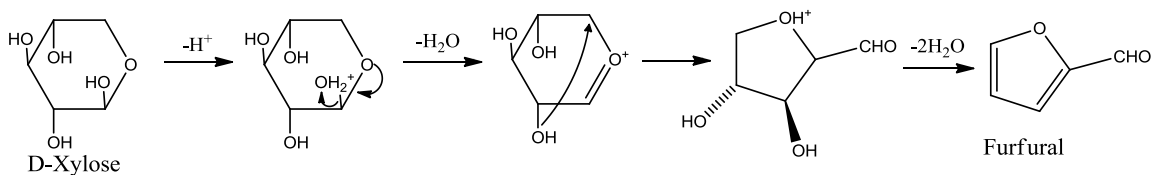


**Fig. 2.5:** Scheme 1 proposed to explain the mechanism of xylose dehydration into furfural via the formation of open-chain intermediates (adapted from Nimlos et al<sup>82</sup>).

The acyclic dehydration schemes were challenged by two new schemes that proposed the dehydration mechanism involved direct rearrangement of the pyranose structure after protonation and dehydration. The difference between these latter schemes lies in the

question of protonation of the oxygen atom (either at C1 or C2)<sup>82</sup>. The basis for these schemes was initially floated by Shafizadeh et al<sup>83</sup> while studying the pyrolysis products of xylan polysaccharides which resulted in thermal cleavage of the glycosidic group, leading to the formation of furfural and the cleaved aglycone. Antal et al<sup>84</sup> investigated both the open-chain hypothesis proposed by Feather et al, and two pyranose rearrangement schemes (Schemes 2 and 3, figure 2.6) using a kinetic model.

**Scheme 2**



**Scheme 3**

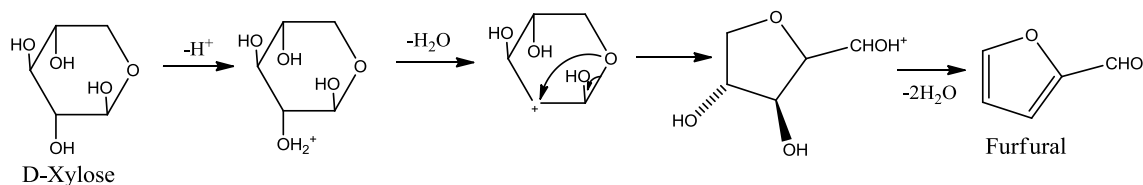


**Fig. 2.6:** Schemes 2 and 3 hypothesizing intramolecular rearrangements within the pyran molecule for the formation of furfural via cyclic intermediates (adapted from Nimlos et al<sup>82</sup>).

The study concluded that the kinetic model constructed for the cyclic dehydration mechanism agreed well with experimental data, lending credence to the latter hypothesis. This hypothesis was further bolstered when Nimlos et al<sup>82</sup> performed quantum mechanical modeling on all three schemes to study the energy barriers of the transition states involved and found that energetics supported intramolecular rearrangement rather

than ring-opening of the pyran, with Scheme 3 shown to have the lowest energy barriers, and therefore, appearing the most plausible.

In addition to these longstanding hypotheses, Binder et al<sup>85</sup> introduced a novel reaction mechanism for furfural production in presence of Cr<sup>II</sup> and Cr<sup>III</sup> catalysts in non-aqueous solvents (ionic liquids and *N,N*-dimethylacetamide containing lithium chloride/ DMA-LiCl). Their observations led to the suggestion of chromium ions influencing the reaction by causing the occurrence of a hydride shift with xylofuranose formed as an acyclic intermediate, which then undergoes deprotonation and dehydration to produce furfural. Although this mechanism is considerably different from those proposed earlier for aqueous solutions, it is thought that such a transformation can occur only in the presence of chromium ions.

Owing to the absence of any consensus in literature regarding the validity of either hypothesis (cyclic versus acyclic intermediates), it was decided to employ a simplified model described by Marcotullio et al<sup>12</sup> based on the formation of acyclic intermediates. Use of this model allowed for a satisfactory explanation of results obtained in this study, without delving into the intricacies of intermediate formation.

For the purposes of improving furfural yield, and to better control the reaction for prevention of losses (explained in Section 2.7), a clear consensus must be reached on the question of the pentose dehydration mechanism. Comprehensive scrutiny of the proposed models to adjudicate the validity of one or more models, or an explanation of the causes for the successes and failings of these models (or the introduction of a new model that

satisfies experimental findings) is sorely needed from future research in furfural chemistry.

Figure 2.7 shows the simplified reaction mechanism for formation of furfural from D-xylose described by Marcotullio et al. In this model, the 1,2-enediol form (structure B) is seen as the target for improvement in furfural yield. This structure is thought to proceed to form furfural by the loss of three water molecules in the presence of an acid catalyst<sup>12</sup>. This model allowed for consistent explanation of improved furfural kinetics observed by Marcotullio et al in the presence of halide ions in solution, assumed to influence the formation of the intermediate.

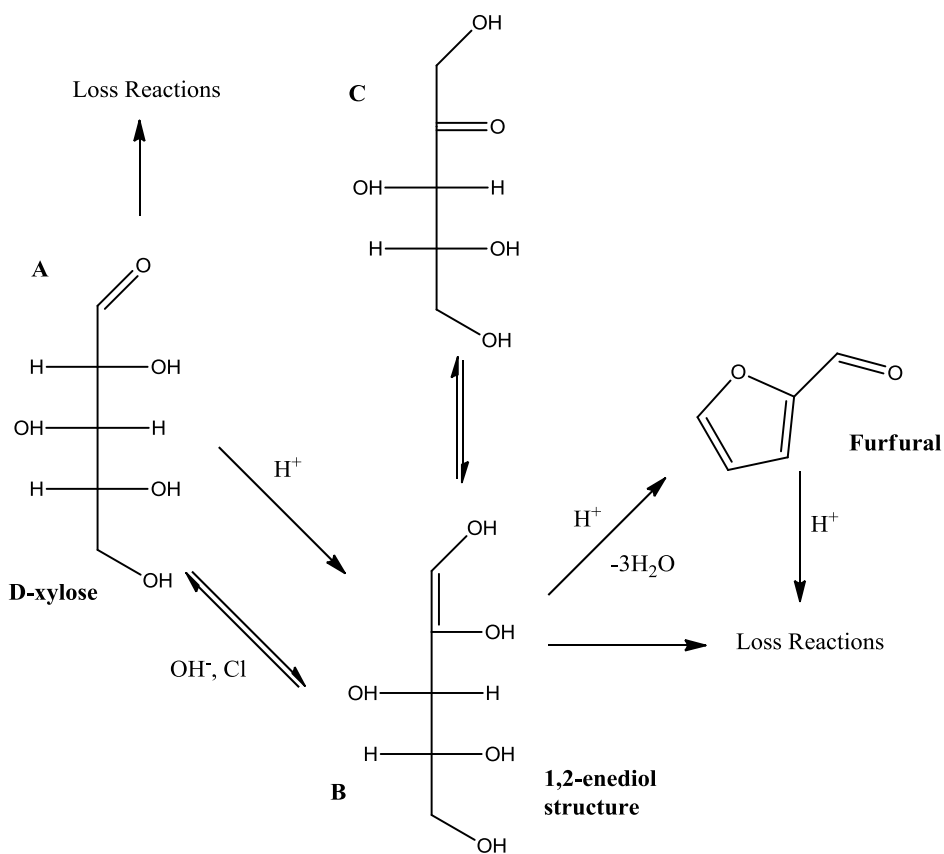


**Fig. 2.7:** Proposed mechanism for formation of furfural from D-xylose<sup>12</sup>.

## 2.6. Reaction losses during the production of furfural

Conventional batch production of furfural is accompanied by the formation of black, resinous loss products called humins. These can be attributed to reactions of furfural with itself (furfural condensation) and reactions of furfural with the 1,2-enediol intermediate (furfural resinification). The latter reaction gives rise to the formation of furfural-pentose, which is the chief loss reaction<sup>6</sup>. Root et al<sup>86</sup>, when studying the kinetics of the dehydration reaction using xylose, showed a direct correlation between lower concentrations of the sugar and higher yields of furfural. This phenomenon has been explained by the formation of furfural-pentose, the occurrence of which is minimized if the initial concentration is low enough, thereby improving the yields.

Industrial processes operating in the conventional batch configuration typically have yields not exceeding 45-50% of the theoretical due to the loss reactions<sup>6</sup>. This is despite the fact that 100% yields have been obtained using analytical methods to produce furfural, including the method to determine pentosan content in biomass following the method of Hughes and Acree<sup>87</sup>. The method involves dehydrating furfural in the presence of 12% hydrochloric acid (with NaCl added to accelerate furfural formation), and distillation to separate furfural from the vapor phase and prevent its degradation in the strong acidic conditions.

Even though the cause of the losses has been extensively studied and established, industrial reactors operate in a configuration similar to the century-old Quaker Oats process and undergo considerable losses. The primary driver for the insistence of this process is the cheap cost of feedstock, which is mostly pentosan-rich residue such as corn

cobs and oat hulls. Improvement in the furfural yield using a process which can be readily adapted for large-scale application is sorely desired, should the idea of a furfural-based biorefinery become more appealing and feasible. A brief review of some of the research undertaken to improve furfural yields, both from xylose and biomass, is presented here.

### **2.7. Research towards improving furfural yields**

Various approaches towards improving the yield of furfural from xylose and pentosan-containing materials have been proposed which involve ways of reducing the occurrence of loss reactions that produce humins. Research has focused on separating furfural from the reaction mixture, and ways to influence the 1,2-enediol intermediate to reduce the formation of humins and improves selectivity towards the production of furfural.

An early attempt to improve the industrial batch process pioneered by the Quaker Oats Company was undertaken by Brownlee<sup>88</sup> investigated a method to improve the furfural yield by hydrolysing pentosan-containing biomass in a reactor, and then dehydrating the pentose sugars to make furfural, which along with water, is removed from the reactor vessel using an inert gas or steam. Yields up to 16% of the dry weight of oat hulls have been reported. Dunlop<sup>73</sup> has provided the potential yield of furfural from oat hulls (based on the method by Hughes and Acree<sup>87</sup>) as 23-34%, which translates Brownlee's furfural yield from oat hulls using his new process as ~70% of the theoretical.

Lessard et al.<sup>10</sup> report obtaining 98% molar yield of furfural by dehydrating xylose using solid acid catalyst mordenite in a biphasic plug-flow reactor comprising of toluene and water at 260°C and 55 atm. High selectivity of 98% and some loss of catalyst activity

were reported in this study, and the improved yields can be attributed to the selective solvation of furfural in toluene as soon as it was formed. Binder et al<sup>85</sup> reported moderate furfural molar yields on the order of 50% using Cr<sup>II</sup> and Cr<sup>III</sup> catalysts in the presence of *N,N*-dimethylacetamide containing lithium chloride (DMA-LiCl) and related non-aqueous solvents. This study sought to explore an alternate mechanism of furfural production in the presence of chromium salts involving the xylulose intermediate. Recently, Weingarten et al.<sup>11</sup> also employed a biphasic system composed of water and methyl isobutyl ketone (MIBK) using a microwave reactor. Furfural formed by the dehydration of D-xylose using HCl in the aqueous phase was selectively transferred into the organic phase, thereby reducing reaction losses and the formation of humins. Similar experiments by the same group<sup>8</sup> using hot water hydrolysates and THF as the organic phase resulted in furfural yields of 92.2%, with NaCl added to saturate the hemicellulose. Marcotullio et al.<sup>12</sup> investigated the kinetics of the acid-catalyzed D-xylose to furfural pathway with the aim of improving the yield by the addition of salts (NaCl). Results from this study indicate that the presence of metal halides improves reaction kinetics by promoting the formation of the 1,2-enediol structure, and consequently, the formation of furfural. A maximum furfural yield of 81.3% was reported in the presence of 5% NaCl (by mass) using 0.05 M HCl, with good selectivity.

Gravitis et al<sup>89</sup> utilized small amounts of strong acids (greater than 10% by mass) to effect differential catalysis of the hydrolysis and dehydration reactions of biomass. Such an approach was designed to increase the furfural yield (increase reported from 55% to 75%), while reducing the degradation of cellulose by a factor of five, though no data has

been presented in support of these claims.

Zeitsch<sup>6, 90, 91</sup> has patented the SupraYield<sup>®</sup> process in which the furfural formed is continuously removed from solution by slow de-pressurization of the reaction between a primary and a secondary temperature. High yields, 50-70%, have been reported and this process has been commercialized in Australia (5 kton/ year) and India (11 kton/ year)<sup>92</sup>.

In a similar fashion, De Jong and Marcotullio<sup>92</sup> have described the use of a Multi-Turbine Column Reactor (MTC) for the hydrolysis of straw and subsequent dehydration to produce furfural. High yields are reported due to continuous removal of furfural by steam stripping from the liquid phase. The reactor column was modelled to provide mass flow rates and estimate process economics, and a furfural yield of over 86% based on hemicellulose sugars was derived from a system model, although no experimental or production data was provided.

The Biofine process, designed for the production of levulinic acid in high yield using a two-stage acid-catalyzed reaction, produces furfural in high yield (~70%) as a byproduct during the first stage of the process. Furfural is made along with HMF in the first stage of the process, where the sugars are degraded to their intermediates in a plug-flow reactor with a residence time of 12 seconds. Furfural and other volatiles are steam-stripped during the first stage, while the HMF is further reacted to produce levulinic acid.<sup>93, 94</sup>

Some of the processes described for improving furfural yields pose inevitable questions related to feasibility and environmental compatibility. The requirement of high concentrations of acid, coupled with usage of salts, lead to issues of corrosion of equipment and the need for specialized alloys to withstand the same. Specialized solid-

acid catalysts and ionic liquids are extremely expensive when compared to sulfuric acid, which finds extensive use in industry owing to its abundance, the ease of application with aqueous media (liquid-phase reactions) and comparatively lower costs. The use of liquid-liquid extraction might not prove to be the most economically feasible way of producing furfural at an industrial scale. The use of solvents gives rise to issues such as the high costs associated with their use and the need for additional recovery operations. In addition, many industrial solvents are known to be hazardous to human health, and concerns of flammability and environmental effects due to their disposal might prohibit their widespread implementation in modern biorefineries of the future.

With the exception of the Biofine process, which produces furfural as a by-product of levulinic acid, the existing furfural production processes do not lend themselves well towards the concept of an integrated biorefinery. The use of biomass as a whole for the production of furfural results in the irrecoverable loss and conversion of hexosan into degradation products. The six-carbon sugars represent valuable sources for recovery and conversion into platform chemicals such hydroxymethylfurfural (HMF) and levulinic acid, and also for the production of cellulosic ethanol and pulp. The ideal biorefinery design will try to incorporate majority of the biomass fractions and convert them into valuable products derivable from each fraction.

## **2.8. Composition of lignocellulosic biomass**

Lignocellulosic biomass is composed primarily of cellulose, hemicellulose, lignin and extractives. These broad constituents make up the woody portion of the plant, the stem and the trunk. Cellulose is the major component of all biomass, both woody and non-

woody, while hemicellulose and lignin form the rest of the plant structure. The cellulose can be visualized as forming a skeletal structure which is surrounded by a hemicellulose matrix, while lignin acts as an encrusting material, cementing the holocellulose (hemicellulose and cellulose)<sup>95</sup>.

The holocellulose contains all the sugars necessary for biofuel production, which can be obtained by the hydrolyzing the biomass. Lignin, which is the encrusting material, interferes with this process, giving rise to recalcitrance. Figure 2.8 shows the composition of lignocellulosic biomass, broken down into the cell wall components ('microfibril' spelt incorrectly as 'macrofibril' in the figure).

The goal of most biological/ chemical pretreatment processes is to improve the accessibility to the sugars by the removal of lignin. The following sections discuss the major components of lignocellulosic biomass in some detail.

### **2.8.1. Cellulose**

Cellulose can be described as a homopolysaccharide composed of  $\beta$ -D- glucopyranose units bonded by (1-4)-glycosidic bonds (figure 2.9). It is a polymer composed of many cellobiose units (a molecule formed by the condensation of two glucose anhydride units). The chemical formula of cellulose is  $(C_6H_{10}O_5)^n$ , where  $n$  is the number of repeating units of glucose, also referred to as the *degree of polymerization* (DP), which is different for different feedstock. Cellulose differs from starch in that the glucose units are bonded by *beta* acetal linkages, while the latter has glucose units bonded by *alpha* acetal linkages. The number of glucose monomer units required for insolubility is about 8, above which the glucan units have a higher affinity towards each other than the aqueous solvent. The

degree of polymerization of cellulose molecules depends on its source, for example, cellulose molecules from the primary cell wall typically contain around 8000 glucose units, while those from the secondary cell wall may contain up to 15,000 glucose units<sup>96</sup>.

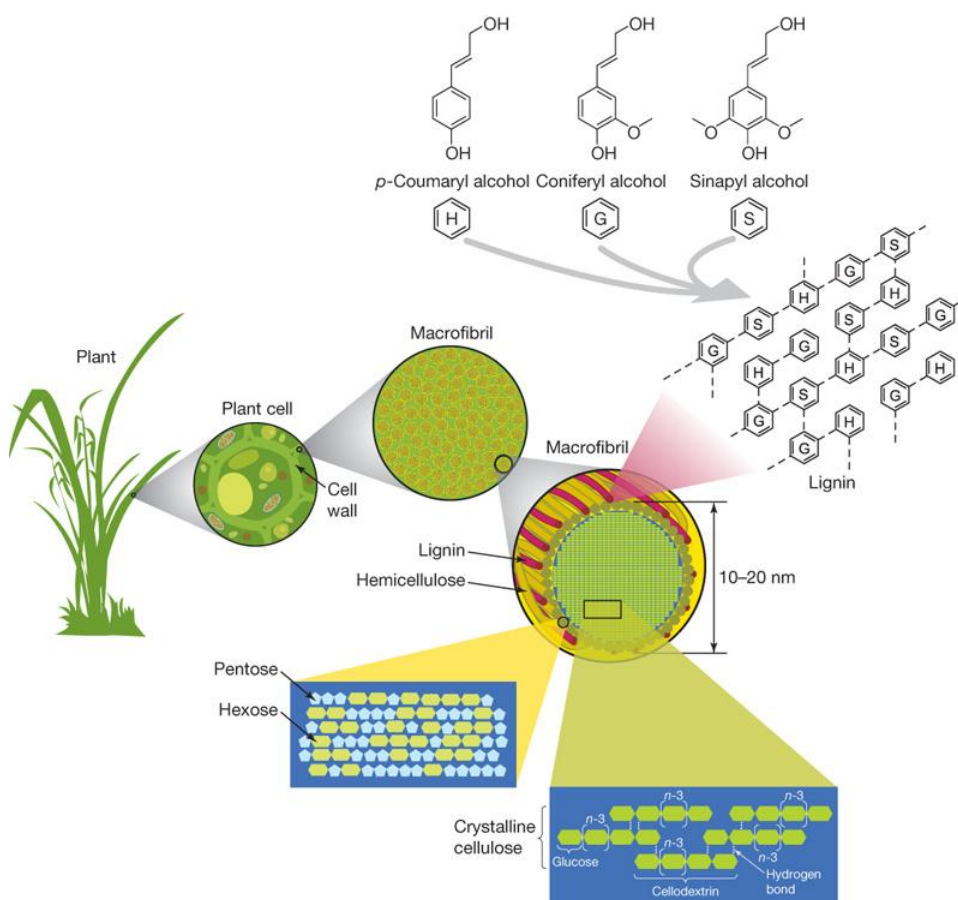


**Fig. 2.8:** The structure of lignocellulose showing the breakdown into its components of cellulose (glucose subunits), hemicellulose (pentoses and hexoses) and lignin (monolignol subunits)<sup>97</sup>.

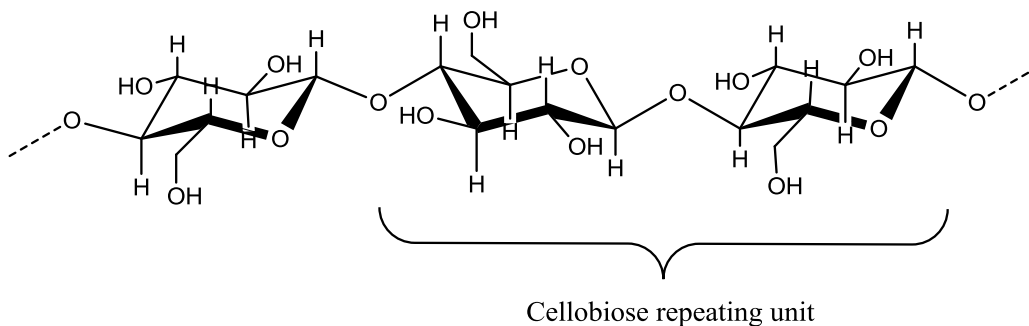


**Fig. 2.9:** The structure of cellulose showing glucose subunits bonded by  $\beta$ -1,4-glycosidic bonds which are broken during hydrolysis (adapted from Keshwani<sup>98</sup>).

The major applications of cellulose as a fiber include the manufacture of pulp (for paper and cardboard) and textiles. It is also used in the production of commercial products such as cellophane, rayon, carboxymethyl cellulose and nitrocellulose<sup>98</sup>.

The structure of cellulose is representative of a highly linear molecule, and the polymeric linkages form the chains in an extended manner, enabling these to fit together snugly over long segments, thus giving rise to powerful associative forces, which contribute to the strength of cellulosic materials. The linearity of cellulose chains arises due to the bond orientation of cellulose molecules. These also have a strong tendency to form intra and intermolecular hydrogen bonds<sup>99</sup>. In plant fibers, cellulose is found in several levels of orientation, with chains arranging over one another, giving rise to regions of crystallinity, which are difficult for penetration using solvents or reagents. When the arrangement is not very compact more amorphous regions are encountered which are more susceptible to hydrolysis reactions. According to the *'fringe micellar model'*, cellulose molecules form completely ordered or crystalline regions, which change into disordered or amorphous regions without any distinct boundary separating the two types of regions<sup>100, 101</sup>.

Even though cellulose forms a highly crystalline structure, individual cellulose fibers are not purely crystalline<sup>102</sup>. Visualization of the indistinct regions of crystallinity and amorphousness of the cellulose fibers can be aided by the notion of a 'lateral order of crystallinity' of cellulose fibers, based on statistics, which ranges from purely crystalline to purely amorphous, with everything else falling within this range<sup>100</sup>. Apart from the amorphous and crystalline regions, cellulose also contains irregularities such as kinks and twists, voids such as micropores, large pits and capillaries. All of these increase the surface area of cellulose as compared to a relatively smooth structure of sugars lacking these irregularities. In addition, of much more importance is the accessibility to water and cellulase enzymes these irregularities provide, the latter accessible by the capillaries and micropores.

Each D- anhydroglucopyranose unit possesses hydroxyl groups at C2, C3 and C6 positions, respectively, enabling it to undergo typical reactions associated with primary (C6) and secondary (C2 and C3) alcohols. The molecular structure of cellulose imparts it with its characteristic properties of hydrophilicity, chirality, degradability, etc<sup>103</sup>.

Individual cellulose molecules undergo self- assembly, aided by associated hemicelluloses, and about 30 of these linear chains pack into structures called protofibrils. Packing of these protofibrils gives rise to microfibrils, which in turn aggregate to give rise to the familiar cellulose fibers<sup>104</sup>. Inter and intramolecular hydrogen bonds stiffen the cellulose molecules and cellulose sheets are held in place by weak intersheet van der Waals forces<sup>105</sup>.

### 2.8.2. Hemicellulose

Hemicellulose is the most abundant polysaccharide in nature<sup>106</sup>, second only to cellulose.

Unlike cellulose however, hemicellulose is not a homopolysaccharide, being composed of various pentose and hexose sugars and uronic acids. Individual sugar monomers found in plant hemicellulose are xylose and arabinose (pentoses) and glucose, galactose and mannose (hexoses).

The main chain of the polyose can contain one sugar (homopolymer) such as xylan, or two or more sugars (heteropolymer) such as glucomannan. The principal pentose sugar is  $\beta$ -D-xylopyranose, which has the 2C and 3C carbons available for O- linked substitution as in xylan, and is used as the simplest representation for hemicellulose. Hemicelluloses are usually bound to cellulose microfibrils by means of hydrogen bonds, which helps stabilize the cell wall matrix and makes it more resistant to enzymatic hydrolysis<sup>68, 107</sup>.

The main types of hemicellulose in softwoods are arabinoglucuronoxylans and galactoglucomannans, while hardwoods are typically composed of glucuronoxylans<sup>108</sup>.

In hardwoods, glucuronoxylans (O-acetyl-4-O-methylglucuronoxylan) represent 15-30% of the dry mass and consist of a linear backbone of  $\beta$ -D-xylopyranosyl units (xylp) linked via  $\beta$ -(1, 4) glycosidic bonds. Some xylose units are acetylated at C2 and C3 and one in ten molecules has a uronic group (4-O-methylglucuronic acid) attached by  $\alpha$ -(1, 4) linkages. The acetyl groups account for 8- 17% of the total xylan, representing 3.5 to 7 acetyl groups per 10 xylose units. The uronic groups are more resistant to acids than the xylp and the acetyl units. The average degree of polymerization of glucuronoxylans is in the range of 100- 200<sup>109</sup>.

Non-woody feedstock (such as agricultural crops) are dominated by arabinoglucuronoxylans (arabino-4-O-methylglucuronoxylan), consisting of a linear  $\beta$ -D-xylopyranosyl backbone containing 4-O-methyl- $\alpha$ -D-glucopyranosyl uronic acid and  $\alpha$ -L-furanosyl linked by  $\alpha$ -(1,2) and  $\alpha$ -(1,3) glycosidic bonds. The typical arabinose: glucuronic acid: xylose ratio is 1:2:8, and might contain low amounts of galacturonic acid and rhamnose, while being less acetylated in comparison to hardwood hemicellulose<sup>108</sup>.

In comparison to cellulose which has crystalline regions, hemicellulose is amorphous and much more susceptible to attack by acids, rendering the hydrolysis a much easier process with dilute acid. Xylans are the most abundant hemicelluloses, these being heteropolysaccharides with homopolymeric backbone chains of 1,4-linked  $\beta$ -D-xylopyranose units. Besides xylose, xylans may also contain arabinose, glucuronic acid, or its 4-O-methyl ether, and acetic, ferulic and p-coumaric acids<sup>106</sup>.

### **2.8.3. Lignin**

Lignin has been described as a polymer of aromatic subunits usually derived from phenylalanine. It functions to provide additional rigidity and compressive strength by forming a matrix around the holocellulose polysaccharides and renders the cell walls hydrophobic and impermeable to water<sup>110</sup>. It has been estimated that 15- 36% of wood dry mass is composed of lignin, making it one of the world's most abundant polymers<sup>111</sup>.

Lignin is a complex polymer formed by the oxidative radical coupling of 4-hydroxycinnamyl alcohols (monolignols), although there are many examples of other phenolics being incorporated into the structure of lignin, besides monolignols<sup>112</sup>. It is

thought that the coupling is formed after the enzymatic dehydrogenation of phenylpropanes, leading to the formation of the lignin polymer<sup>113</sup>.

Almost all plant lignin is composed of three units: guaiacyl (G), syringyl (S) and p-hydroxyphenyl (H) moieties, their relative amounts differing amongst the type of biomass. Softwood lignin is primarily composed of guaiacyl units which originate from the predominant precursor, trans-coniferyl alcohol. Hardwood lignin is best represented by both syringyl and guaiacyl units, originating from trans-sinapyl and trans-coniferyl alcohols, respectively. Lignin from grasses is primarily composed of the third moiety, p-hydroxyphenyl units derived from trans-p-coumaryl alcohol<sup>113</sup>.

In the purest sense, lignin biosynthesis occurs by the radical coupling of the three monolignols (H, G and S) initiated by the action of enzymes called peroxidases, which cleave the covalent bond between the phenolic oxygen and its hydrogen atom. Since the result of these coupling reactions would be the production of a polydisperse polymer unit with no distinct sequence of repeating monolignol units, lignin polymers are classified based on the relative amounts of the monolignols that compose it. In addition, characterization is realized by the distribution of the interunit linkages in the lignin polymer: C-C ( $\beta$ -5,  $\beta$ - $\beta$  biphenyl, 5-5, etc) and ether linkages ( $\beta$ -aryl ether,  $\beta$ -O-4, diphenyl ether,  $\beta$ -O-5, etc)<sup>113</sup>.

The generalization of lignin from various feed types should provide insight into the requirements and challenges associated with delignification of these biomasses. In general, C-C bonds are much more stable than C-O-C ether bonds, and the latter are

hydrolyzed more easily than the former<sup>114</sup>, especially as witnessed during kraft pulping<sup>115</sup>. In syringyl units, the C3 and C5 carbons are bonded to methoxy units, and hence, this unit is limited to forming ester bonds instead of C-C bonds. Syringyl is the predominant unit in hardwood lignin, which makes the delignification of hardwood lignin easier than softwood or herbage lignin, in which the predominant units, guaiacyl and hydroxyphenyl (one and two free carbon atoms) are free to form C-C bonds.

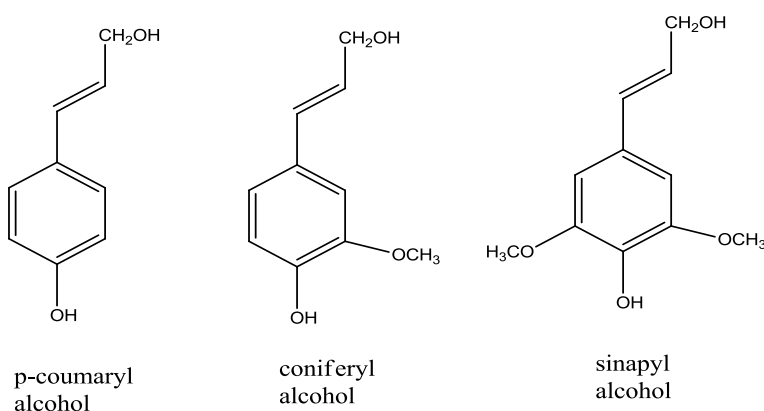


**Fig. 2.10:** Structures of the three monolignols that constitute lignin. p-coumaryl alcohol is the primary monolignol in herbage, while coniferyl and sinapyl are the major constituents of softwood and hardwood lignin, respectively (adapted from Keshwani<sup>98</sup>).

There is, however, some ambiguity with regards to the reactions leading towards lignin polymerization and lignin dimerization. Lignans, which are formed by the dimerization of monolignols (another radical coupling reaction) are rarely encountered during the process of lignin biosynthesis. The relative amounts of lignans are very low compared to the lignin polymer, being less than 1% in softwoods and typically less than 3% in hardwoods and grasses<sup>116</sup>.

Other ways of characterizing lignin structures from various sources is by estimating the relative amounts of the various linkages that make up the polymer, and also by the relative amounts of the functional groups present in lignin<sup>117</sup>. An example of characterization based on the functional groups (methoxyl, phenolic hydroxyl and benzyl alcohol) present in hardwoods and softwoods is shown below. The functional groups are expressed as the number of functional groups that are present in the polymer structure per 100 monomer units.

**Table 2.1:** Representative values of the functional groups present in hardwood and softwood lignins per 100 lignin monomer units (from Helm<sup>117</sup>)

Functional Group	Softwood Lignin	Hardwood Lignin
<i>Methoxyl</i>	95	150
<i>Phenolic Hydroxyl</i>	23	12
<i>Benzyl Alcohol</i>	35	45

#### 2.8.4. Extractives

In addition to the macromolecular compounds (holocellulose and lignin) that constitute woody cell wall, wood also contains minor components that are soluble in water or organic solvents, which are referred to as extractives, and are not part of the cell wall structure. These are generally distributed in the lumen and specific tissues such as the resin canal, without interacting with the cell wall components of wood. These are mostly low molecular weight compounds and typically make up less than 5% of the wood in relation to cellulose, hemicellulose and lignin<sup>118</sup>. The types of extractives can be broadly classified into three categories, depending on the solvent they are extracted using:

- a. Lipid extractives, comprising of aliphatics (fatty acids, fatty acid esters, waxes and suberin (a polyester) and terpenoids (monoterpenes, diterpenes and triterpenes)
- b. Phenolic extractives, comprising of simple phenolics (gallic acid and vanillin), stilbenes, flavonoids (most abundant phenolic extractives) and lignans
- c. Other extractives (alkanes, proteins, monosaccharides and derivatives)

Terpenoids are generally limited to softwood species only, occurring as constituents of essential oils. Terpenes are generally hydrocarbons, while terpenoids are compounds that contain oxygen atoms with functional groups such as alcohols, aldehydes and ketones<sup>119</sup>.

### **2.9. Pretreatment of biomass: Hot-water hydrolysis for hemicellulose extraction**

Among the pretreatment methods currently employed for the production of cellulosic ethanol, hot-water hydrolysis of biomass represents a very attractive form of overcoming the recalcitrance of lignocellulose (by depolymerizing and solubilizing some of the hemicellulose, thereby increasing enzyme accessibility towards cellulose)<sup>120</sup> and for the relatively milder operating conditions that result in the extraction of hemicellulose sugars, while ensuring that the cellulose fraction is not degraded. Depending on the source, hot-water hydrolysis has been categorized as either a form of physical<sup>121</sup> or as physicochemical pretreatment<sup>122</sup>, because no extraneous chemicals are added to the process, while the hydrolysis depends to a large extent on the activity of weak acids generated during the process. In very general terms, hot water hydrolysis is described as the treatment of biomass with water at 150 °C and beyond, at elevated pressures<sup>123</sup>. Some

of the numerous applications of hot water hydrolysis include: removal of hemicelluloses during fractionation or pulping processes, defibration during the production of fiberboard, and as one of the many pretreatment options for the enzymatic hydrolysis of cellulose<sup>124</sup>. Of these, the most attractive application of autohydrolysis seems to be for the pretreatment of lignocellulosic biomass for improving the accessibility of the hydrolysing enzymes towards the cellulose fraction of biomass by solubilizing the lignin and hemicellulose portions<sup>122</sup>. Removal of the hemicellulose results in an increase in the pore volume of the biomass, thereby improving the surface area available for the action of hydrolyzing enzymes<sup>125</sup>. In comparison, the primary objective of pretreatment during chemical pulping is the solubilization and/or selective removal of lignin to ensure that the fiber strength and pulp integrity are maintained<sup>126</sup>.

Some of the advantages of hot-water extraction over other pretreatment technologies are described as the absence in the need for neutralization (as acids are not added to the process), the ability to utilize biomass that has not undergone prior comminution, the improved digestibility of the cellulose fraction for hydrolyzing enzymes, and the extraction of a relatively high yield of hemicellulose sugars<sup>121</sup>. Compared to steam explosion (another form of hydrothermal pretreatment), liquid hot water pretreatment results in the solubilization of lower amounts of hemicellulose and lignin products such as furfural and lignin condensation products which reduces the likelihood of interference with enzymatic hydrolysis for cellulosic ethanol production<sup>127</sup>.

The hydrolysis and extraction of hemicellulose sugars is catalyzed by the cleavage of *-O*-acetyl and uronic acid groups from the hemicellulose matrix, resulting in the formation of

acetic and other organic acids. The combined action of  $H^+$  ions from water and the resulting acids catalyzes the formation and subsequent conversion of oligosaccharides into sugar monomers<sup>121, 124</sup>. The unique properties of water come into play to cause the breakdown of the lignocellulosic matrix. In the sub-critical state, water assumes an extremely low dielectric constant, comparable to that of polar organic solvents such as pyridine or tetrahydrofuran. At the same time, a high value of the ionic product renders it a very effective amphoteric catalyst for the hydrolysis of ether (and ester bonds), breaking down the holocellulosic oligosaccharides. For this reason, hot water offers the advantage of simultaneously being both a solvent and a reactant for lignocellulosic pretreatment<sup>123</sup>, without the express requirement of additional chemicals.

Mok et al<sup>128</sup> showed that all of the hemicellulose present in lignocellulosic biomass could be hydrolyzed (resulting in a weight loss of 40-60%), while 90% of the hemicellulose could be recovered in the monomeric form, based on an analysis of woody and herbaceous feedstock. Significant amounts of the lignin were also solubilized, along with the dissolution of small to moderate amounts of cellulose, though the authors do not report about the quality of the cellulose in the extracted solids.

From the perspective of hemicellulose extraction prior to pulping, the concept of value prior to pulping (VPP) towards the establishment of the integrated forest products biorefinery (IFBR) has been promoted<sup>129, 130</sup>. Tunc and van Heiningen<sup>129</sup> discuss the advantages of incorporating a hemicellulose-extraction scheme into an existing pulping operation, which include experience of the forest products industry which would mean easier adaptation to new extraction and conversion processes, the availability of

wastewater treatment and boiler systems, etc. A prime advantage with integration into a 'state of the art' Kraft pulp mill, it is reported, will be the utilization of a net energy surplus (of 30%) towards the production of energy-intensive biofuels, so as to increase the overall profitability of the facility. Since the hemicellulose sugars are currently underutilized in Kraft pulping for producing energy recovery of low heating from combustion, it is suggested that a more economical use for these would be towards the conversion to value-added products, following extraction. Hot water extraction of biomass under elevated pressures has been shown to be a viable idea for the development of a biorefinery model incorporated both into a pulp mill, and cellulosic ethanol plant owing to its simplicity, zero dependence on external reagents or solvents (making it an environmentally-friendly alternative to other pretreatment technologies), the mild conditions of extraction employed (translates into better economics) and the significant extraction of hemicellulose sugars while ensuring that the degradation of cellulose is minimal. Along these lines, it is easy to envision a process that fractionates biomass into a solid stream which might be the natural feedstock in a pulp mill or a cellulosic ethanol process, and a hemicellulose-rich hydrolysate which can be subjected for conversion into pentosan-derived, value-added chemicals such as furfural.

## **Chapter 3- Materials, Chemicals, Experimental and Analytical Techniques**

### **3.1. Introduction**

This chapter discusses the treatment of materials (biomass feedstock, yeast, etc.) and the sourcing of chemicals used in this research. A detailed explanation of various experimental techniques and analytical methods adopted throughout the course of the research is also provided. Sections in subsequent chapters will refer back to the topics outlined in the present chapter when dealing with specific methods employed. Particular emphasis is placed on a detailed explanation of instruments and equipment used for sample preparation, conducting experiments and analysis of samples obtained. The order of methods discussed in this chapter follows the same order in which they are talked about in subsequent chapters. The dehydration of aqueous xylose solutions, untreated biomass and biomass hydrolysates using batch reactive distillation (BRD) is not discussed in this chapter, as it was felt that since the process was devised drawing inspiration from the concept of batch reactive distillation, it would be better introduced and discussed separately in Chapters 4 and 5.

### **3.2. Materials and Chemicals**

#### **3.2.1. Biomass feedstock: Harvest and treatment**

Hybrid poplar (*Populus maximowiczii x nigra*), representative of a short- rotation woody bioenergy crop, was harvested from northern Wisconsin after ten years of age and seasoned for three months before use. The wood was debarked by hand, chipped, screened (2-8 mm) and air- dried. As an agricultural residue presenting value for conversion to bioenergy, corn stover (*Zea mays*) was collected from Lodi, Wisconsin,

aged for three months before being chopped and screened to one inch samples, and air-dried. To account for high- yield bioenergy crops, switchgrass (*Panicum virgatum*) and miscanthus (*Miscanthus giganteus*) were sourced from the University of Wisconsin agricultural research stations (Arlington and West Madison, respectively). The two samples were harvested after senescence, air-dried, chopped and screened to one-inch plus size.

Complete characterization of all four biomass feedstock was performed in a previous study<sup>131</sup>, and these results are shown in table 3.1.

**Table 3.1:** Composition of the biomass feedstock used in this study as estimated by Wipperfurth<sup>131</sup> (standard solutions were not hydrolyzed during analysis; acetic and levulinic acids, and fractions of furfural and HMF were measured as artefacts from the analytical method)

Component (wt%)	Poplar	Miscanthus	Switchgrass	Corn Stover
<i>Arabinose</i>	0.29	2.20	3.06	3.30
<i>Galactose</i>	0.46	0.62	1.26	1.40
<i>Glucose</i>	40.74	38.19	40.54	38.62
<i>Xylose</i>	13.30	18.89	19.71	21.23
<i>Mannose</i>	3.01	0.47	0.88	0.69
<i>Total sugar</i>	57.80	60.37	65.45	65.24
<i>Acetic Acid</i>	3.71	3.37	2.39	2.60
<i>Levulinic Acid</i>	0.38	0.19	0.19	0.25
<i>HMF</i>	0.47	0.73	0.46	0.40
<i>Furfural</i>	1.14	1.97	1.58	1.76
<i>Total Furans/Acids</i>	5.70	6.26	4.62	5.01
<i>Total Sugar</i>	57.80	60.37	65.45	65.24
<i>Total Furans/Acids</i>	5.70	6.26	4.62	5.01
<i>Acid insol. Lignin</i>	22.19	24.02	18.95	17.28
<i>Acid sol lignin</i>	3.63	2.15	2.76	3.06
<i>Ash</i>	0.93	3.69	5.95	6.89
<i>Total</i>	90.25	96.73	97.73	97.48

Except the poplar samples, the remaining feedstock used in this study were different from

those characterized by Wipperfurth<sup>131</sup>, but the storage and handling was similar in both studies. The sugar content data obtained from this source was used to estimate furfural yields obtained from the dehydration of biomass (poplar) and biomass hydrolysates.

### **3.2.2. Chemicals and Reagents**

The experiments conducted in the model compound dehydration section (chapter 4) all used xylose (Acros Organics, New Jersey, USA) in different amounts, with some of the batch reactions conducted in the presence of sodium chloride (Fisher Scientific, New Jersey, USA). In chapters 4 and 5, furfural (TCI, Tokyo, Japan) was used to generate the standard curves both for the UV spectrophotometric and HPL chromatography analyses. Experiments conducted in the section on fermentation of samples dosed with furfural utilized Red Star® Active Dry Yeast (Lesaffre Yeast Corp, Milwaukee, WI, USA) as the organism. Preparation of the YPD (yeast extract, peptone and dextrose/glucose) growth media utilized glucose (Acros Organics, New Jersey, USA), yeast extract and bacto-peptone (latter two chemicals from Fisher Scientific, Fair Lawn, New Jersey, USA). For analysis, furfuryl alcohol and furoic acid (both from Acros Organics, New Jersey, USA) were used in making standards and estimating yields.

## **3.3. Experimental Techniques**

### **3.3.1. Dehydration of aqueous xylose solutions using the batch process**

For the batch dehydration reactions transforming xylose (aqueous solutions, 17.6% by mass), the experiments were carried out in a 600-ml Parr 4560 series mini benchtop pressurized reactor cast in Hastelloy C-276, operated using a Model 4848 reaction controller (to control the temperature and the stirring speed). Figure 3.1 shows a simplified schematic of the reactor setup, control and sampling, while figure 3.2 depicts a

closer view of the reactor itself, with the sampling port assembly in closer detail. The temperature was monitored using a thermocouple held in place in a Hastelloy well. The reactants (xylose, water and sulfuric acid) were mixed within a glass liner placed inside the reactor vessel to minimize corrosion to the vessel, especially when using high concentrations of acid and salt.

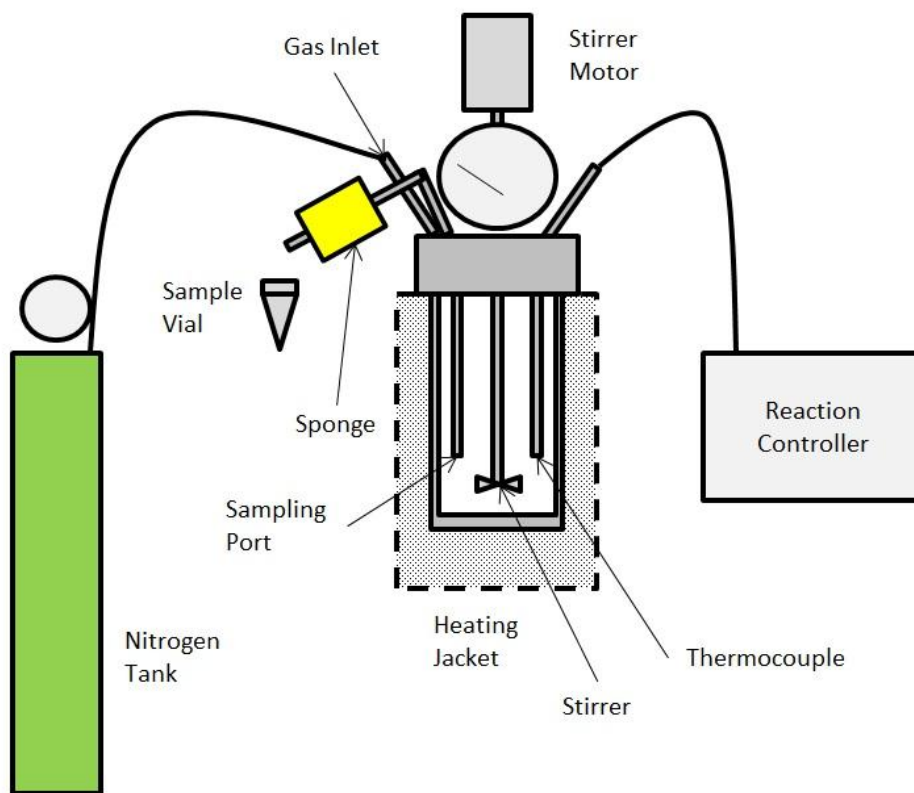


**Fig. 3.1:** A simplified (not-to-scale) schematic of the setup, control and sampling operation of the batch reactor for the dehydration of xylose solutions to produce furfural.

Sampling was carried using a sampling port inside the vessel fitted with a screen to filter out insoluble humin particles. These samples were used for conducting xylose and furfural analysis based on reaction time, observed using a stopwatch. The sampling tube

was purged after sampling using nitrogen gas supplied from a gas inlet, and also to make up for the small amount of pressure lost when the sampling valve was opened to let out the sample. This way, it was ensured that uncontaminated, time-based liquid samples were obtained each time.

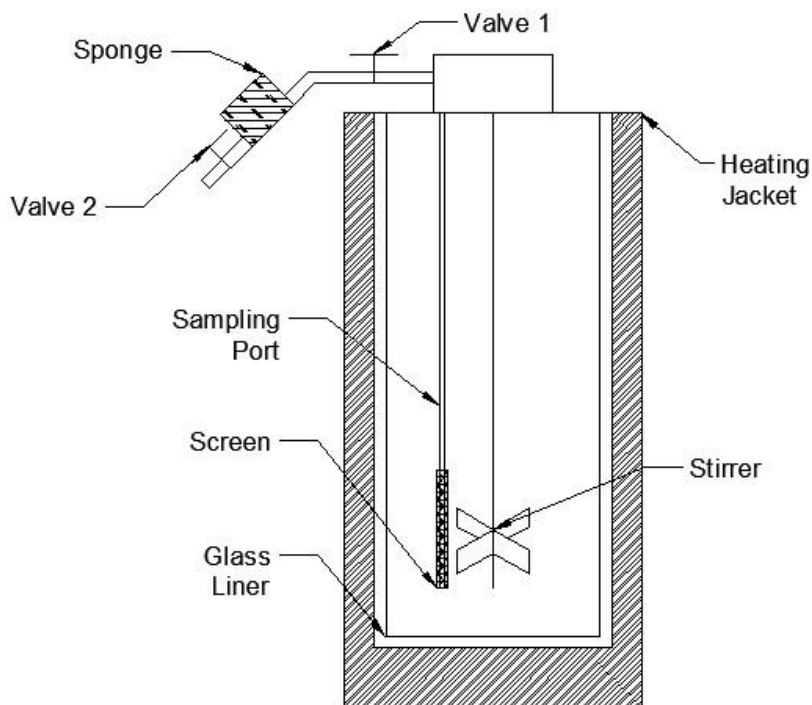


**Fig. 3.2:** Simplified schematic of the batch reactor (not to scale) showing the sampling tube and the way sample was withdrawn from the sampling port, collected using valves 1 and 2, and cooled using the sponge before being saved for analysis. The samples obtained were stored in vials for analysis of xylose (after neutralization) and furfural (following dilution).

Each time-based sample was held in the small sampling tube outside the reactor for 1-2 minutes to allow it to cool down using an ice water-soaked sponge wrapped around the tube. With reference to figure 3.2, valve 1 was opened at time  $t$  to draw out the sample

while valve 2 remained shut and the cold, wet sponge was wrapped around the sampling tube. Following the passage of 1-2 minutes, valve 2 was opened to collect the sample in a vial. The tube was then purged with N<sub>2</sub> gas to adjust for any lost pressure, and also clean out the sampling tube. The cooling ensured that the sample was not boiling before it was collected in small 1.5-ml sampling vials for analysis later on.

### **3.3.2. Determination of biomass moisture content**

The moisture content of biomass samples (both untreated and water-extracted) is needed in order to account for the amount of water already present in the biomass samples before they are subjected to any pre- or post-treatment. In this case, it was important to know the initial amount of water present in the biomass samples that contributed to their weight, so that the liquor-to-wood ratio could be adjusted accordingly when performing the hot-water hydrolysis. Use of this quantity is also made during estimation of the heating value of pre- and post-extracted biomass samples and for conversion between lower and higher heating values (LHV and HHV). The procedure described here has been devised from the ASTM (American Society for Testing and Materials) Standard E1756-08<sup>132</sup> and the TAPPI (Technical Association of the Pulp and Paper Industries) Standard T 412 om-11<sup>133</sup> (in particular for solids pretreated using liquid hot water).

Biomass stored in plastic bags was taken from three different (top, middle and bottom) portions of the bag to get samples that were representative of the entire bag. 1 to 2 g of these samples were placed in pre-weighed tin dishes and put in the oven at 105 °C overnight. The samples were weighed and put back in the oven for another hour, following which the weights were recorded again. If the difference in both measurements

exceeded 3%, the samples were dried for another hour till the difference was negligible.

The moisture content of all biomass samples was estimated in triplicates according to the convention stated above.

The moisture content of biomass was estimated using equation 3.1 as under:

$$MC(\%) = 100 \left[ 1 - \frac{\{(Final\ Mass)_{D+S} - (Init\ Mass)_D\}}{\{(Init\ Mass)_{D+S} - (Init\ Mass)_D\}} \right] \quad (\text{eqn 3.1})$$

Where,

*MC* refers to the moisture content (in %)

*Init* and *Final Mass* denote the mass of the samples at the beginning and the end of the overnight drying period (in g)

*D* and *S* denote the dish and the sample, respectively; (*D+S*) indicates mass of the sample as well as that of the aluminum dish (in g)

Moisture contents for all four biomass feedstock used in this study were estimated in triplicates and are tabulated in table 3.2

**Table 3.2:** Moisture contents of the four untreated biomass feedstock used in this study with standard error (for triplicate measurements)

Feedstock	Moisture Content (%)
Hybrid Poplar	17.57 ± 0.5
Miscanthus	5.31 ± 0.07
Switchgrass	5.07 ± 0.07
Corn Stover	6.71 ± 0.14

### 3.3.3. Hot-water extraction/ hydrolysis of biomass

Biomass samples were hydrolyzed using water to separate a fraction of the pentosan content into the liquid phase, with the goal of dehydrating it to produce furfural. The reaction conditions were optimized to maximize the pentosan extracted into the liquid phase, while minimizing the degradation of cellulose that would be a likely result of the hydrolysis reaction.

All four biomass samples were air-dried and chopped to 1-inch size prior to the hydrolysis. The hot-water extraction was performed using a 23-liter, steam-jacketed rotating digester at the Forest Products Laboratory, Madison, WI. A schematic of the digester is provided in figure 3.3, which shows a simplified profile view of the digester, and the valves used to control it. Figure 3.4 shows a picture of the digester during operation.

The liquor-to-wood ratio (L/W) based on the dry weight of the solids used for all four feedstock was 6:1, reacted for 1 hour at 170 °C. These conditions were identified in an earlier work as being suitable for maximum removal of hemicellulose while preventing the degradation of cellulose<sup>131</sup>.

Prior to operation, the digester was pre-heated with water to around 170 °C so that the metal is kept hotter, which would reduce the ramp-up time once the biomass was put into the digester. Dry biomass samples were weighed into the basket (0.75 to 1.5 kg, based on the bulkiness of the samples) and put into the digester.

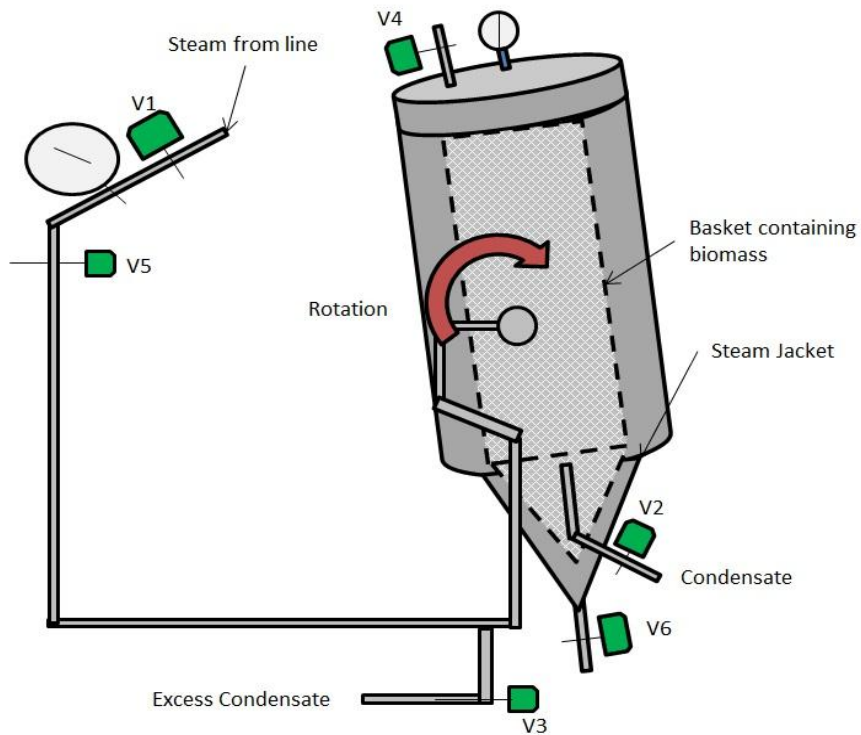


**Fig. 3.3:** Simplified schematic of the rotating digester at the Forest Products Laboratory, used for performing the hot-water hydrolysis of feedstock samples showing the various valves used to control and regulate the steam pressure (and hence, the temperature).



**Fig. 3.4:** Picture of the rotating digester in operation at the Forest Products Laboratory.

All of the valves are kept shut at this point. Water, accounting for a L/W ratio of 6:1, was poured into the digester vessel and the main steam valve, V1, was opened. Valves V5 and V3 are the main controls so as to ensure that the temperature is not overshot; the latter valve is used to release excess condensate and also to reduce steam loss from the steam inlet into the digester (at the axis of rotation). Valve V2 is also opened to let the condensate escape as fresh steam is fed into the jacket.

Once the digester temperature reaches 170 °C, the stopwatch is started and the reaction is carried out for 1 hour. The temperature can be read both from the temperature gauge on the digester lid, as well as confirmed from the pressure gauge and referring to steam tables. After the reaction is finished, valve V4 is slowly and progressively opened to let out the steam and reduce the pressure in the vessel. Once the pressure has fallen to zero, the sampling valve, V6, is opened to collect the sample from the bottom of the vessel.

The solid portion of the feedstock, retained in the basket, was removed, washed and squeezed in thick cotton bags to recover any additional sugars that might remain attached to the surface of the solids. The amount of water used for performing the washing amounted to the original 6:1 L/W ratio, based on the dry mass of the original biomass samples.

The hot liquor and the washed liquor were allowed to cool and frozen in 1-gal Nalgene HDPE containers, while the washed solids were cooled down and frozen in Ziploc bags.

#### **3.3.4. Determination of higher heating value (HHV) of biomass and extracted solids using oxygen bomb calorimetry**

The energy content of biomass samples and water-extracted solids was determined using a Parr 6772 oxygen bomb calorimeter. The oxygen bomb calorimeter is a device used for estimating the gross heating value of combustible solid or liquid samples. It works on the principle of measuring temperature change in a bucket of water induced by the complete combustion of a sample inside a bomb. Ignition is accomplished by passing current across a nickel alloy fuse which is in contact with the sample. The biomass samples used in this procedure were dried, milled and pelletized using a Parr 2811 Pellet Press.

Milled biomass samples are pelletized by filling the die with the sample and compressing it using the plunger. The weight of the pellet was then recorded (and entered into the calorimeter under 'Sample Preweigh'), and it was placed in the sample cup, held in the metal loop. Approximately 10 cm of the nickel fuse wire was taken and its ends were inserted into the eyes of the electrodes in the lid of the bomb, and the wire was just touching the surface of the pellet. The lid on the bomb was then tightened and the entire bomb pressurized to 30-35 atm with oxygen. The bomb was placed in the water-containing bucket and the 'Start' button was pressed to ignite the fuse and combust the sample. Upon completion of the test, the printer connected to the calorimeter prints out the change in temperature and the gross heating value (HHV) of the biomass sample.

### **3.3.5. Fermentation experiments using Red Star active dry yeast**

The fermentation experiments carried out to reduce furfural into furfuryl alcohol by microbial activity using Red Star active dry yeast were all performed in semi-sterile conditions. All of the apparatus was sterilized in an autoclave at 121 °C for 15-20 minutes (in addition to heating and cooling phases), and transfers from the media bottles

to the fermentation flasks were performed in the presence of flame, once the area had been sprayed with ethanol for disinfection. The absence of ultraviolet irradiation could not guarantee complete sterility, even though precautions were taken to avoid contamination.

The growth media used for all the experiments was YPD (20 g/l glucose, 20 g/l peptone and 10 g/l yeast extract). Aqueous glucose solutions (dosed with furfural samples apart from controls) were sterilized separately from 5X YP media (to prevent caramelization<sup>134</sup>) in glass bottles, and these were later mixed into 125-ml sterile flasks along with the yeast. All of the flasks were equipped with a sampling apparatus as shown in figure 3.5.

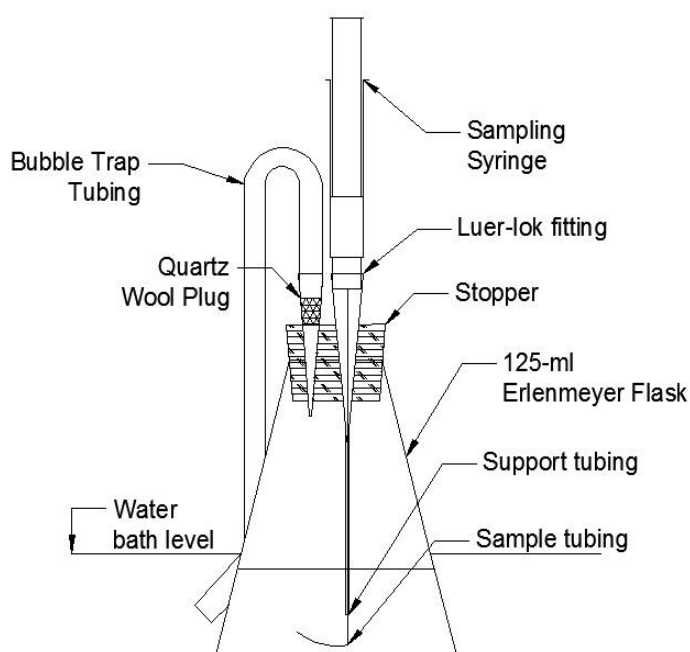


**Fig. 3.5:** Setup used for conducting the furfural reduction experiments using active dry yeast, showing the apparatus used for sampling with time.

All the flasks were maintained at anaerobic conditions at 30 °C in a water bath without stirring. A stopper, drilled with two holes for holding pipette tips as shown, was used to keep the conditions anaerobic. One of the tips was plugged with quartz wool and attached with rubber tubing that dipped into the water bath (attached to the flask with tape) to act as a bubble trap. The second tip had a 1/32" luer-lok ended plastic tubing going through it, affixed at the top to hold the latter in place. The luer-lok fitting was held in place snugly by the wider mouth of the tip. The other end of the sample tubing dipped into the level of the media in the flask. Since the sampling tubing was not stiff, it was guided through a support tubing (PVC, 1/8") to keep it upright instead of curling up and away from the contents of the flask. 1-ml samples were withdrawn from the flasks at specific time intervals using sterilized syringes. The barrel of the syringe twisted into the luer-lok fitting that stuck out at the top of the sampling tip, and then the plunger was pulled to collect samples. The sampling tube was purged each time before sampling by pushing in ~0.5 cc air to clear the tubing. All of the flasks were gently swirled to mix the contents before sampling.

### **3.4. Analytical Techniques**

Several sections of the current study necessitated the identification and estimation of chemical compounds generated during the reaction. Sugars and inhibitors (organic acids and furans) were measured for characterization of the biomass hydrolysates. Xylose and furfural were monitored and measured for the batch and the BRD dehydration reactions using the model compound. For the BRD dehydration reactions using biomass hydrolysates, the pentose sugars arabinose and xylose were measured along with furfural

that was produced. Glucose, furfural, furfuryl alcohol and furoic acid were measured for experiments conducted using yeast. This section presents the techniques employed for all these measurements.

#### **3.4.1. Measurement of furfural**

Furfural was measured using two different techniques: UV/Vis spectrophotometry, and HPL chromatography. The former technique did not employ any prior separation, and therefore, was susceptible to errors caused by other UV-absorbing compounds. This limited its use towards monitoring the reaction and the production of furfural with time. For calculation of yields, HPL chromatography was employed, except in the case of the experiments using the model compound: pure xylose. Since the product of dehydration in this case does not involve any other UV-absorbing products apart from furfural, it was felt that this method can be relied upon for accurate results, while saving time and resources.

##### ***3.4.1.1. Using UV Spectrophotometry***

Furfural was analyzed using UV/Vis analysis performed with a Shimadzu UVmini 1240 spectrophotometer run at 276 nm (absorption maximum for furfural). Figure 3.6 shows a standard curve generated for furfural (at the time these experiments were performed) at different concentrations, which enabled conversion of absorbance into units of concentration (M). Application of the Beer-Lambert law yielded a furfural molar absorptivity value of  $1.23 \times 10^4 \text{ M}^{-1} \text{ cm}^{-1}$ . This agrees well with the findings of Martinez et al<sup>135</sup>, who observed that furans (furfural and HMF) accounted for the major fraction of the peak at 278 nm in biomass dilute acid hydrolysates.

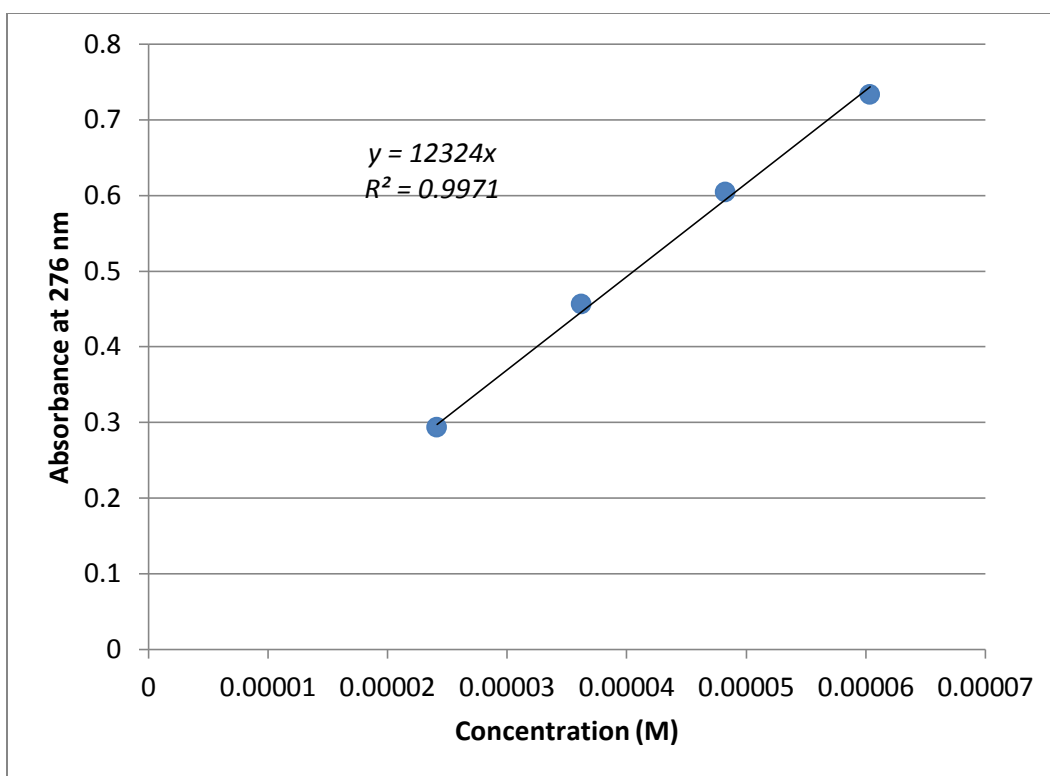


**Fig. 3.6:** Standard curve generated for furfural using UV absorbance spectroscopy

Samples collected during and after the batch dehydration reactions were centrifuged for ten minutes at 10,000 rpm, diluted and analyzed. The calibration curve generated using pure furfural was used for estimating furfural concentrations and for calculating the final yield based on the initial amount of xylose in the reaction.

For the BRD dehydration samples using the model compound, samples taken based on the mass of the vapor fraction collected were similarly analyzed to estimate the concentration of the furfural produced.

Figure 3.7 shows a comparison of absorption spectra for pure furfural at 0.0362 mM and a typical reaction product obtained from one of the optimized center point runs using pure xylose (BRD product).

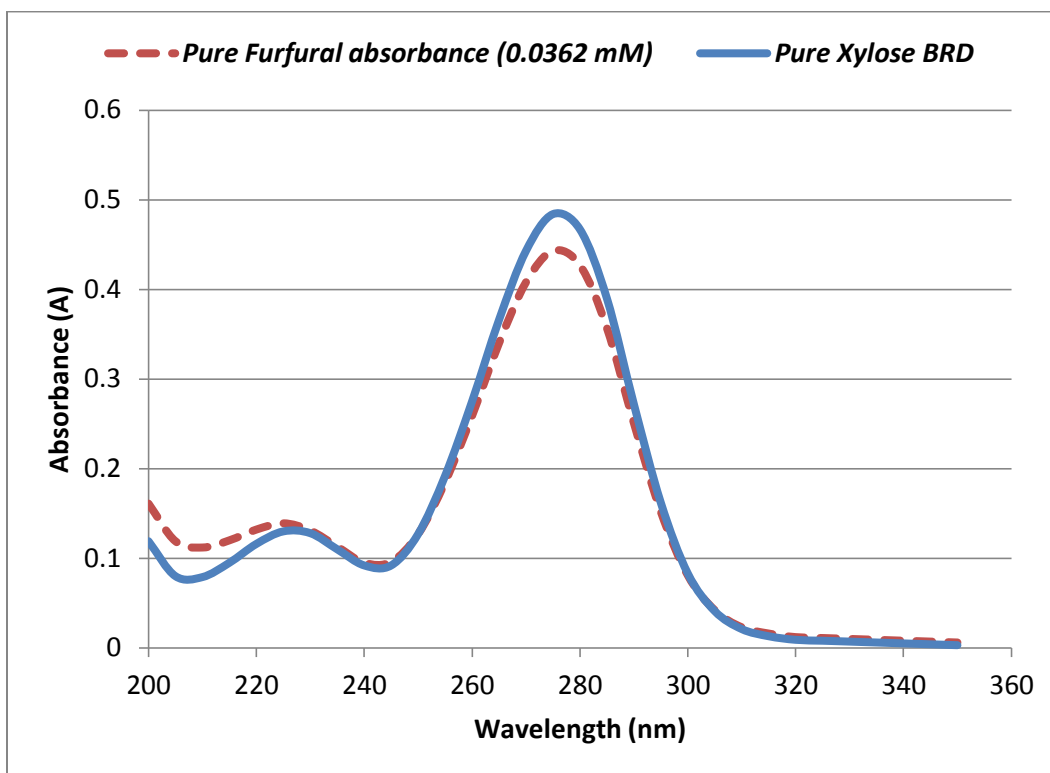


**Fig. 3.7:** Comparison of the ultraviolet absorption spectra of pure furfural and the BRD reaction product showing the furfural absorption maximum at 276 nm.

Appreciable agreement between the absorption spectra of pure furfural and the BRD reaction product, and also the agreement with existing literature<sup>135, 136</sup> has prompted the use of UV spectroscopy to determine and measure furfural concentration, and estimate the yield based on this value (for model compound BRD dehydration).

#### **3.4.1.2. Using HPL Chromatography**

Furfural concentration was estimated using HPL chromatography consisting of an acid-based column and a UV absorbance detector. The apparatus consisted of a Dionex ICS-3000 system equipped with a Supelcogel C- 610H column, maintained at 50°C, and detected using UV absorbance at 210 nm. Phosphoric acid at a rate of 0.7 ml/ min (isocratic flow) was used as the eluent. This technique, being more time and resource-consuming, was used only for calculation of the final furfural yield values from the BRD dehydration of biomass hydrolysates. This method was capable of measuring other potential inhibitors of microorganisms during fermentation, such as formic acid, acetic acid, levulinic acid, furoic acid, and hydroxymethylfurfural. A representative chromatogram of a standard composed of these chemicals is shown in figure 3.8. These standards were run at five different concentrations to generate a standard curve for the compound(s) of interest and estimate their concentration in samples.

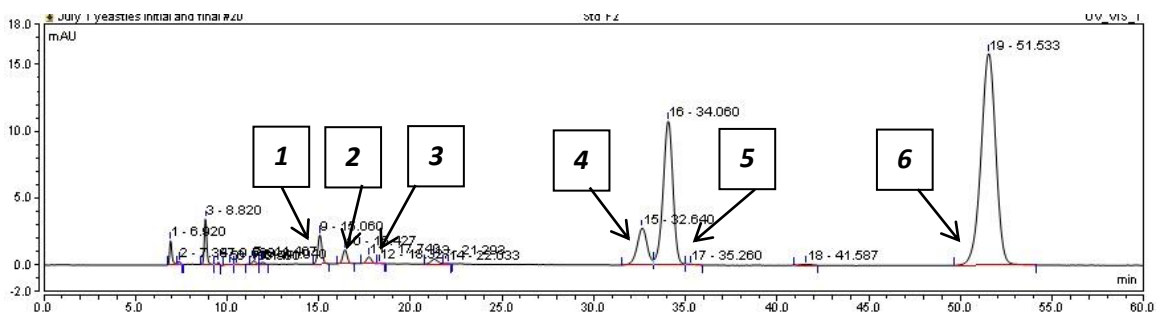


**Fig. 3.8:** Chromatogram showing the composition of the standards and their order of elution (1 through 6): formic acid (15 min), acetic acid (16.4 min), levulinic acid (18 min), furoic acid (32.6 min), HMF (34 min) and furfural (51.5 min).

### 3.4.2. Measurement of sugars

The five common wood sugars (arabinose, galactose, glucose, xylose and mannose) present in the biomass hydrolysates, model compound experiments and fermentation

experiments using dry yeast were measured using ion-exchange chromatography. The apparatus comprised of a Dionex ICS-3000 system integrated amperometric detector and CarboPac PA20 guard and analytical columns maintained at 30 °C. Detection was performed by pulsed amperometry (PAD) using a disposable gold electrode. Eluent was provided at the rate of 0.35 ml/min according to the following gradient: 0.1 to 20.0 min: 100% water, 20.5 to 35.0 min: 75% 0.1 M NaOH and 35.0 to 45.0 min: 100% water. A representative chromatogram of a standard composed of these sugars is shown in figure 3.9. These standards were run at five different concentrations to generate a standard curve for the compound(s) of interest and estimate their concentration in samples.

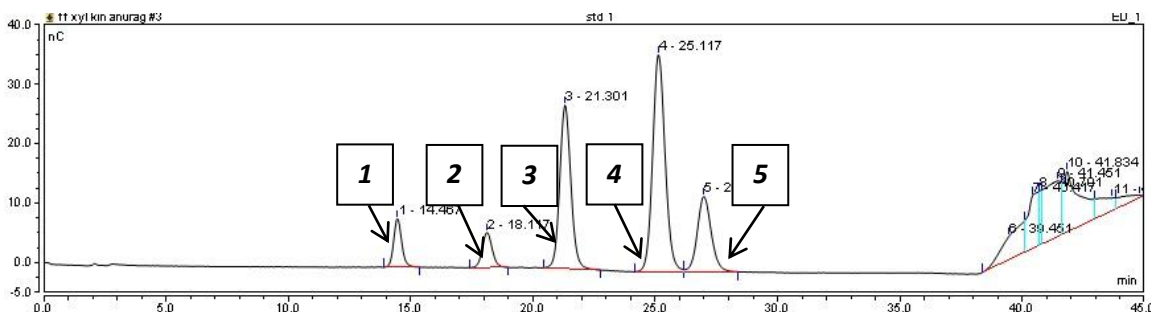


**Fig. 3.9:** Chromatogram showing the composition of the sugar standard and their order of elution (1 through 5): arabinose (14.5 min), galactose (18.1 min), glucose (21.3 min), xylose (25.1 min) and mannose (26.9 min).

### 3.4.3. Measurement of cell growth and estimation of furfural and furfuryl alcohol concentrations

Yeast cell growth was measured with time by determining the optical density (OD) at 600 nm using UV absorbance (with distilled water used as the blank). Measurement of the optical density provides with an indication of the turbidity of the solution, which in the absence of any other particulates, points to the ultraviolet light absorbed by yeast cells. The disadvantage of the OD method for monitoring growth is that it does not discriminate

between dead and viable cells. A constant OD measurement over time generally indicates a lack of growth. The optical density is calculated by diluting the liquid broth and measuring the absorbance at 600 nm using equation 3.3 as under:

$$OD = (Abs_{600\text{ nm}}) \times (DF) \quad (\text{Eqn. 3.2})$$

Where,  $Abs_{600\text{ nm}}$  is the UV absorbance at 600 nm

$DF$  is the dilution factor used

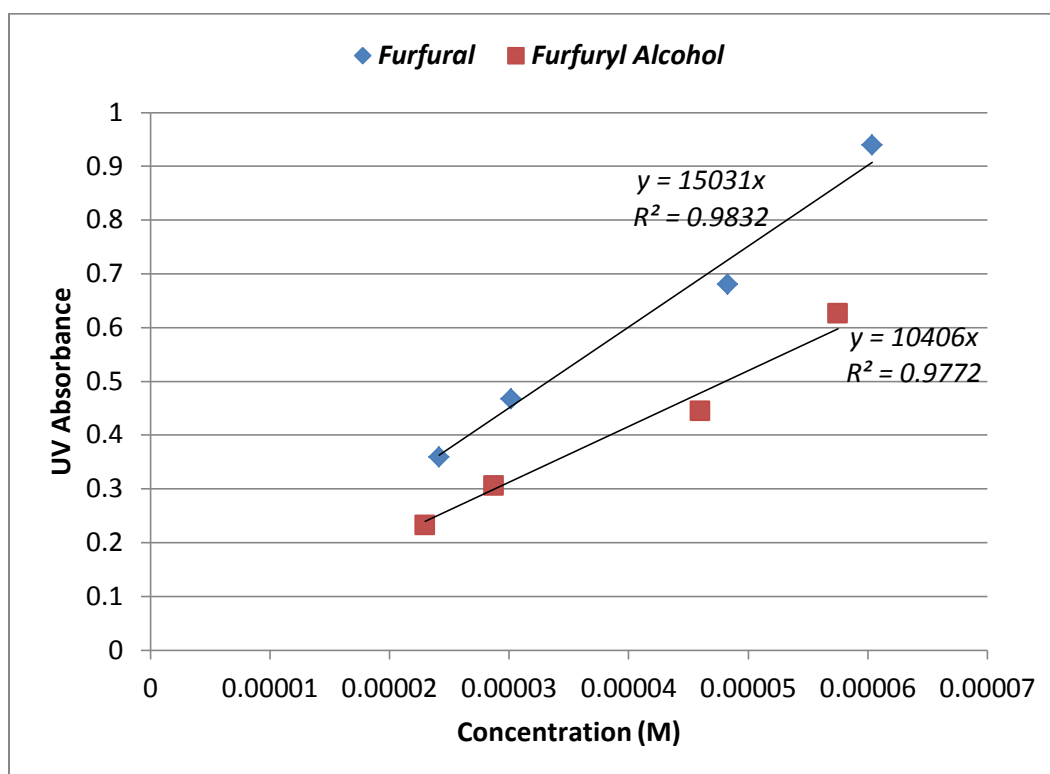


**Fig. 3.10:** Calibration curve generated for a mixture of furfural and furfuryl alcohol at different concentrations using ultraviolet absorption spectroscopy.

Estimation of the concentrations of furfural and furfuryl alcohol was also made using UV absorbance. By running pure samples of both compounds, it was found that furfural and furfuryl alcohol had maximum absorbance at 276 and 215 nm, respectively. Calibration curves were generated using a mixture of both compounds at different concentrations (figure 3.10).

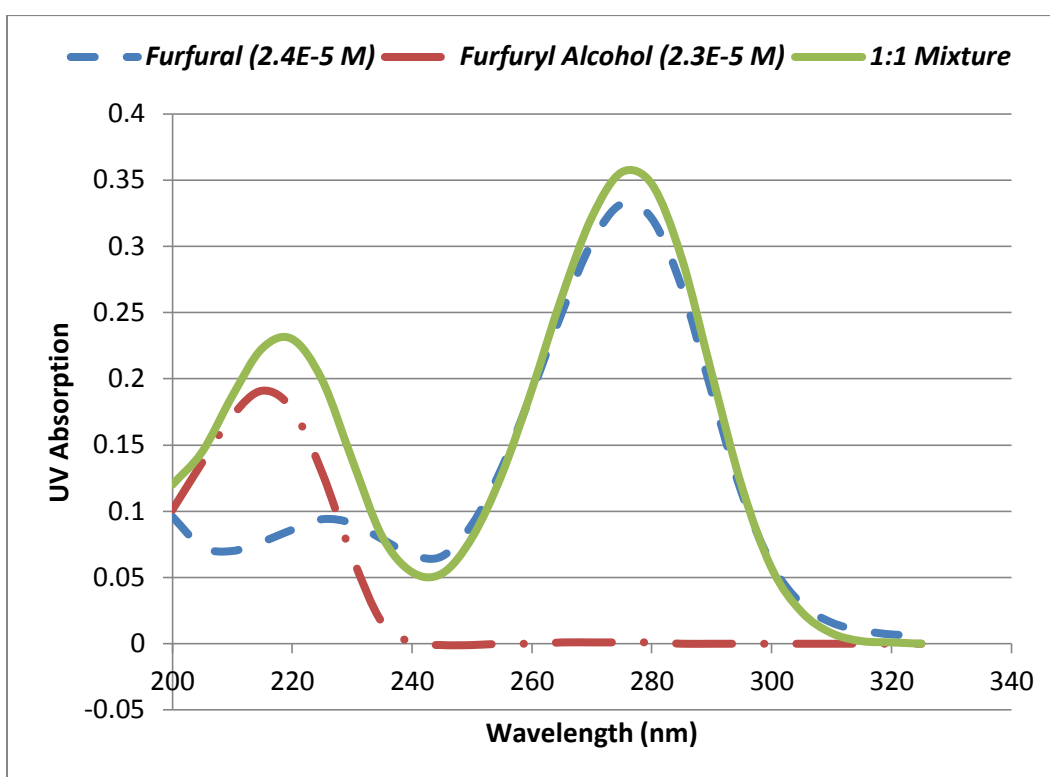


**Fig. 3.11:** Absorption spectra generated for furfural, furfuryl alcohol, and a mixture of both chemicals ( $[\text{Fur}] = 2.4\text{E-}5 \text{ M}$ ,  $[\text{FA}] = 2.3\text{E-}5 \text{ M}$ ).

To correct for this anomaly, standard curves were generated for the absorbance of furfural at 276 nm and 215 nm, and the ratio between the absorbance values at these wavelengths was plotted against furfural concentration (figure 3.12).

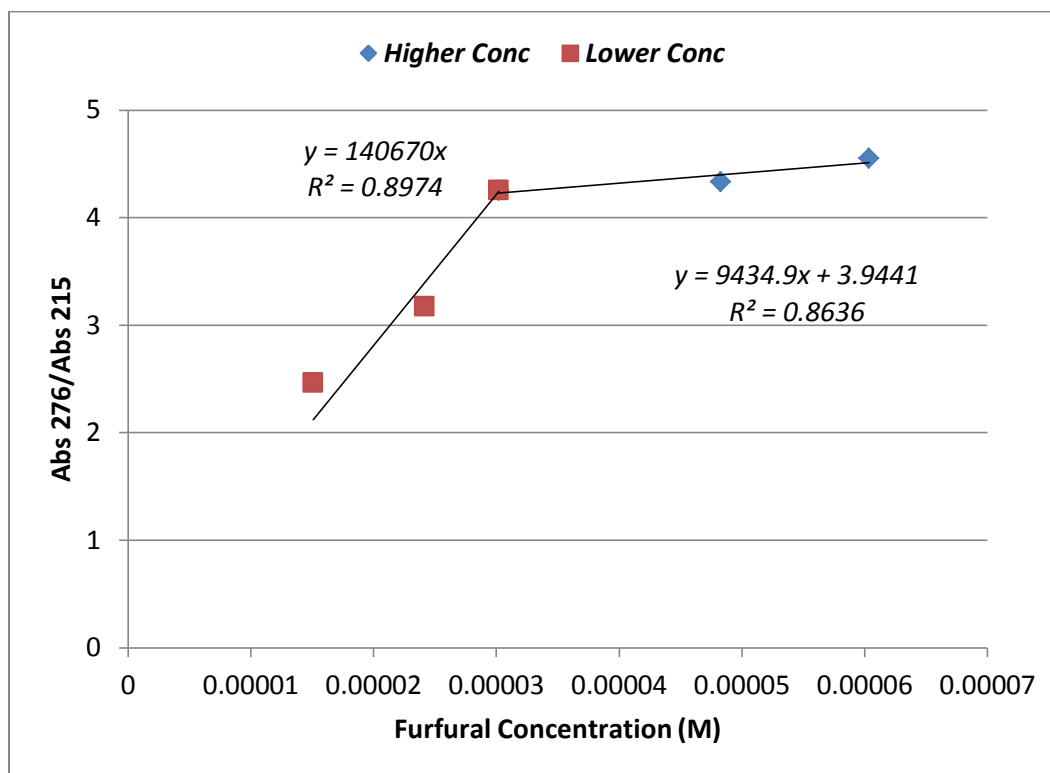


**Fig. 3.12:** Plot of the ratio of absorbance values for furfural at 276 and 215 nm, with two linear relationships assumed depending on the furfural concentration range.

Based on the value of furfural estimated from the UV absorbance at 276 nm, the ratio of the absorbance at 276 and 215 nm can be found from figure 3.13 to estimate the height of the smaller furfural peak which interferes with measurement of the furfuryl alcohol peak at 215 nm. This value can then be subtracted from the absorbance at 215 nm to provide the absorbance of furfuryl alcohol at this wavelength.

## Chapter 4- Model Compound Dehydration

### 4.1. Introduction

Furfural serves as the precursor of many furan-based compounds such as furfuryl alcohol, tetrahydrofuran (THF), furan, furoic acid, 2-methylfuran (2-MF), etc. It has also been classified as one of the upcoming platform chemicals, deserving of attention and research towards the goal of a furfural-based biorefinery. A natural product of pentose dehydration, furfural yields obtained using conventional methods are typically low (~50%). The application of furfural as the basis for the design of an integrated biorefinery demands research into the improvement of these marginal yields in ways that are feasible and scalable.

Research performed towards the improvement of furfural yields has taken several paths towards achieving this end. Marcotullio et al<sup>12</sup> have sought to influence the formation of the 1,2-enediol structure, which equilibrates between the aldopentose form and furfural, and is seen as crucial towards the formation of the latter (figure 2.7). This was done by the addition of metal halides (sodium chloride), which not only caused a slight elevation in boiling point (though this effect is minute in comparison to the high pressures employed in the reactions), but also suggested an increase in the rate of formation of the enediol structure as evidenced by the reaction kinetics. A maximum furfural yield of 81.3% was reported in the presence of 5% NaCl (by mass) using 0.05 M HCl, with good selectivity.

Furfural forms a minimum-boiling azeotrope with water, and this behavior has been documented by Curtis and Hatt<sup>137</sup> (figure 4.1). At atmospheric pressure, the azeotrope,

containing 35% furfural (by mass), boils at 97.9 °C. This behavior propagates at higher pressures as well, and exploitation of this property to distil and condense furfural as it was being produced seems to offer the prospect of a ‘single-pot’ reaction and separation of furfural from the aqueous phase. In this context, the relatively new technology of batch reactive distillation (abbreviated as BRD henceforth) was emulated to perform the dehydration reaction and recover the furfural produced.

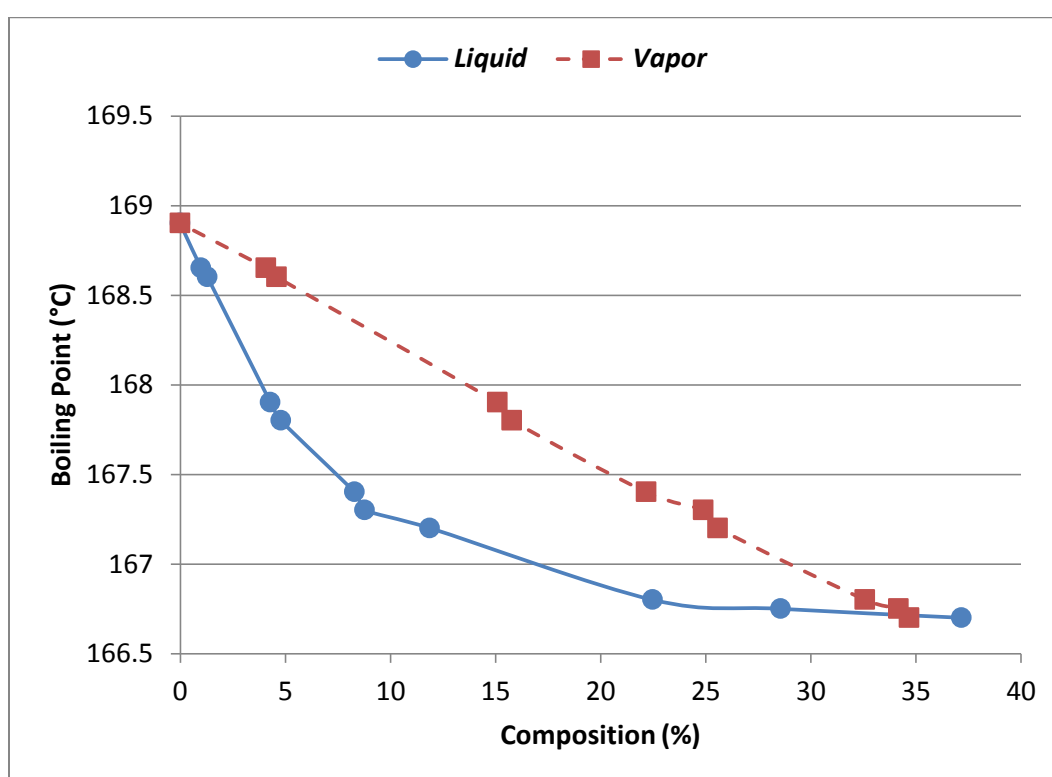


**Fig. 4.1:** Vapor-liquid equilibrium (VLE) data of furfural and water showing the formation of a minimum-boiling azeotrope at 111.5 psi (adapted from Curtis and Hatt<sup>137</sup>).

BRD has been identified to offer advantages over conventional batch reactions in cases where the chemical reactions may be limited by equilibrium, or if the reaction descends

into the formation of undesired byproducts. The removal of one or more products from the reaction mixture during BRD increases the conversion of equilibrium-limited reactions (Le Chateliers' principle)<sup>138</sup>. Several studies have utilized BRD for the production of chemicals such as methyl acetate, methyl tertiary butyl ether (MTBE), etc. Reactive distillation operations in the continuous processing phase have been shown to lower process costs and reduce environmental emissions<sup>139</sup>. As furfural is primarily produced in the batch configuration, it would be prudent to combine it with the batch/continuous distillation operation to reap the benefits offered by reactive distillation. In this context, the BRD process investigated in this study combines batch reaction with continuous distillation, giving rise to a 'semi-continuous' batch reactive distillation operation. Figure 4.2 shows a schematic of a BRD device with the condenser performing reflux to concentrate the product, which is collected in the receiver.

While batch rectifiers are incapable of eliminating a binary minimum-boiling azeotrope to produce a pure product, limitations of equipment available in the current study led to the integration of the batch reaction with rectification. This handicap of the rectifier is due to the fact that even if reaction kinetics allow the still composition to exceed the azeotropic composition, the top product that is recovered from the column is always the minimum-boiling azeotrope, as it is the lightest-boiling entity in the system<sup>140</sup>.

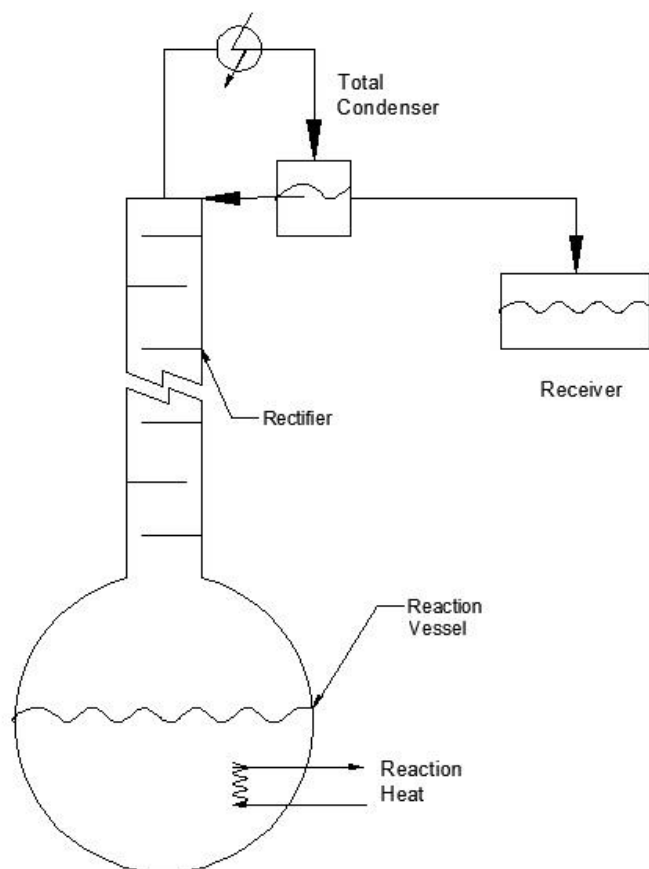


**Fig. 4.2:** Schematic of an ideal BRD device (adapted from Gadewar et al<sup>138</sup>).

Prevention of loss reactions and the formation of humins is essential for improving furfural yields from pentoses, and this can be accomplished by extracting the furfural produced from the reactive aqueous phase. Continuous removal of furfural will isolate it from the reactive aqueous phase where furfural can undergo condensation reactions with pentose and result in the formation of undesired byproducts. Unlike liquid-liquid extraction of furfural<sup>8, 10, 11</sup>, where furfural is selectively transferred into an organic solvent, BRD

may be employed to this effect using the azeotropic properties of furfural with water minus the requirement for solvent separation and recovery operations.

Xylose has traditionally been chosen as the starting material for most research in furfural chemistry, and for good reason. Xylose is the predominant pentose in biomass (the other being arabinose), and can, for most practical purposes, be assumed to be the only source for furfural formation. Much literature dealing with the chemistry and kinetics of furfural and its production have used xylose as the starting material<sup>6, 10-12, 85, 86</sup>, and for these reasons, aqueous solutions of xylose were subjected to dehydration, with the assumption that these results can be applied towards biomass experiments.

The goal of this phase of research is to find ways of improving the furfural yield from xylose. To achieve this end, conventional batch reactions were set as a benchmark, and experiments were performed using sodium chloride to influence the reaction kinetics. As an exploratory process being investigated, BRD was employed on aqueous xylose solutions with the aim of increasing the furfural yield in comparison to the conventional batch process.

## **4.2. Materials and Methods**

### **4.2.1. Chemicals and Reagents**

Xylose solutions were prepared at a fixed concentration of 17.6% (by solution mass), and sulfuric acid was used to catalyze the reaction, its concentration varied between 1 and 3% (by solution mass). Sodium chloride was added to some of the reactions at 10% (by solution mass) to observe its effect on the reaction yield. Pure furfural was used for the

preparation of standard solutions for analysis using both UV/Vis spectrophotometry and high-performance liquid chromatography.

#### 4.2.2. Apparatus

All the batch experiments were conducted in a 600-ml Parr 4560 series mini benchtop pressurized reactor cast in Hastelloy C-276, operated using a Model 4848 reaction controller (refer to section 3.3.1 detailed operating procedure). The sampling port was equipped with a screen to filter out insoluble materials such as humins formed during the reaction. Nitrogen gas was used for purging the sampling tube after samples were taken, and also to make up for any pressure lost during the sampling.

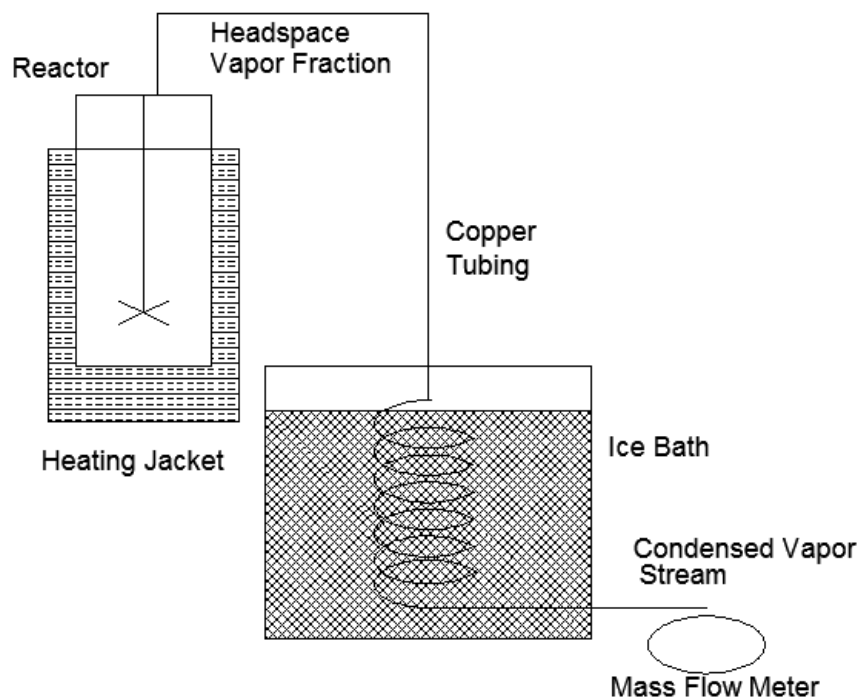


**Fig. 4.3:** Simplified schematic of the batch reactive distillation (not to scale): the vapor fraction is pulled from the headspace and condensed within the copper tubing immersed

in the ice bath. The ‘mass flow meter’ constitutes the beaker placed on a balance, and the furfural accumulation is monitored using a stopwatch.

For the BRD experiments, a copper coil condenser was attached to the vapor release valve of the Parr reactor so as to extract the vapor fraction from the headspace (figure 4.3). The condenser was made by running copper tubing through an ice box filled with ice, which cooled the vapor down considerably, and was collected in liquid form in a beaker placed at the end of the coil.

#### **4.2.3. Methodology**

The batch experiments were conducted according to the procedure described in section 3.3.1 (figures 3.1 and 3.2). For the 20 minute runs, samples were taken every 2 minutes, while for the 60 minute runs, samples were taken every 6 minutes. Later runs did not involve sampling as the behavior of the furfural yield with CSF was seen as the primary objective, and only the final sample was necessary for this purpose.

Experiments using the BRD configuration were conducted by opening the vapor release valve once the reactor was heated to the set-point temperature. The valve opening, and consequently the flow rate, was small enough so that the energy from the heating jacket could manage with the pressure loss due to vapor removal, so as to provide with a nearly constant temperature for the duration of the reaction. The vapor was condensed and collected in a beaker at the end of the coil, and time-based samples were collected from the contents of the beaker to provide an accumulated concentration of furfural extracted from the reactor headspace. For all experiments, 300 g was taken as the initial reactant mass (xylose, sulfuric acid and water), and 200 g was withdrawn from the vapor space, so

as not to run the reactor dry. Samples were taken at every 20 g of accumulation in the beaker, and the time, temperature and pressure were recorded for each sample.

#### **4.2.4. Analysis**

Furfural was analyzed using UV/Vis spectrophotometry run at 276 nm as explained in section 3.4.1.1

Xylose was measured using a ion-exchange chromatography system as described in section 3.4.2.

### **4.3. Results and Discussion**

#### **4.3.1. Xylose dehydration in the batch configuration**

##### ***4.3.1.1. Impact of CSF on the furfural yields***

Sulfuric acid- catalyzed batch dehydration of aqueous xylose solutions in the presence of salt, in general, showed a significant improvement in furfural yield in comparison to experiments where salt was excluded from the reactant mixture. The results are summarized in figure 4.4 against the CSF, which is defined as under:

$$CSF = \log R_0 - pH \quad (\text{Eqn. 4.1})$$

Where,

$$R_0 = \exp\left(\frac{T - 100}{14.75}\right) \times t$$

*T* is the temperature (in °C) with 100 °C chosen as the reference temperature, and

*t* is the time of the reaction (in min)

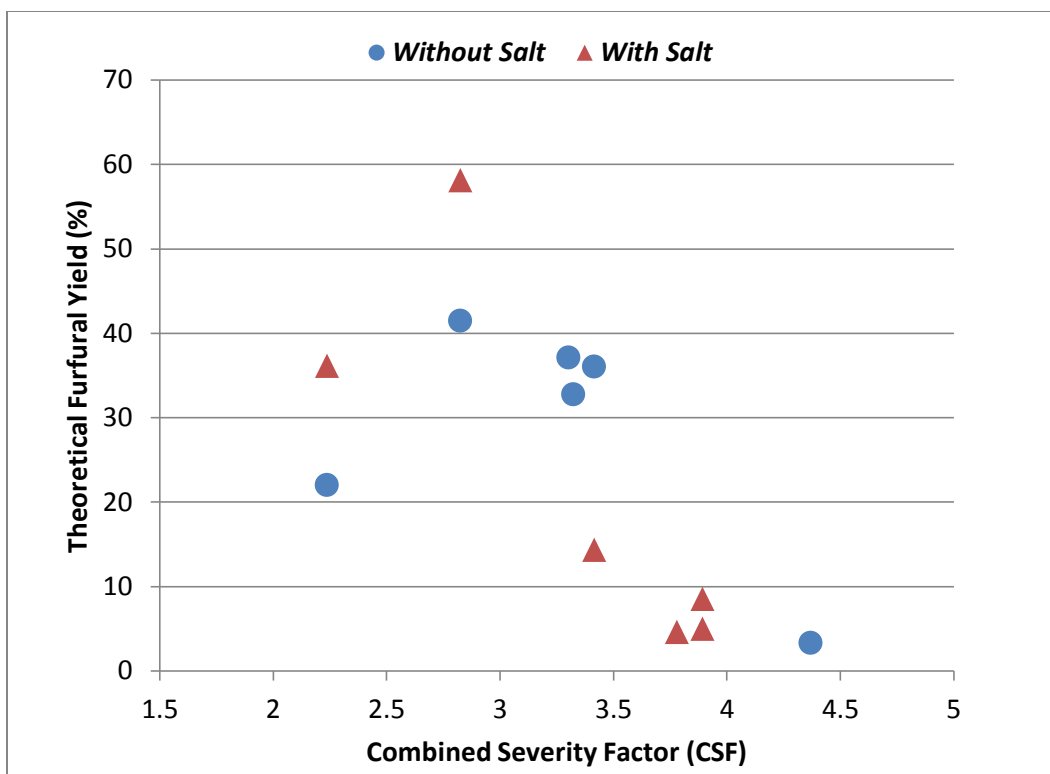


**Fig. 4.4:** Plot showing the dependence of furfural yield on the CSF, both in the presence and absence of salt (NaCl).

The results immediately point out the benevolent effect of salt on the furfural yields at low to moderate values of the CSF. The effect is reversed as the CSF is increased at and beyond a value of 3.30. A maximum theoretical furfural yield of 58.1% was obtained at a CSF of 2.83 in the presence of salt, versus 41.42% in its absence.

The sharp decrease in furfural yields as the CSF is increased beyond an optimum value can be explained by the occurrence of loss reactions of furfural in the reaction mixture. Higher degrees of harshness of reaction conditions have a negative effect on the yield by readily converting any furfural produced into humins- loss products arising out reactions

of furfural with itself (resinification) and with xylose (condensation). This explanation is given credence from a typical time-based furfural concentration plot (figure 4.5), which shows a gradual loss of furfural in the reaction mixture for a higher value of CSF (2.83 through 3.89) for four of the 20 minute experiments. From the plot, it is evident that the furfural produced during the dehydration reaction is subsequently transformed, most likely, into humins as long as it remains exposed to the harsh conditions in the reactant mixture. The most probable explanation for this loss is that furfural is converted into humins as long as it remains in the reactant mixture.

Between the runs with CSF of 3.33 and 3.42, the latter run has a slightly higher furfural concentration (and consequently, a slightly higher furfural yield), and it can be observed that the slightly greater reaction severity leads to a faster rate of furfural production within the first six to eight minutes.

The lowest value of the CSF (2.83) shows the highest concentration of furfural produced, but some of it inevitably gets converted into loss products towards the end of the reaction. Offering a stark contrast to this is the run with a CSF of 3.89 where it was observed that the furfural concentration shows a constant decline right from the beginning of the reaction, suggesting that the conditions were harsh enough that any furfural that was produced became extremely susceptible for degradation into humins.

The general trend shown from the batch results also leads to the inference that the reaction time needs to be very short while producing furfural in the batch configuration to prevent its transformation to humins.

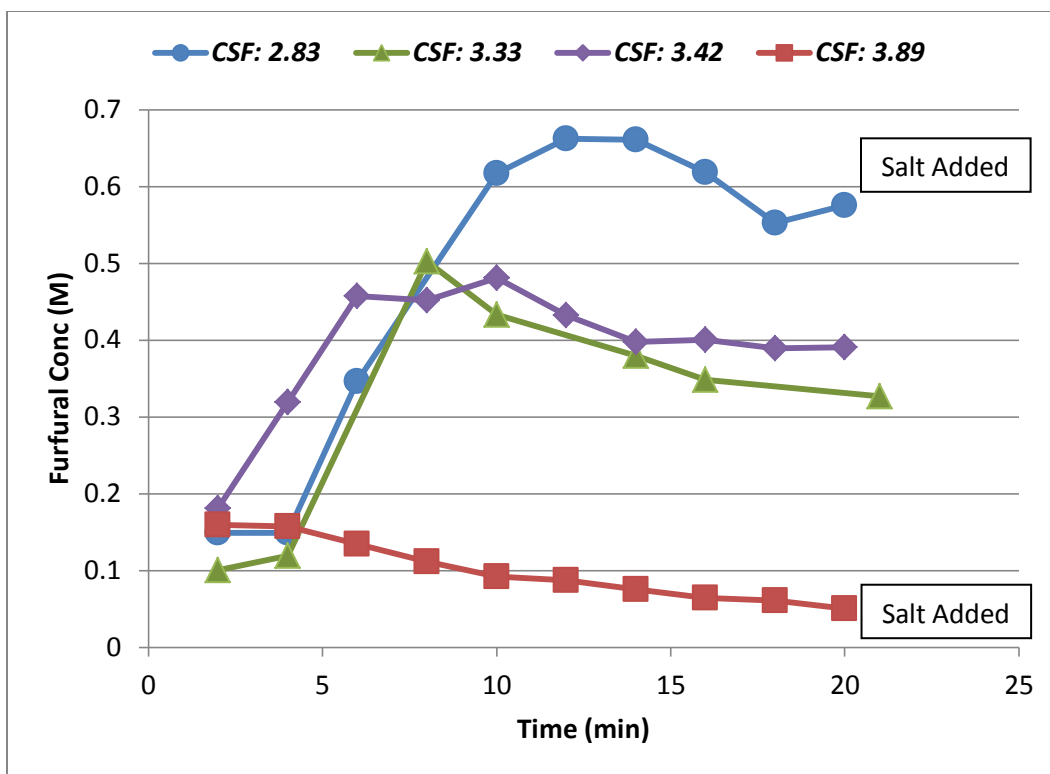


**Fig. 4.5:** Plot showing the effect of CSF on furfural concentration with time for four of the 20 minute runs, indicative of the subsequent transformation of furfural into loss products.

The furfural yield from pure xylose was calculated using equation 2:

$$FF \text{ Yield } (\%) = \left( \frac{\text{mol } FF}{\text{mol } Xyl} \right) \times 100 \quad (\text{Eqn. 4.2})$$

The presence of chloride ions in the reaction mixture leading towards the production of furfural has improved the furfural yield from ~41% to over 58%, conceivably, by influencing the formation of the pentose-furfural intermediate. These results can be corroborated from the work of Marcotullio et al, who first showed the effect of metal halides on furfural yields at elevated pressures. At 200 °C, a maximum yield of 62.1% using 0.21 g/l (0.22 M) formic acid in the presence of 100 g/l (10 %) NaCl, is reported.

Better yields were reported using 18.23 g/l (0.05 M) HCl and 100 g/l NaCl, with the additional Cl<sup>-</sup> ions from the acid adding to the overall chloride ion concentration and the overall yield reported as 74.4%. The yield dropped to 68.7% under similar conditions in the absence of the salt, indicating a strong influence of chloride ions on the conversion of xylose to furfural. A two- point improvement in selectivity was also reported due to the presence of salt in the reaction mixture.

The significantly better results obtained by Marcotullio et al can be attributed to the choice of reactor used in their study and the operating conditions employed. A coiled tube was used, which resembled a plug- flow reactor operated at over 870 psi (60 bar), without any mixing. In contrast, the current study involved a completely mixed batch reactor which operated between 130 and 203 psi as dictated by the vapor pressure at the operating temperature.

Results obtained in this study, in addition to corroborating and further expanding on the effects of salt on furfural production, also shed new light on the importance of CSF as a factor affecting furfural yield in reactant solutions containing salt. At higher values of CSF, salt has a deleterious effect on furfural yields, probably because the faster reaction kinetics subject the furfural produced to loss reactions that form humins. This impact of the severity of reaction conditions on furfural yields deserves consideration, and has not been documented in terms of the CSF so far.

#### ***4.3.1.2. Impact of CSF on xylose conversion***

The effect of CSF on the conversion of xylose was also analyzed for six of the total thirteen runs conducted. A time profile of xylose conversion (shown as concentration in

g/l) is plotted in figure 4.6, for four different values of the CSF, two experiments in the presence of salt (CSF: 3.781 and 3.893), and two in its absence (CSF: 3.304 and 4.37). The ordinate begins at 6 minutes (without assuming 0 minutes to be the initial xylose concentration of 176.47 g/l, or 17.6% by mass), in order to more clearly distinguish the behavior of the curves at slightly lower concentrations.

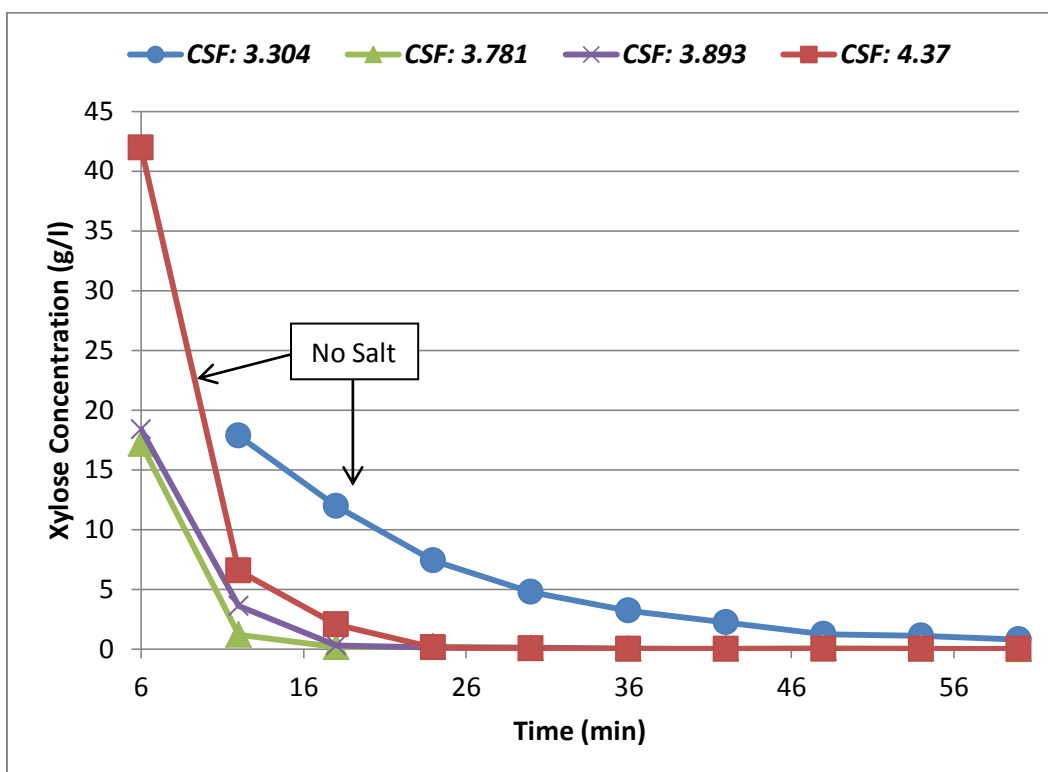


**Fig. 4.6:** Plot showing the concentration of xylose as it is being converted with time, for four different values of the CSF (both in the presence and absence of salt), beginning with the first sample (at 6 min for 60 min reactions).

As expected, higher values of CSF lead to greater conversion of xylose, which is explicitly witnessed for the CSF values of 3.304 and 4.37 in the absence of salt.

Significantly greater conversion of xylose occurred in the presence of salt even at lower

values of CSF, further lending credence to the inference that the metal halides influenced the formation of the intermediate 1,2-enediol structure.

An unlikely observation is made within the two experiments that were performed in the presence of salt (CSF values of 3.781 and 3.893), in that greater conversion of xylose was observed in the experiment with the lower CSF value. Given that the CSF values for the two runs are very close, and so are the estimated xylose concentrations, it is very likely that this result is anomalous.

#### **4.3.2. Xylose dehydration using the BRD configuration**

Preliminary experiments were performed to run the Parr reactor in a BRD configuration, and for determining the important variables necessary for the construction of a statistical model to provide with optimum reaction conditions for maximum furfural yield. These included opening/regulation of the condenser valve which would ensure a nearly constant reaction temperature, the energy loss due to vapor removal being balanced by the heat provided by the heating jacket. Figure 4.7 shows a typical plot of furfural accumulation with time.

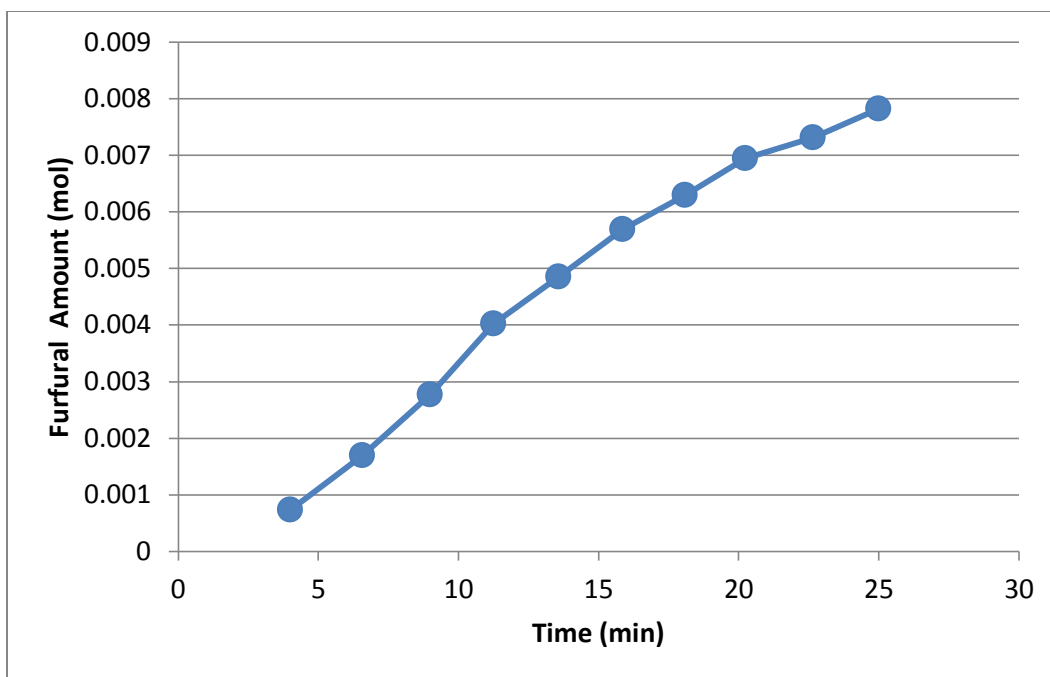


**Fig. 4.7:** Plot showing a typical time-based furfural formation curve for one of the preliminary experiments. Reaction conditions: 0.5% xylose, 2% sulfuric acid and 170 °C; Yield = 80.2%.

Based on preliminary results, the xylose concentration was fixed at 0.5% (by solution mass), and the condensate valve was opened to 60° to ensure a nearly constant temperature. As before, CSF was made use of to compress the reaction conditions into one term, and the results from individual experiments as a function of CSF are shown in figure 4.8.

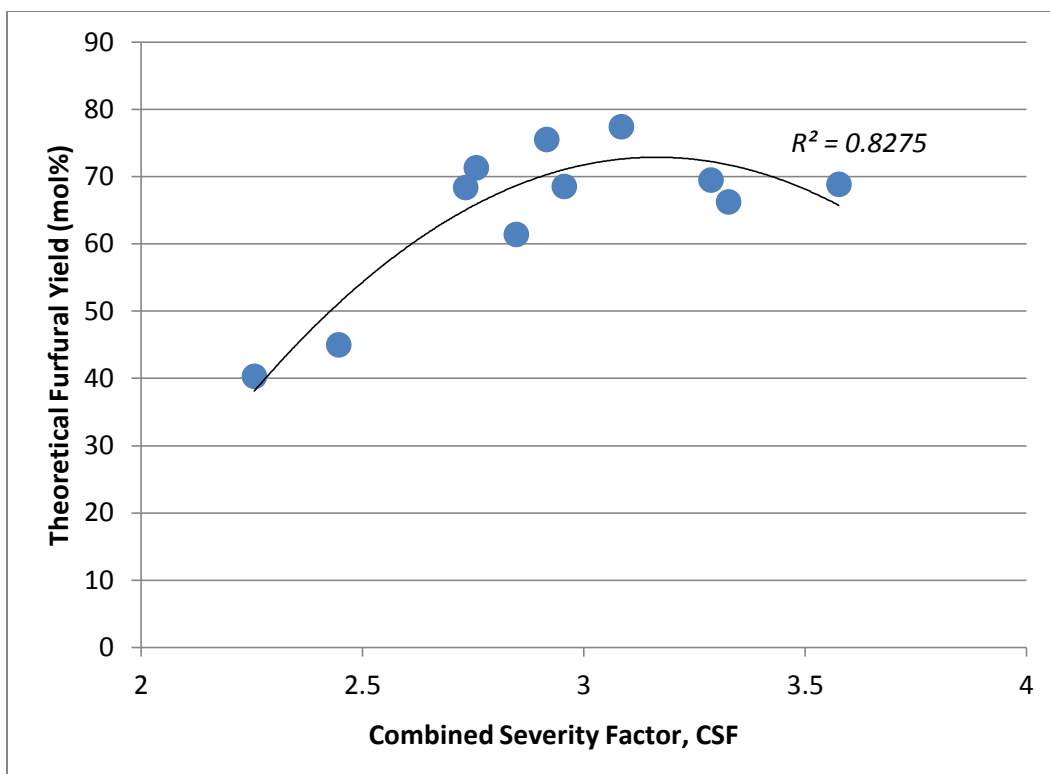


**Fig. 4.8:** Plot showing the effect of CSF on furfural yield for the range of experiments conducted using BRD. A 2<sup>nd</sup> order polynomial fit was constructed to generalize the behavior as before.

Increase in the CSF results in a steep increase in the furfural yield using the BRD configuration, and the yield attains a maximum of 77.5% at a CSF value of ~3.1. Beyond this, there is a slight decrease in the yield, indicating a slight detrimental effect of increasing reaction severity on the furfural yields.

This behavior can be explained by the fact that as the reaction conditions are made harsher, furfural is produced sooner, but since the flow rate is low and constant (to maintain a constant temperature), the furfural produced becomes exposed to the reactant

mixture, and is highly susceptible to undergo loss reactions, resulting in the formation of humins.

The reduction in the furfural yield with higher values of the CSF for the BRD reactions, however, is not as pronounced as was witnessed in the case of the batch reactions.

Possible explanations for this apparent disparity are: (1) the much lower concentration of xylose used for the BRD experiments as compared to the batch experiments (0.5% versus 17.6%), and (2) the inherent nature of the BRD process which involves separation of the furfural-water azeotrope as it is being produced. Lower concentrations of xylose used in the dehydration reaction reduce the probability for the occurrence of the condensation loss reaction(s) which lead to the formation of furfurals-pentose. This effect of xylose concentration on the yield has been demonstrated by Root et al<sup>86</sup>, and it is very likely that this could have played a significant role in decreasing the loss in furfural yield.

Figure 4.9 shows a typical plot of furfural produced with time for one of the experiments from the model. Concentration of furfural obtained in the vapour phase slowly increases with time, reaches a point of maximum concentration, and then decreases. It can be inferred that furfural continues to be extracted with the azeotrope and boils over as long as it is being produced by the dehydration of xylose. Some loss reactions are inevitable due to limitations of the reactor, and as the furfural concentration falls, more of the water in the solution is now being extracted. Towards the end of the reaction, even though furfural continues to be extracted, it may not be wise to continue extraction as this might lead to the reactor being run dry. The low concentrations of furfural obtained in the vapor phase reiterate the fact that the furfural-water azeotrope is being withdrawn from the

reactor headspace, and it is hard to recover pure furfural as the difference in boiling points of furfural and that of the azeotrope at elevated pressures is small<sup>137</sup> enough to evade the precision of the reactor temperature controller.

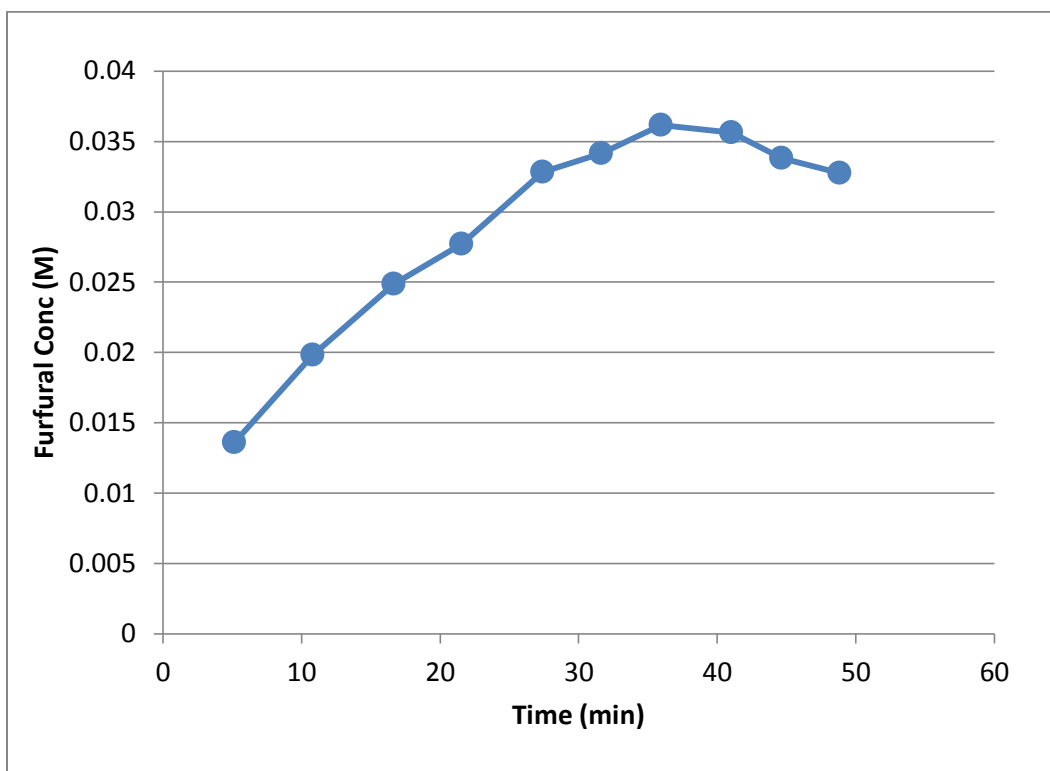
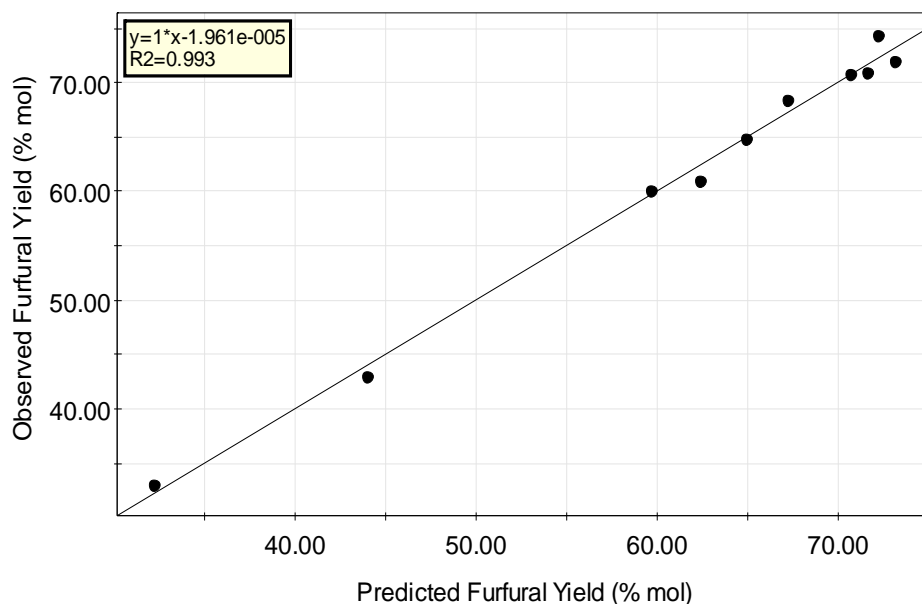


**Fig. 4.9:** Plot showing the time-based accumulation of furfural extracted from the vapor phase for a typical xylose BRD reaction.

A three-level, central composite face (CCF) statistical model was constructed in MODDE 7.0.0.1, with sulfuric acid concentration and temperature treated as the main variables. The acid concentration was varied between 0.1 and 0.3 M, while the temperature was varied between 150 and 170 °C, with the model optimized for maximizing the furfural yield. The model predicted optimum furfural production at reaction conditions of 168.5°C and 1.6 wt% acid, or a CSF of 2.41. A predicted v/s actual plot obtained from

MODDE is shown in figure 4.10, suggesting a very good fit ( $R^2 = 0.993$ ). At the optimum conditions suggested by the model the yield was predicted to be 76.2%, while triplicate experiments conducted at these conditions provided with an average furfural yield of 75.0  $\pm$  0.674%.



MODDE 7 - 5/5/2012 1:16:16 PM

**Fig. 4.10:** Plot showing the predicted versus observed theoretical furfural yields from MODDE fit for the xylose BRD experiments.

Coefficient plots obtained from MODDE also pointed out to a greater effect of temperature on furfural yield than the concentration of acid. The scaled and centered coefficient plot, shown in figure 4.11, suggests that when the sulfuric acid concentration is kept constant at its average value, an increase in temperature has almost twice the impact on the yield of furfural as compared to the sulfuric acid concentration.

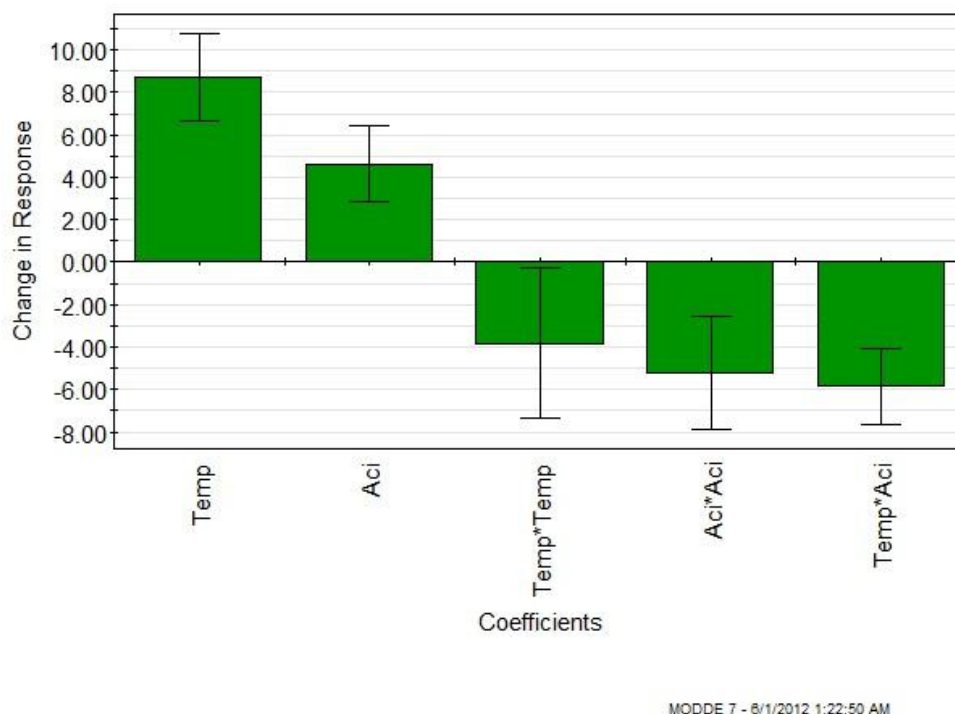


**Fig. 4.11:** Coefficient plot obtained for the statistical model constructed in MODDE showing the effect in response (furfural yield) when the value of one of the factors is increased from the medium to the high setting, while the other factor is kept at its average value.

This observation leads to the inference that if the reactor needed to be reconfigured in such a way as to increase the furfural yield beyond what the current BRD setup offers, it should involve performing the reaction at much higher temperatures, which might lead to a reduction in the amount of sulfuric acid needed.

#### 4.3.3. BRD dehydration using acid-injection

Instead of having the acid present in the reaction vessel with xylose during the reactor heating phase, experiments were carried to introduce the acid once the temperature was reached in order to minimize degradation of any furfural produced before the condensate valve was opened to extract furfural from the vapor phase. Allowing the acid to be

present along with xylose will increase the chances that any furfural produced before opening the valve will be exposed to potential condensation loss reactions. Based on results from the coefficient plot, it was presumed that employing acid-injection will allow for the exploration of higher reaction temperatures. This was not possible with the original BRD process (with the acid being part of the reactants during the heating phase) as the time needed to reach temperatures ~190 and 200 °C was a lot greater, and by then, a significant amount of furfural would have been generated and become the target of loss reactions. This was one reason why lower furfural yields were witnessed at higher temperatures during initial experimentation with the BRD process.

Sulfuric acid was introduced into the reactor using a stainless steel acid-holding chamber that was injected using nitrogen gas (maintained at a slightly higher pressure than the reactor pressure) when the requisite temperature was reached. Four such reactions were conducted, at higher temperatures (180 and 190 °C) and lower acid concentrations (0.2 and 0.5% by mass). An additional reaction was conducted at the optimum conditions predicted by the model (168.5 °C and 1.6% acid by mass). The xylose concentration was also varied for the high temperature experiments (0.5 and 2% by mass).

Furfural yields from all the acid injection experiments at higher temperatures were lower (60 to 66.1%), and the furfural yield obtained at the optimum conditions was slightly lower as well, at 71.7%, compared to an average of 75% without the use of acid injection. These results are contrary to the expectation that introduction of the sulfuric acid at a later stage, after the temperature had been reached, would reduce the formation of humins. It is highly likely that a small fraction of furfural is being produced during the

heating phase (as evidenced by the slightly higher yield when the acid was part of the reactants) and that any means of improving the yields by introducing the acid later on was not possible using the existing BRD reactor setup. The combination of higher temperatures and lower acid concentrations led to much lesser furfural yields, which seem to indicate that a minimum acid concentration was necessary even when the temperature was increased. This is only a presumption, and the existence of such a minimum necessary acid amount was not evaluated, and all future experiments employing the BRD process reverted back to the method where the sulfuric acid was present as part of the reactant mixture during the temperature ramp-up phase as well.

#### **4.4. Conclusions**

Significant improvement in the yield of furfural was achieved by experimenting with two different methods: (1) the addition of salt to the reaction mixture, and (2) operation of the dehydration reaction using the BRD configuration. The concept of the Combined Severity Factor (CSF) was utilized as the primary tool for evaluating the effect of reaction conditions on the yield of furfural, and xylose conversion. In both cases for improving the furfural yield, an optimum value of CSF was observed, beyond which, any effort to increase the severity of the reaction renders a detrimental effect on the furfural yield. Use of this composite term should enable insights into a basis for evaluating reaction conditions that conform to an optimal value of the CSF.

The utilization of UV spectroscopy for estimating furfural concentrations in both the batch and BRD experiments provided with a fast and reasonably accurate method, as opposed to relatively expensive and time-consuming chromatography methods. This is

seen as a valuable way of measuring furfural in the absence of lignin and other furans, such as HMF, which also absorb around the same wavelengths.

A maximum theoretical furfural yield of 58.1% was obtained in the presence of salt, as opposed to 41.4% in its absence. Using the BRD configuration at lower xylose concentrations, the furfural yield was significantly improved to  $75 \pm 0.674\%$  at conditions predicted by the statistical model constructed in MODDE, optimized for maximum furfural yield. These results urge for the evaluation of the BRD process towards producing furfural in higher yields over the conventional batch process (even with the use of salt).

Apart from the slightly lower yields (compared to the BRD), a major disadvantage of using salt in the reaction medium is the danger of corrosion associated with doing so. Even with Hastelloy C-276 reactor equipment, a significant amount of corrosion was witnessed in the reactor clamps and within crevices. For this reason, this manner of improving furfural yields is not seen as being feasible on a large scale.

Favorable results obtained using the BRD process indicate a real potential to produce furfural in high yields. The dehydration of biomass and biomass hydrolysates using the BRD configuration is expected to allow for the production of furfural in high yields. It is anticipated that the optimized conditions obtained from the model can be applied to dehydrate biomass and hydrolysates, producing similar or even slightly higher furfural yields. The reasoning behind this assumption is that biomass and hydrolysates comprise of pentose oligomers (along with monomers), and will undergo simultaneous hydrolysis

reactions (breakdown of the oligomers into monomers) in addition to the dehydration reaction to produce furfural. In case of the pure xylose solutions, all of the sugar was available as a lump for conversion into furfural, increasing the likelihood of exposing the furfural so produced to the formation of loss products. Occurrence of the hydrolysis reactions in case of the biomass and hydrolysates will likely reduce the probability of degrading the furfural produce into humins (primarily the condensation loss product, furfural-pentose).

## Chapter 5- Biomass Fractionation and BRD Dehydration of Biomass and Water-Extracted Hydrolysates

### 5.1. Introduction

Furfural has received recognition as a valuable biobased chemical<sup>3</sup>, as a precursor for the production of sugar-derived platform chemicals such as levulinic acid<sup>2</sup>, and for the production of furan-based chemicals such as furfuryl alcohol, furoic acid, furan and THF, 2-methylhydrofuran, etc.<sup>6,7</sup> The industrial batch process of producing furfural from pentosan-rich materials such as corncobs, bagasse, etc., results in low furfural yields (~50%)<sup>5,6,11</sup>, which presents a strong incentive to find ways of improving the yield using biomass. The previous chapter dealt with the evaluation of two different processes for increasing the furfural yield from aqueous solutions of pure xylose. Use of sodium chloride in the reaction mixture to realize this resulted in a maximum theoretical furfural yield of 58.1%, but this process was not seen as being feasible for scale-up, given the significant amount of corrosion witnessed due to the presence of salt. As a novel process for producing furfural, batch reactive distillation (BRD) of xylose solutions was developed and investigated by extracting the vapor fraction from the reactor headspace and condensing the product. At optimum conditions predicted by a three-level statistical model constructed in the experimental design software MODDE 7.0.0.1 (Umetrics AB, Sweden), the furfural yield was increased significantly to  $75.0 \pm 0.674\%$ . Due to the much greater yields afforded by the BRD process, and the apparent ease of scalability and feasibility of the process led to its application on biomass, and later on biomass hydrolysates.

It was hypothesized that the conditions obtained by the statistical treatment of pure xylose experiments can be applied to the BRD dehydration of biomass and biomass hydrolysates, and this would still provide with similar or even better furfural yields. The reasoning behind this hypothesis is that in the case of biomass and hydrolysates, there are simultaneous hydrolysis and dehydration reactions occurring. The hydrolysis of pentosan oligomers into monomers will restrict their immediate availability for the dehydration reaction to occur and effect their transformation into furfural. This is not the case with pure xylose, which means that the scope for the furfural produced to undergo condensation loss reactions with xylose, forming humins, is much greater.

## **5.2. Materials and Methods**

### **5.2.1. Materials and Reagents**

A total of four different biomass feedstocks were evaluated for this study. While all four were subjected to water hydrolysis and subsequent dehydration using the BRD process, only hybrid poplar was dehydrated using the BRD process as a solid untreated biomass. For the BRD dehydration of raw biomass, poplar chips were air-dried, milled and screened to 3 mm with no further pretreatment.

Hybrid poplar (*Populus maximowiczii x nigra*), representative of a short- rotation woody bioenergy crop, was harvested from northern Wisconsin after ten years of age and seasoned for three months before use. The wood was debarked by hand, chipped, screened (2-8 mm) and air- dried. As an agricultural residue presenting value for conversion to bioenergy, corn stover (*Zea mays*) was collected from Lodi, Wisconsin, aged for three months before being chopped and screened to one inch samples, and air-

dried. To account for high- yield bioenergy crops, switchgrass (*Panicum virgatum*) and miscanthus (*Miscanthus giganteus*) were sourced from the University of Wisconsin agricultural research stations (Arlington and West Madison, respectively). The two samples were harvested after senescence, air-dried, chopped and screened to one-inch plus size.

As before, sulfuric acid (Fisher Scientific, New Jersey, USA) was used to catalyse the dehydration reaction in all the experiments.

### **5.2.2. Apparatus**

The hot-water extraction of all four air-dried, chopped and screened biomass samples was performed using a 23-litre rotating, steam-jacketed digester at the Forest Products Laboratory, Madison, WI. The milling of the hybrid poplar samples was performed using a Wiley Mill equipped with a 3 mm wide screen.

All of the dehydration reactions were performed using the BRD reactor setup as described in Chapter 4 (figure 4.1) using milled biomass samples, and using biomass hydrolysates.

Estimation of the energy content of original and water-extracted biomass samples was performed using oxygen bomb calorimetry with a Parr 6772 calorimeter as explained in section 3.3.4. Samples were milled, oven-dried and pelleted using a Parr 2811 Pellet Press before being tested for their HHV. All experiments were performed in triplicates, and calibration was performed using Parr 3415 benzoic acid pellets.

### **5.2.3. Methodology**

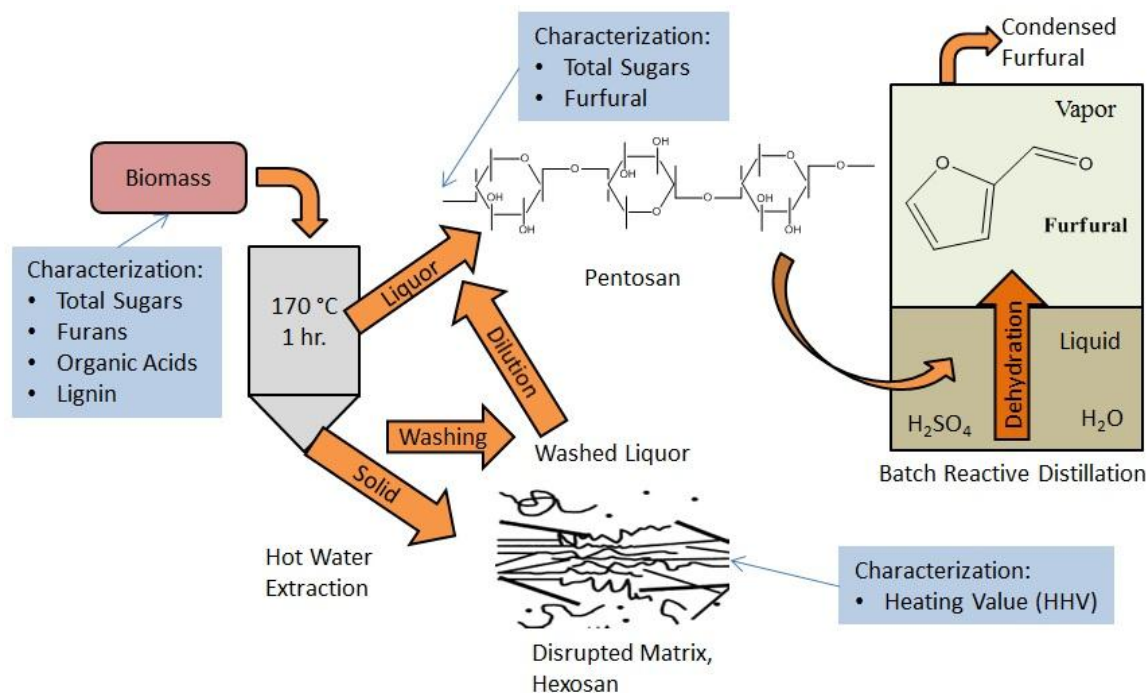


**Fig. 5.1:** Schematic showing the strategy employed for the fractionation of the biomass and subsequent dehydration to produce furfural using the BRD process. The type of characterization performed on each stream is also shown (inset of disrupted cell matrix image from Mosier et al<sup>121</sup>).

The overall strategy employed to fractionate and characterize the biomass, the hydrolysates and the solids, and then the BRD dehydration of the hydrolysates is shown in figure 5.1. All four biomass feedstocks were characterized in earlier work<sup>131</sup>, and were subject to hot-water hydrolysis giving rise to liquid and solid streams. The solids were washed to provide with ‘wash liquor’, and all three streams were characterized- the liquor streams for sugars and furfural, while the water-washed solids were tested for their heat content (higher heating value, HHV).

Hot-water hydrolysis of the biomass was carried out in the rotating digester as described in section 3.3 (figure 3.3), and the liquid samples (liquor and washed liquor) were frozen

for chemical analysis and dehydration experiments. The solid samples were frozen for calorimetric analysis.

The hybrid poplar samples, which were milled to 3 mm size, were reacted with sulfuric acid and water in the BRD configuration based on the optimized conditions obtained from the model- temperature: 168.5 °C and acid concentration: 1.6% by solution mass. Based on biomass characterization performed earlier<sup>131</sup>, the amount of sample dehydrated in this manner corresponded to 0.5 wt% of total pentose (this quantity is explained in section 5.3.1).

Liquor and washed liquor samples were mixed in specific amounts so as to provide with a total pentosan (TP, g/l) content of 0.5% (by mass). The original liquor samples obtained from the hydrolysis had a higher TP concentration, so it was necessary to dilute them by mixing with the washed liquor samples to bring the TP concentration down to 0.5% (to be consistent with the xylose concentration of 0.5 wt% used in the model compound experiments). The mixed stock of the liquor and the washed liquor was dehydrated at the optimized conditions obtained from the model compound experiments.

The heating value of all four water-extracted solids was performed using oxygen bomb calorimetry, as described in section 3.3.4. The solids were oven-dried, to make them moisture-free, and then tested for their heat content. While complete characterization of the solid fraction of the hydrolysis was not performed, estimation of the energy content allowed for confirmation with prior work<sup>131</sup>, along with casting light on the value of the product as a combustible fuel source.

#### **5.2.4. Analysis**

Raw hybrid poplar samples were not characterized as part of this research, but these results were obtained from prior work. Analysis of hydrolysates (liquor and washed liquor samples) for the five common wood sugars (arabinose, galactose, glucose, xylose and mannose) was performed in triplicates using ion-exchange chromatography as described in section 3.4.2. Duplicate and triplicate analyses were performed at a lower flow rate (0.35 ml/min) due to particle buildup in the analytical column, using the following gradient: 0.1 to 20.0 min: 100% water, 20.5 to 35.0 min: 75% 0.1 M NaOH and 35.0 to 45.0 min: 100% water. The post column eluent used was 0.5 M NaOH.

Analysis for furfural in hydrolysates and in BRD product samples was done using high performance liquid chromatography (HPLC), as explained in section 3.4.1.2.

## **5.3. Results and Discussion**

### **5.3.1. Hot-water extraction of biomass feedstock**

Results from the hot-water fractionation of all four biomass feedstock confirmed the intent of the operation, which was to obtain much of the hemicellulose pentose sugars, without extracting most of the hexose sugars from the cellulose fraction of biomass.

Figures 5.2 through 5.5 show the amounts of the five sugars (in percent) of the original biomass feedstock extracted into the liquor and washed liquor samples, as obtained from triplicate analyses of the hydrolysates.

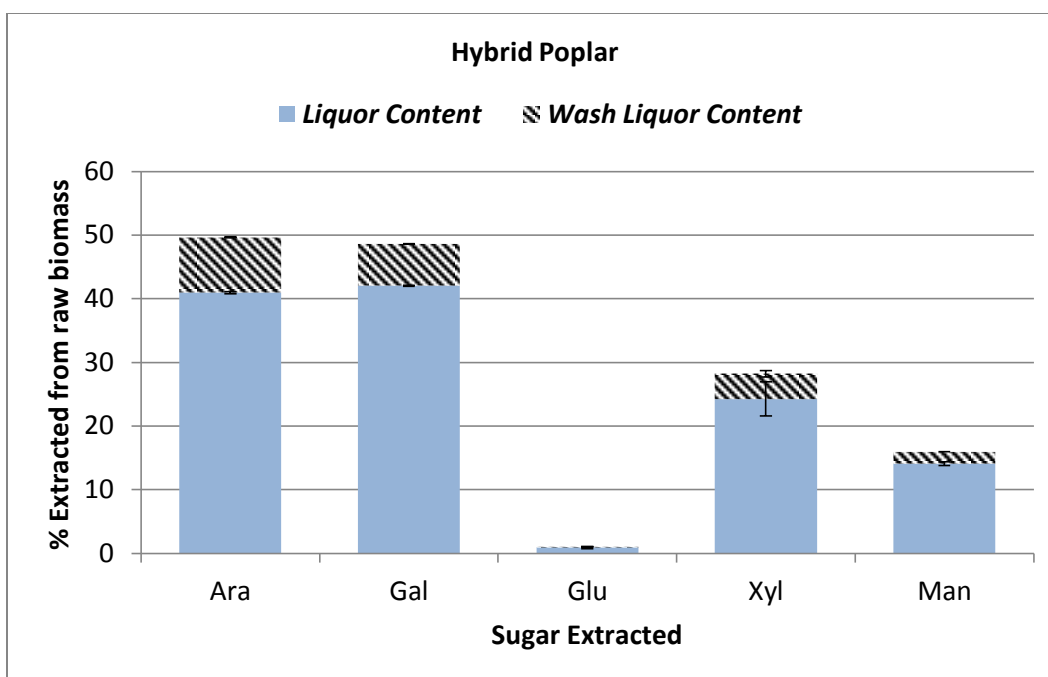


**Fig. 5.2:** Hybrid poplar sugar extracted from autohydrolysis (grey column: extraction and white column: wash liquor) with standard error.

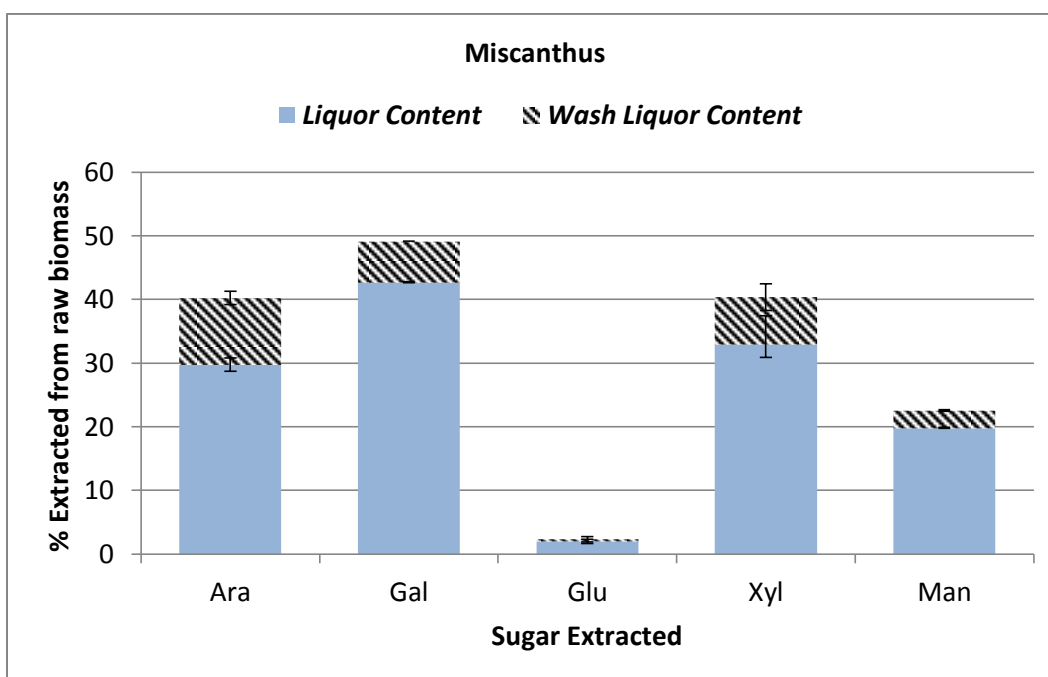


**Fig. 5.3:** Miscanthus sugar extracted from autohydrolysis (grey column: extraction and white column: wash liquor) with standard error.

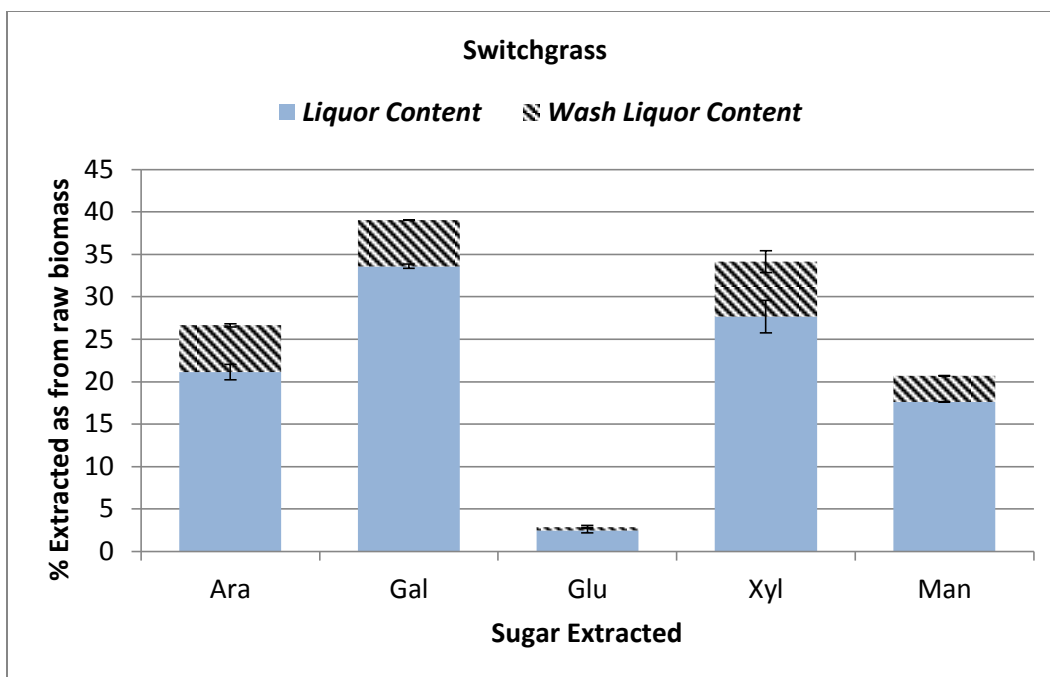


**Fig. 5.4:** Switchgrass sugar extracted from autohydrolysis (grey column: extraction and white column: wash liquor) with standard error.

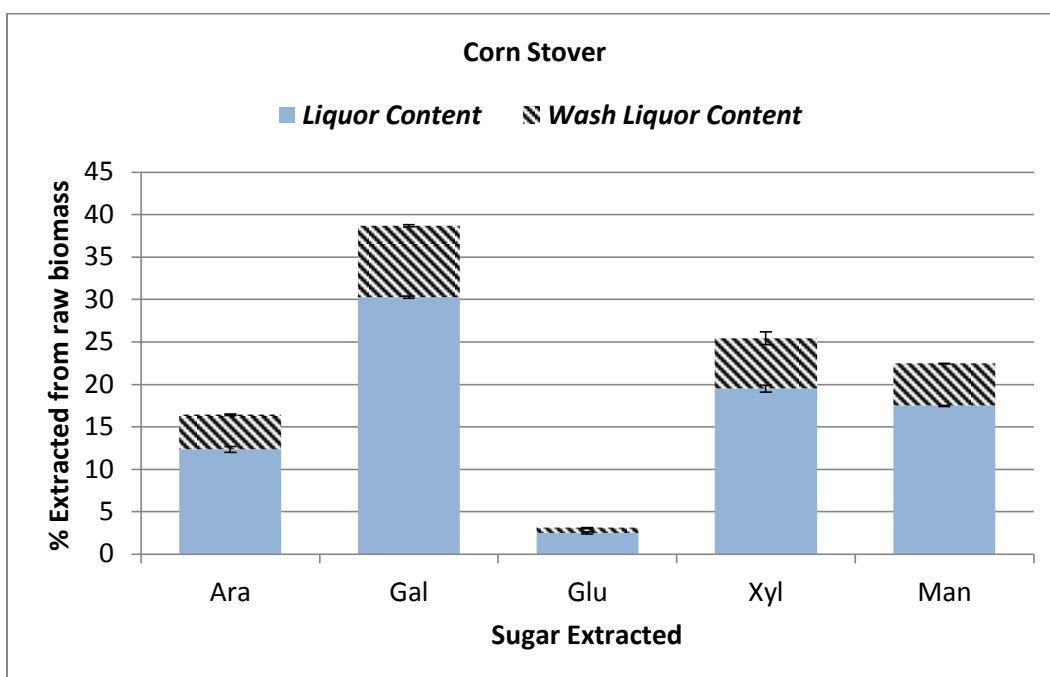


**Fig. 5.5:** Corn stover sugar extracted from autohydrolysis (grey column: extraction and white column: wash liquor) with standard error.

Anywhere from 19.5 to 33% of the original xylose present in the biomass was extracted into the liquor fraction from the hot-water hydrolysis step. A further 4 to 7.5% of the xylose was recovered by washing the biomass solids after the extraction, and was obtained in the washed liquor samples. Evidence of minimal cellulose degradation is provided from the fact that only 1 to 2.5% of the original biomass glucose content was extracted into the liquor samples, and much less was recovered from washing the water-extracted solids, even though it could have originated either from the cellulose or the hemicellulose fractions of the biomass.

The hydrolysate characterization results also shed light on the potential advantage of washing the extracted solids to recover additional sugars. The washed liquor was used in this research for diluting the pentose in the liquor for the dehydration reactions, and was considered beneficial for this purpose. The benefit of washing to recover additional sugars will have to be considered separately for other processes which employ hydrolysis, and assess whether a 4 to 7.5% gain of sugars is worth the additional unit operation, and also on the end-use of the hydrolysate or the extracted solids. For example, in the case of cellulosic ethanol fermentation following steam explosion pretreatment, washing the solids with water is suggested as necessary for the removal of degradation products that may be inhibitory to microbial growth, enzymatic hydrolysis and fermentation, along with the water-soluble hemicellulose<sup>141</sup>.

As a way to quantize the amount of pentose sugars available for dehydration into furfural (both monomeric and oligomeric), the term ‘total pentose’ was devised as shown in equation 5.1:

$$TP(g/l) = \{Ara_{II}\} + \{Xyl_{II}\} + \left\{ (Fur_{II} - Fur_I) \times \left( \frac{150.13}{96.08} \right) \right\} \quad \text{(Eqn. 5.1)}$$

Where,

*Subscripts I and II are pre- and post-hydrolyzed samples, respectively,*

*TP is total pentose concentration,*

*Ara is measured arabinose concentration,*

*Xyl is measured xylose concentration,*

*Fur is measured furfural concentration,*

*150.13/96.08 is the conversion factor of pentose MW/furfural MW*

Even though the hydrolysate samples primarily contain sugars as oligomers, the nomenclature of ‘total pentose’ rather than ‘total pentosan’ was chosen to prevent confusion when discussing the conversion of pentose sugars into furfural. Since the furfural yield is calculated based on the amount of pentose available, the term ‘total pentose’ refers to the total available pentose sugars (present both as monomers and oligomers), and the chemical conversion into furfural is independent of the hydrolysis of oligomers into monomers.

The six-carbon sugars (galactose, glucose and mannose) were used to derive the ‘total hexose’ content which provides with the concentration of these sugars in the liquor, in both the monomeric and oligomeric forms. This quantity was calculated using equation 5.2 as under:

$$TH(g/l) = \{Gal_{II}\} + \{Glu_{II}\} + \{Man_{II}\} \quad \text{(eqn. 5.2)}$$

*Where,*

*Subscript II refers to post-hydrolysis samples*

*Gal, Glu and Man refer to the 6-carbon sugars galactose, glucose and mannose, respectively*

It was assumed that the sugars did not significantly degrade into HMF during the hydrolysis step, and this was evident from the analysis where the concentration of HMF did not change appreciably before and after hydrolysis. The TH content provides the total amount of the six-carbon sugars that are present in solution in both the monomeric and oligomeric forms, and it was assumed that in the hydrolysis step, the oligomers broke down into monomers and were measured along with the initial monomers (pre-hydrolysis) without getting converted into degradation products.

Figure 5.6 shows the concentration (g/l) of the pentose and hexose sugars extracted into the liquor following hot-water extraction for the four biomass feedstock based on triplicate analyses. Anywhere from about 14 to 21 g/l of the pentose sugars were extracted into the hydrolysate, while only 3-5% of the hexose sugars were extracted. Much of these hexoses could have originated from the easily hydrolyzed hemicellulose portion of biomass as opposed to the cellulose. This is evident from the low concentrations of glucose extracted into the hydrolysate (figures 5.2 through 5.5), the principal fraction of which originates from cellulose and the much lower amounts of the remaining C6 sugars present in the biomass to begin with.

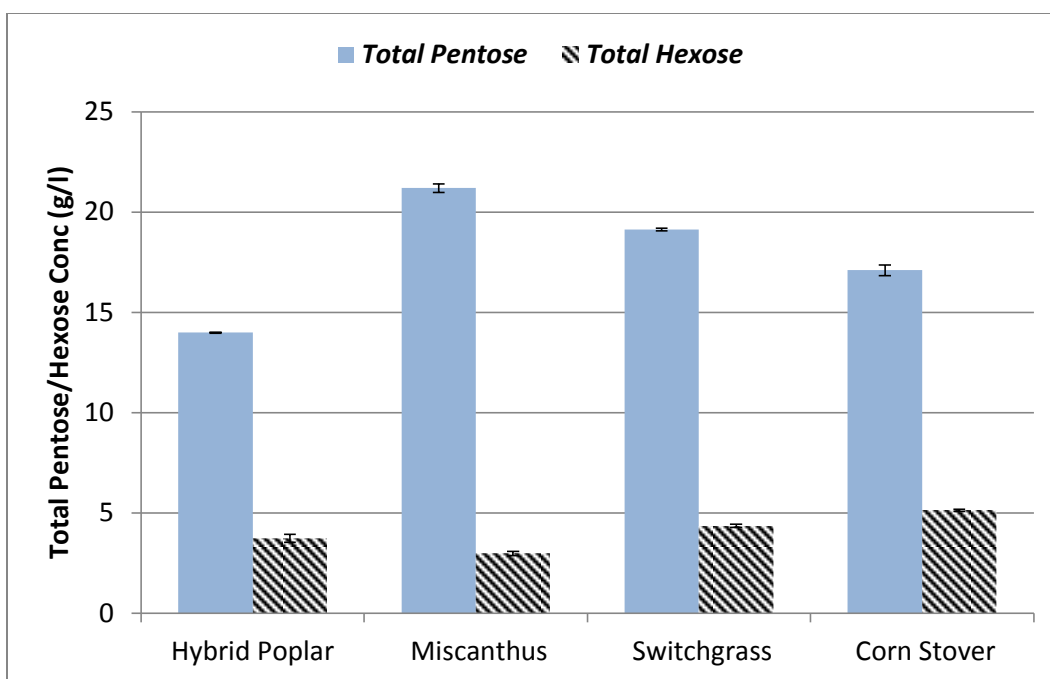


**Fig. 5.6:** Plot showing the concentrations of total pentose and hexose sugars (as measured in the monomeric form) obtained from the hot-water hydrolysis for all four biomass feedstock with standard error.

### 5.3.2. BRD dehydration of untreated poplar

To determine if the BRD reaction scheme could also apply to biomass, hybrid poplar samples were dehydrated using the batch reactive distillation method at the optimum conditions suggested by MODDE for pure xylose solutions. Poplar chips were oven-dried and milled (3 mm screen) and reacted with sulfuric acid in amounts to give a total pentosan content of 5.01 g/l (9.78 g of sample for a 300 g solution). Performed in triplicates, the reaction provided an average furfural yield of  $79.8 \pm 2.66\%$ . The yields are slightly greater than those obtained with pure sugar experiments. The higher yields, it is assumed, are due to the presence of oligomers of the pentose sugars xylose and arabinose (pentosan) which are gradually hydrolyzed into their monomers during the reaction,

thereby slowly releasing the latter for dehydration. The simultaneous occurrence of the hydrolysis and dehydration reactions ensure that the furfural produced during the dehydration reaction is not exposed to as much pentose (monomers) as it would have in case of the pure xylose reactions (reducing the possibility of the condensation loss product between furfural and pentose from forming). Therefore, in the same amount of time, the chances of interaction between furfural produced and the pentose monomers derived from hydrolysis are reduced significantly, which are translated into a higher furfural yield.

The results indicate that the batch reactive distillation process works well with both xylose solutions and biomass samples, producing high yields consistently. The question now remains of how to integrate into a biorefinery to allow the hexose materials to be preserved for other value streams. Therefore, extraction of the hemicelluloses prior to performing the dehydration reaction is implicit on a comparison of the value of the solid cellulose-rich stream available for further conversion versus the costs of performing the extraction.

### **5.3.3. BRD dehydration of biomass hydrolysates**

Conditions obtained from the model compound optimization were used to dehydrate the biomass hydrolysates obtained following the hydrolysis. Triplicate runs were performed for each biomass feedstock by dehydrating a stock solution prepared by diluting the hydrolysate liquor with the wash liquor.

Average yields based on triplicate characterization for all four biomass feedstock are shown in figure 5.7. Amongst the feedstock, the highest average yields were obtained for

miscanthus (~94.4%) and switchgrass (~93.5%), followed by hybrid poplar (~87.7%) and corn stover (~85.1%). The standard errors were combined using the method suggested by Baker and Nissim<sup>142</sup>. Table 5.1 summarizes the results obtained by the BRD dehydration of biomass hydrolysates, showing the values of furfural yield and selectivity from three separate characterization analyses and triplicate runs. Results indicate that the furfural yield from hybrid poplar hydrolysate may be improved by finding ways of increasing the selectivity of the reaction, while yields from corn stover may benefit from ways to improve the conversion (defined as Yield/Selectivity) of the pentosan into furfural, as the majority of the pentosan for corn stover water extract seems to be bound up in its oligomeric form.

The yield was calculated by measuring the number of moles of furfural produced, correcting for the initial amount of furfural present in the hydrolysate (obtained from characterization of hydrolysate), and dividing the net furfural produced with the number of moles of total pentose (though it is inaccurate to refer to TP as a chemical compound/entity, such a reference aids in understanding of the concept) present in the stock solution that was dehydrated. This way, any furfural that was present initially in the hydrolysate (both from the biomass, and that formed during the hydrolysis step) was not counted towards estimating the yield from the dehydration reaction.

Similar research dealing with prior hydrolysis of biomass for pentosan extraction, followed by dehydration of the hydrolysates has shown to improve furfural yields over simple batch dehydration of untreated biomass. Singh et al<sup>143</sup> produced furfural as a byproduct from sugarcane bagasse in a two-step process: hydrolysis of hemicellulose and

dehydration to produce furfural, and the subsequent hydrolysis cellulose in the solid fraction using acetic acid to produce glucose (for fermentation into ethanol). A maximum theoretical furfural yield of 37.2% was reported in this study. The slightly lower furfural yields obtained by Singh et al can be explained by the choice of catalyst used (acetic acid) in order to minimize degradation of cellulose with the goal of producing cellulosic ethanol. This study outlines the advantage of biomass fractionation, separation into cellulose and hemicellulose-rich streams for conversion into ethanol and furfural.

Mansilla et al<sup>46</sup> observed that furfural yields from a two-stage process (sulfuric acid-catalyzed hydrolysis and dehydration) were higher than a one-stage conversion of raw rice hulls. A maximum furfural yield of 10.5 wt% (on dry biomass) was reported using the two-stage process, which translates into a theoretical yield of 58.6% (based on a pentosan content of 28 wt% for rice hulls) compared with 18.66% in the presence of 20 wt% sulfuric acid for the one-stage process. Despite using conventional dehydration methods, the two-stage process was shown to result in considerably higher yields of furfural using rice hulls at similar conditions.

Xing et al<sup>8</sup> utilized solvent extraction to separate furfural produced by dehydrating aqueous hemicellulose solutions obtained by the hydrolysis of wood chips. Experiments were performed using a two-zone (for hydrolysis and dehydration) biphasic reactor containing the aqueous phase (where the dehydration would occur) and an organic phase (into which the furfural produced would be dissolved as it is produced to prevent it from degradation), with sodium chloride added to saturate the hemicellulose. An optimum furfural yield of 90% (at a high selectivity of 90.5%) was reported by the dehydration of

biomass water extract containing 10.7% xylose by mass. The advantage of employing solvent extraction is the significantly higher concentration of pentose that can be converted into furfural. Results with using the BRD process revealed a decrease in furfural yield with increase in xylose concentration (using pure xylose), necessitating that the pentose concentration be kept low. This may be explained as being a virtue of the batch process (from which the BRD is derived) when the furfural produced has a higher probability of reacting with pentose monomers in solution to form the condensation loss product of furfural-pentose when a higher concentration of pentose is reacted<sup>6, 86</sup>.

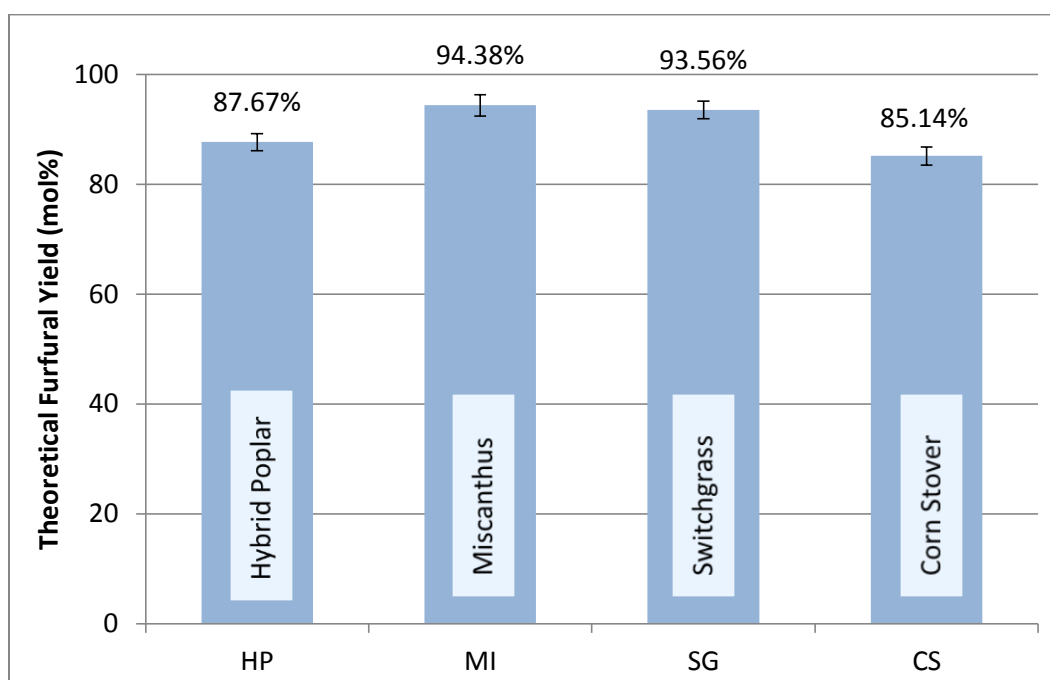


**Fig. 5.7:** Average furfural theoretical yields obtained from all four biomass hydrolysates with standard error. HP is hybrid poplar, MI is Miscanthus, SG is switchgrass and CS is corn stover.

**Table 5.1:** Table showing the theoretical furfural yield (average for triplicate runs, based on three different hydrolysate characterization results) and the selectivity towards the dehydration reaction for all four biomass feedstock

Feedstock	Average Furfural Theoretical Yield (%)	Average Reaction Selectivity (%)
Hybrid Poplar	87.7 ± 1.52	88.3
Miscanthus	94.4 ± 1.93	95.2
Switchgrass	93.6 ± 1.58	94.2
Corn Stover	85.1 ± 1.61	94.6

#### 5.3.4. Heating value of water-extracted solids

Oxygen bomb calorimetry was employed to determine the heating value of the water-extracted, oven-dried biomass solids, and to assess the change in the heating content induced by performing the hot-water extraction. Apart from providing an estimate of the combustibility of the water-extracted biomass residue, it also allowed for confirmation of the solid product obtained from hydrolysis with prior research that led to the establishment of the optimum conditions<sup>131</sup>. Performed in triplicates, the range of the HHV (higher heating value) of all four oven-dried, water-extracted biomass and untreated biomass samples is shown in figure 5.8. The values were corrected for discrepancies in the calibration of the calorimeter using benzoic acid pellets.

**Table 5.2:** Comparison of the higher heating values of all four biomass feedstock

Feedstock	Original biomass HHV (Btu/lb)	Fractionated solids HHV (Btu/lb)	Change in HHV (%)
Hybrid Poplar	7,912.8 ± 82.33	8,538.6 ± 62.98	7.91
Miscanthus	7,904 ± 33	8,648 ± 116.12	9.41
Switchgrass	7,613.5 ± 25.93	8,703.5 ± 134.8	14.32
Corn Stover	7,453.6 ± 102.11	8,739.8 ± 127.02	17.26

Partial extraction of the hemicellulose sugars using hot-water hydrolysis led to an increase in the higher heating value of the extracted solids for all four biomass samples, ranging from ~8 to 17.3% (hybrid poplar and corn stover, respectively). The increase in the heating value of the extracted solids over the untreated biomass can be attributed to an increase in the lignin concentration (due to extraction of the hemicellulose sugars), which has a higher energy content than the sugars (~8,000 versus ~10,000-11,000 Btu/lb between the holocellulose and lignin<sup>144</sup>) 1. Demirbas<sup>144</sup> has found a positive correlation between the lignin content of biomass and its energy content, with the heating value increasing with the amount of lignin present. By increasing the amount of lignin (upon removal of the hemicellulose sugars), the heating value of the extracted solids is driven up (on a mass basis), and the latter is a function of the biomass lignin content (as evidenced from a mathematical relation derived by Demirbas, using a regression fit between the lignin content and the HHV<sup>144</sup>).

Similar experiments performed by Pu et al<sup>145</sup> to assess the heating value of water extracted mixed hardwoods at 170 °C for one hour (amongst a host of other conditions) resulted in an increase in the heating content of the extracted wood over the untreated wood of ~2.7%. The smaller increase in the heating value (compared with ~4% obtained for poplar samples in the current study) observed by Pu et al can be attributed to a value for the HHV of the original wood chips that was derived from an older study. The HHV of the original mixed hardwood chips used in the study by Pu et al was also much lower than that of the poplar chips (and the remaining three biomass feedstock) to begin with, which could have further exacerbated the discrepancy.

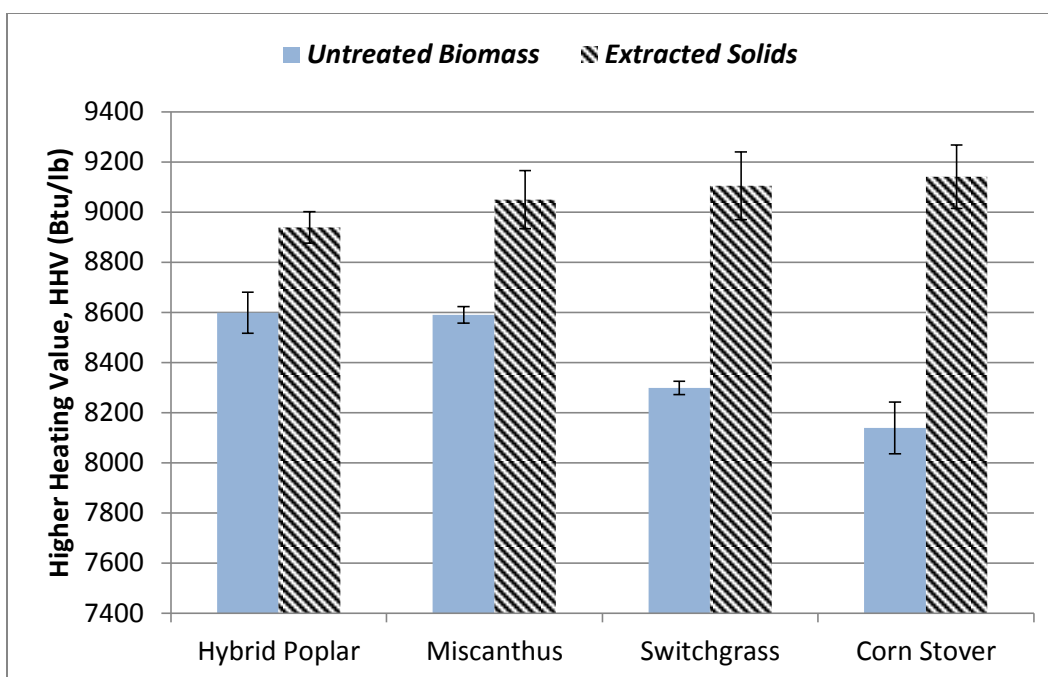


**Fig. 5.8:** Plot showing the higher heating value (HHV, Btu/lb) of untreated, oven-dried and water-extracted, oven-dried biomass solids obtained using oxygen bomb calorimetry, performed in triplicates with standard error.

Though there is an apparent increase in the HHV of the extracted solids, their high moisture content renders the solid fraction unsuitable for direct implementation as a solid fuel. A better application of the extracted solids would be towards the production of cellulosic ethanol by fermentation. The extraction of significant amounts of the pentose sugars into the liquid fraction reduces the potential for the formation of compounds that are inhibitory towards the microorganisms (acetic acid, furfural, etc) that carry out the saccharification and fermentation reactions<sup>14, 15, 146</sup>. Partial removal of the hemicellulose is shown to improve enzyme accessibility towards the cellulose microfibrils by increasing the mean pore size of the lignocellulosic substrate<sup>122, 147</sup>. Moreover, hot water extraction has been shown to improve the enzymatic digestibility of the extracted solids, and present

cellulose chains with a much lower degree of polymerization<sup>148</sup>. The result is a substrate that is much better suited for enzymatic saccharification and fermentation into ethanol.

Another potential application is the utilization of the extracted solids in the production of pulp for making paper. According to the concept of Value Prior to Pulping (VPP), the hemicellulose sugars, which are underutilized/ wasted during conventional pulping practice, are extracted before the biomass is processed into pulp<sup>149</sup>. In a process called 'PureVision', Kadam et al<sup>150</sup> have described a biorefinery model in which pulp made from fractionated (two-stage hydrolysis) corn stover is blended with hardwood pulp for making linerboard without significantly degrading the pulp properties. A brief discussion on the use of the extracted solids for producing short fiber pulp and dissolving pulp is also provided.

A substantial amount of research has shown hot-water hydrolysis to be a good pretreatment procedure for production of cellulosic ethanol, for the production of solid fuel according to the Value Prior to Combustion (VPC) strategy, and the production of various grades of pulp according to the Value Prior to Pulping (VPP) strategy. Based on the modest increases in the heating content obtained in the current study, combined with the fact that a large fraction of the glucose sugars were preserved unscathed in the extracted solids, the VPC strategy might not be the best option at current operating conditions. The extracted solids might be better suited for the production of cellulosic ethanol, especially since a significant amount of the hemicellulose sugars have been removed, reducing the chances of forming inhibitors. Replication of this work with the

solids fraction derived from hot-water extraction is deemed to be beyond the scope of this thesis.

#### **5.4. Conclusions**

Four different biomass feedstock (representing woody, energy and herbaceous crops, and agricultural residues) were fractionated using hot-water hydrolysis and the liquid fraction was dehydrated to produce furfural using the BRD process in high yield (greater than 86%). Furfural yield from the biomass hydrolysates significantly exceeded the yield from pure sugar dehydration and from the dehydration of untreated biomass (hybrid poplar). In addition, the BRD process was shown to exceed yields from the conventional batch process of producing furfural (by dehydrating aqueous solutions of pure xylose in the presence of sodium chloride), using a variety of feedstock, which ascribe towards the consistency of the process.

Figure 5.9 summarizes the various methods of producing furfural investigated in this study: batch production (without and without the presence of salt), BRD dehydration of pure xylose, of untreated poplar and of all four biomass hydrolysates.

Furfural yields greater than 85% were realized by employing the BRD process over biomass hydrolysates. Furfural obtained by the BRD process is very dilute and relatively pure (as indicated by chromatograms) which might need very little purification. An added advantage to doing so is realized in the salvage of a highly porous cellulose stream during fractionation that can be committed to further processing and production of pulp or cellulosic ethanol. The cellulose sugars thus obtained are relatively free of pentose sugars which can cause inhibition of microorganisms during fermentation by the production of

chemicals such as furfural and hydroxymethylfurfural<sup>15, 151</sup>. The cellulose sugars can be recovered only by fractionating them prior to dehydration, and conventional methods of furfural production do not indulge in this. The BRD process only relies on the separation of the vapor stream from the reactor headspace, and thus, does away with any need for toxic and expensive solvents. It is believed that significantly less capital may be needed for the adoption of the BRD configuration as opposed to the employment of solvent recovery units or reactors cast out of alloys in order to withstand corrosion.

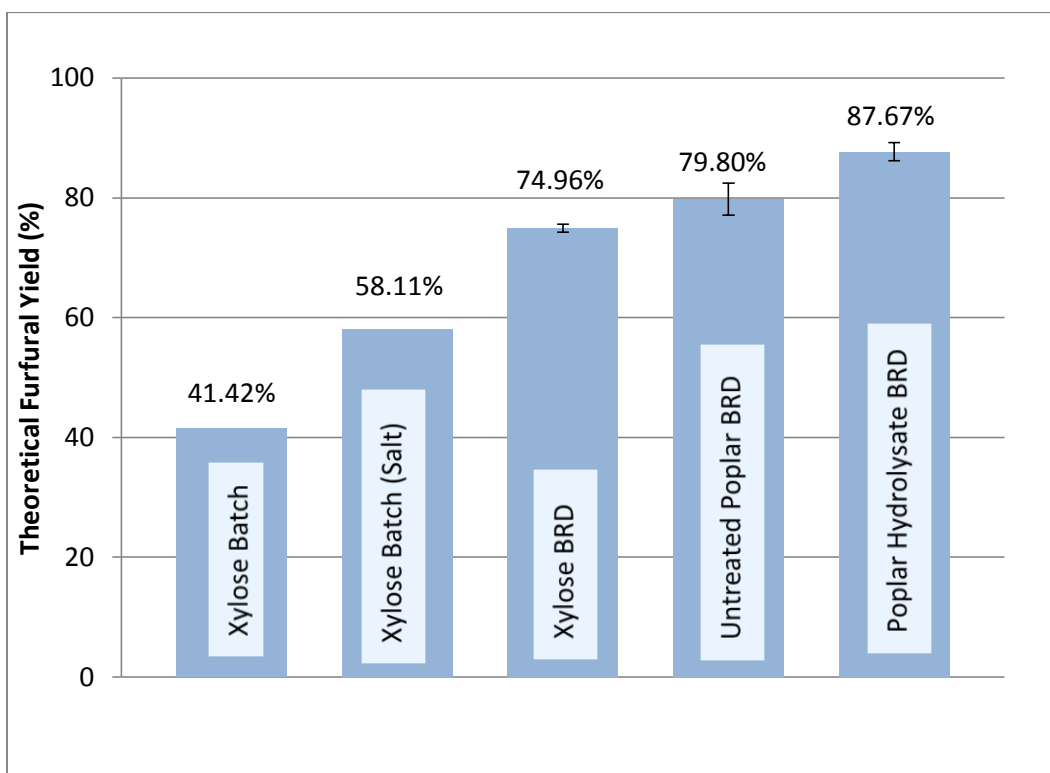


**Fig. 5.9:** Summary of the furfural yields obtained using various methods of acid-catalyzed dehydration: the conventional batch dehydration (in the absence and presence of salt), the batch reactive distillation reaction (BRD) using pure xylose, untreated poplar and poplar hydrolysate (with standard error for the BRD results).

The process is not without its shortcomings, however, as the pentose concentration

needed with the current BRD reactor setup is very dilute, and so is the furfural concentration obtained in the vapor stream. This will give rise to the need for larger reactors and distillation apparatus to process biomass amounts similar to conventional furfural plants. The water requirement is also immense, and a complete economic and energy analysis is needed before lauding the feasibility of the BRD process.

Future work in this area will focus on improving the BRD process in order to produce furfural in high yields while being able to increase the concentration of pentosan converted, and thus, that of the furfural produced as well. Current concentrations of furfural are extremely dilute, and might be uneconomical for the BRD to be considered as a stand-alone process. Research into realizing reactor designs that accomplish true reactive distillation, continuous flow setups, utilization of acid recycle, or the evaluation of heterogeneous catalysts that allow for easier separation of the products from the catalyst. Kinetics of the BRD process will help produce insights into optimizing the reaction and lead to better control over the reaction conditions. The use of a constant temperature throughout the reaction was done owing to shortcomings of the equipment and the heating apparatus, while research has shown that implementation of a two-stage reactor setup with different temperatures for the hydrolysis and dehydration reactions might reduce furfural losses<sup>46, 143, 152, 153</sup>. Economics of the process need to be evaluated, with special emphasis on the value of the cellulose stream recovered during fractionation of the biomass. Conversion of the cellulose fraction into valuable bioproducts will enable the formulation of a furfural-based integrated biorefinery, and would lead us closer to the reality of bio-based economies.

## Chapter 6- Microbial Conversion of Furfural into Furfuryl Alcohol

### 6.1. Introduction

Furfural was produced in high yields (greater than 85%, theoretical) by dehydrating four biomass hot-water hydrolysates using the batch reactive distillation (BRD) process.

Furfural yields obtained in this fashion significantly exceeded those from the conventional batch process used in industry. Despite the high furfural yields obtained, the low concentration of furfural in the product stream might make the concept of a furan-based biorefinery (dependent on the BRD process) economically challenging. Distillation of highly dilute product stream to recover pure furfural would incur significant energy expenditures, and increases the overall process costs. In addition, since furfural forms a low-boiling azeotrope with water<sup>137</sup>, expensive azeotropic distillation must be employed, adding to the production costs.

Further conversion/ upgrading of furfural (primarily catalytic reactions) require a purified reactant and expensive catalysts at harsh operating conditions. As an example, the hydrogenation of furfural into furfuryl alcohol requires pure, distilled furfural and copper chromite catalyst (with limited activity) to react at high pressures (~1,500 psi) in the industrial process. While the conversion of furfural into furfuryl alcohol would seem to be a natural next step (given that ~62% of furfural produced globally is currently converted into furfuryl alcohol<sup>5</sup>, the dilute furfural from the BRD process will prove to be challenging to convert into furfuryl alcohol using the commercial conversion process.

In order to overcome these obstacles and to upgrade to a higher-value product, the next phase of research was focused on the microbial conversion of furfural into furfuryl

alcohol. This conversion has been realized as a way to reduce the inhibitory effects of furfural on microbial growth during fermentation for the production of cellulosic ethanol. Several strains of yeast and bacteria have been investigated which are capable of tolerating furfural concentrations to an extent and effect the conversion into furfuryl alcohol by using the latter as a carbon source. Furfuryl alcohol is less inhibitory to these microorganisms than furfural. Since furfuryl alcohol does not form an azeotrope with water, its purification using distillation will be relatively straightforward, and this approach has been taken to circumvent the impediment of azeotropic distillation required for the purification of furfural. In addition, the low temperature required for yeasts and the selectivity requirement of the reaction may make the BRD product stream more suitable for a microbial conversion. Finally, a microbial conversion would avoid the need for chromite-based catalysts and the environmental concerns associated with their use in conventional catalytic furfuryl alcohol production.

## **6.2. Mechanism**

During anaerobic growth, organisms utilize glucose mostly for the production of energy in the form of the energy carrier molecule, ATP (adenosine triphosphate) and very little (~5%) of this energy goes towards growth. This chemical energy is used for driving the biosynthetic reactions that contribute to the many anabolic pathways involved in the biotechnology of the organism. Glycolysis and oxidative phosphorylation are seen as the two catabolic pathways that lead to the production of ATP in *S cerevisiae*, where glucose is consumed in order to produce ATP and ethanol<sup>154</sup>.

The ability of *S cerevisiae* to conduct this biotransformation is seen as the reason for the increased tolerance displayed by this organism to inhibitors such as acetic acid, furfural and HMF, making it the preferred organism in the ethanol fermentation industry over other candidates such as *E coli*, *Z mobilis*, *P stipitis* and *C shehatae*<sup>155, 156</sup>. In a separate study, Delgenes et al<sup>157</sup> found that *Z mobilis* showed higher tolerance to furfural inhibition towards both growth and ethanol production than *S cerevisiae*, although this difference could be due to the particular strains used in both studies.

Furfural is reduced to furfuryl alcohol as a way of biodegradation, thought to be undertaken by the action of the enzyme alcohol dehydrogenase (ADH), as demonstrated by studies on *P stipitis* in aerobic conditions<sup>158</sup>. It was determined that furfural added to *P stipitis* during aerobic growth inhibited respiration, and was rapidly converted into furfuryl alcohol, which seemed to influence growth. Banerjee et al<sup>159</sup> have observed that the presence of furfural affected the activity of dehydrogenase, thereby causing inhibition of growth and glycolysis in *S cerevisiae*. In batch culture, the specific growth rate of *S cerevisiae* was found to decrease with increasing furfural concentration and inoculum size<sup>160</sup>. It was observed that the inhibitory effect of furfural on growth was much smaller than its effect on ethanol production, because growth may be influenced by several metabolic cycles, while furfural was thought to stimulate some processes which provided energy for growth.

Figure 6.1 shows a simplified scheme of pathways for glycolysis, leading to growth and the production of ethanol, in the presence of furfural, constructed by Palmqvist et al<sup>14</sup> as part of a carbon mass-balance. The coefficients  $\alpha$ ,  $\beta$  and  $\gamma$  are part of this carbon balance

with regard to the quantity of NADH oxidized to  $\text{NAD}^+$  during various pathways. Furfural, by the action of ADH, was reduced to furfuryl alcohol, with the  $\text{H}^+$  derived from the oxidation of NADH into  $\text{NAD}^+$ . An interesting observation from this study was that the presence of furfural retarded the formation of glycerol, leading to the oxidation of an equivalent amount of NADH (corresponding to the amount of glycerol that would have been produced in the absence of furfural). The reduction of furfural into furfuryl alcohol acts as a redox sink for the regeneration of  $\text{NAD}^+$ , reducing the need for glycerol production to serve this purpose<sup>161</sup>. The excess NADH formed as a result of biosynthesis was oxidized by both the reduction of furfural, and glycerol production, but the latter occurred only after all the furfural was depleted<sup>14</sup>.

In addition, the presence of furfural led to the excretion of significant amounts of acetaldehyde (extracellular) which has shown to limit growth, but not metabolic activity. The depletion of intracellular acetaldehyde (due to excretion) is reflected in the reduced amounts of acetate observed (which was reported to be low in the beginning of the reaction due to the inhibition of aldehyde dehydrogenase (ALDH) in the presence of high concentrations of acetaldehyde). The excretion of acetaldehyde is also reflected in the reduced amounts of ethanol produced (by the reduction of acetaldehyde by the action of ADH) in the presence of furfural. The formation of furoic acid as a byproduct has been shown to be the effect of oxidation of furfural by ALDH, even though its activity towards furfural is low<sup>14</sup>.

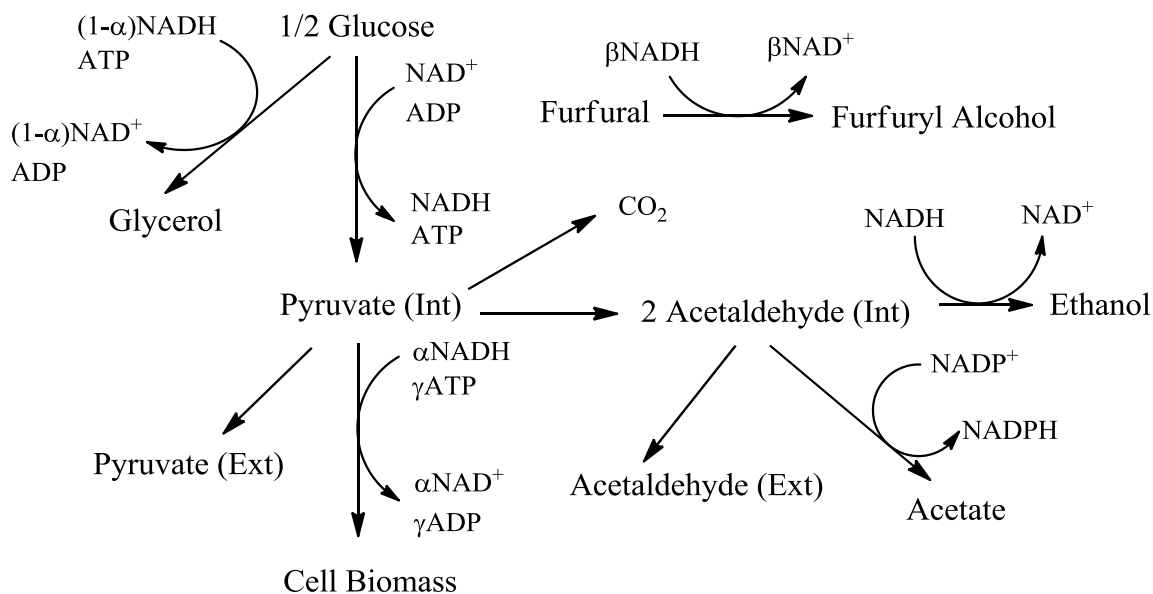


**Fig. 6.1:** Proposed pathway for the transformation of furfural into furfuryl alcohol in conjunction with the fermentation of glucose (Adapted from Palmqvist et al<sup>14</sup>); ‘Int’ and ‘Ext’ refer to intracellular and extracellular, respectively.

This chapter deals with preliminary experiments and observations in the use of microbial methods for conversion of furfural into furfuryl alcohol. Since the goal was to observe whether conversion could be successfully accomplished and sufficiently monitored, it was presumed that these experiments could be performed using commercial bakers’ yeast (Red Star ® Active dry yeast) in semi-sterile conditions. Some previous studies<sup>162-164</sup> have utilized active dry yeast to perform fermentation experiments, and it was assumed that the next phase of studies could be conducted on industrial strains of inhibition-resistant yeast provided current experiments yielded favorable results.

### 6.3. Materials and Methods

#### 6.3.1. Chemicals

All of the experiments were performed with the yeast being maintained on the YPD growth medium (yeast extract: 10 g/l, bacto-peptone: 20 g/l and dextrose/ glucose: 20 g/l)<sup>165</sup>

For the fermentation of the BRD product, the media was added to the BRD product itself (20 g/l glucose and 5 times YP separately) after mixing four different samples obtained from the BRD dehydration of hybrid poplar hydrolysate. For comparison, samples were dosed with pure furfural at the average concentration that was obtained by mixing the BRD samples.

### **6.3.2. Apparatus**

All of the experiments conducted to induce the microbial conversion of furfural were performed in the apparatus and sampling setup described in section 3.3.5 under semi-sterile conditions. The yeast used were not culture-grown as is the convention, and ultraviolet radiation was not available to completely sterilize the media and sampling apparatus. The plastic vials, syringes, flasks and tubing were all autoclaved at 121 °C for 20 min for sterilizing, but chances of contamination were increased when transfers were performed not in an irradiated area, but in an area sprayed with 20% ethanol (by volume) next to an open flame.

### **6.3.3. Analysis**

Optical density (OD) analysis, to give an indication of the turbidity of the solution, was conducted to monitor the growth of the cells with time. This was performed using ultraviolet absorbance at 600 nm in a Shimadzu UVmini 1240 spectrophotometer to estimate the concentration of cells at any particular time, though this was not expressed in

units of dry weight-per-volume. As only the turbidity of the solution is provided by this method, the OD does not discriminate between viable and dead cells. This is explained in more detail in section 3.4.3.

The OD was recorded in singular measurements for the preliminary set of experiments (performed using pure commercial furfural), while it was performed in duplicates for the last batch of experiments that involved conversion of the BRD furfural product.

The concentrations of furfural and furfuryl alcohol were estimated using UV absorbance at 276 and 215 nm as described in section 3.4.3.

Samples were also analyzed for furfural, furfuryl alcohol and furoic acid using HPL chromatography as explained in section 3.4.3. Estimation of furfuryl alcohol using HPL chromatography with the existing columns was found to be not possible, presumably as the furfuryl alcohol condensed into polymers due to the acidic eluent used, creating numerous small, contiguous peaks without a good baseline.

## **6.4. Results and Discussion**

### **6.4.1. Preliminary experiments with pure furfural to find maximum furfural dosage**

Preliminary experiments using pure furfural were conducted by dosing the active dry yeast-containing YPD media with 5, 10, 15, 20, 30, 40 and 50 g/l furfural. The objective of these experiments was to determine the tolerance of the yeast towards furfural by finding a maximum furfural dosage. If the data suggested that a high furfural concentration could be tolerated by the yeast, the BRD product could be concentrated to provide with higher furfural concentrations. The control contained no furfural, and

similar concentrations of dry yeast and YPD media. The concentration of dry yeast used was 10 g/l to ensure that a surplus of yeast were available for the conversion (10 g/l dry yeast =  $2 \times 10^8$  cells/ml, based on personal communication from Dr. Jacobson- Advisor, Lesaffre Yeast Corp).

#### **6.4.1.1. Optical Density results**

The OD results for the control and dosed samples (0: control, 10 and 30 g/l) are shown in figure 6.2. The data suggests that the optical density of the yeast remained constant (with very little variation) throughout the duration of the experiments. Growth was not expected, as during strictly anaerobic conditions, the glucose is converted for use in respiration, producing ethanol as a byproduct, with very little contributing towards growth<sup>166</sup>. Also, the amount of yeast used (10 g/l) might be overwhelming for the amount of glucose added (20 g/l), which is why an initial growth is not observed/ noticeable (despite the presence of some oxygen in the headspace of the flask).

The optical density data proved to be too erratic to generate a linear regression between  $\ln(\text{OD})$  and the time to provide with a specific growth rate ( $\mu$ ).

The nearly constant OD values were helpful for monitoring the fermentation and to ensure that the conditions were anaerobic for the duration of the experiment. The absence of growth is observed as predicted by the fact that (1) during anaerobic phase, very little of the glycolysis products contribute to growth<sup>14</sup> and (2) the concentration of yeast used was very high, which would have placed limits on the substrate (glucose) availability towards growth (latter point based on personal communication with Dr Jacobson- Advisor, Lesaffre Yeast Corp). Any increase in the OD in comparison to that of the

control would indicate that the assimilation of furfural by the yeast contributed towards growth, which was not observed even at much higher doses of furfural (up to 50 g/l). This observation is consistent with that observed by Palmqvist et al<sup>14</sup>, who found that the cell mass yield on glucose actually decreased in the presence of furfural. This is hard to observe in the current study because of the high initial loading of yeast, which hindered growth on the substrate.

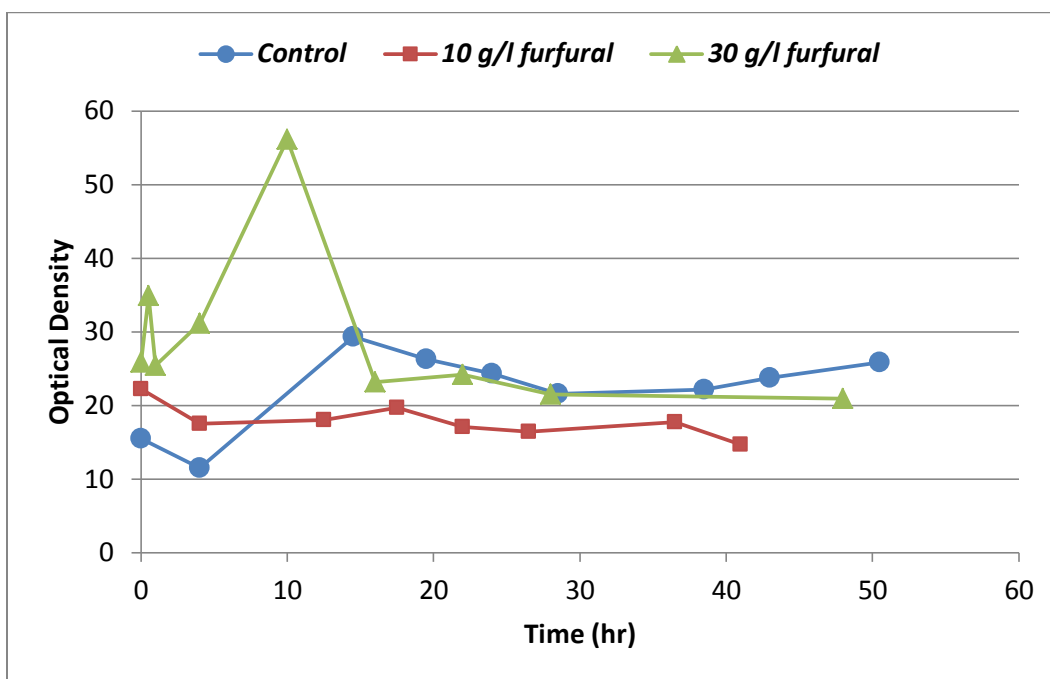


**Fig. 6.2:** Plot showing the change in optical density of yeast with time for the control (no furfural added) and flasks with 10 and 30 g/l furfural added.

#### 6.4.1.2. Transformation of furfural

Results revealed that most of the conversion of furfural into furfuryl alcohol occurred within the first ten hours of the start of the reaction. Also, uptake of furfural by the yeast occurred immediately, as the samples taken at 0.083 hours (assumed to be five minutes

after the yeast were put into the fermentation flasks) showed reduced amounts of furfural in the solution, which led to a disparity between the actual furfural concentration put into the solution and the initial concentration calculated using the standard curve. Results of the conversion are shown in figure 6.3. The results also suggest that the uptake of furfural occurs much faster than its conversion and release into solution by the yeast. Furfuryl alcohol continues to be observed in increasing amounts in the solution after all the furfural has been consumed.

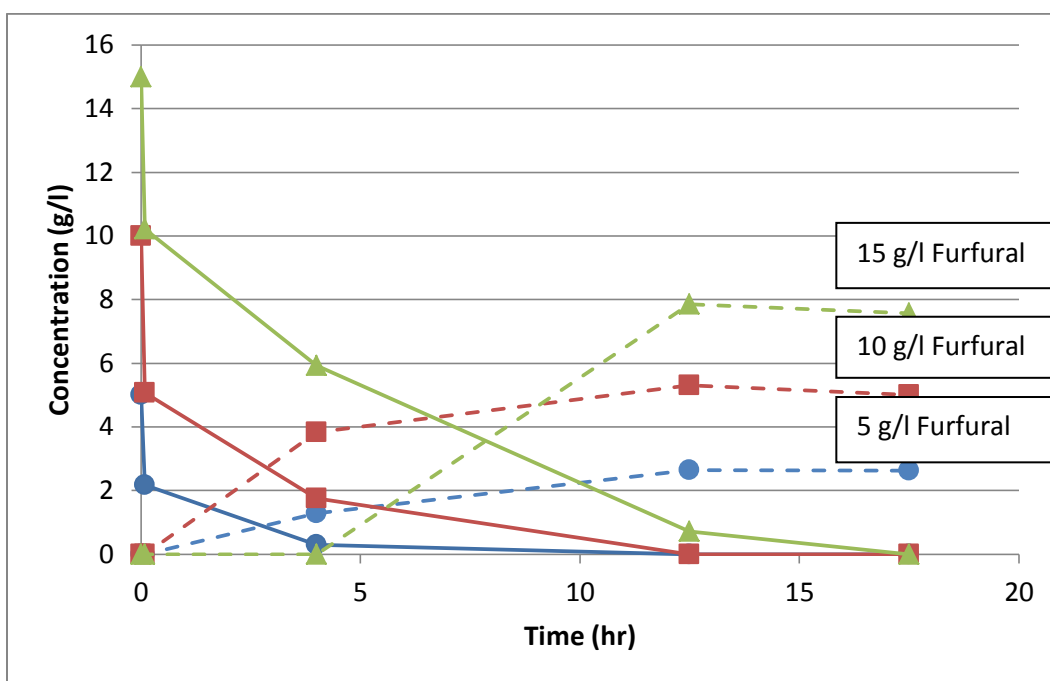


**Fig. 6.3:** Disappearance of furfural (solid lines) and appearance of furfuryl alcohol (dashed lines) shown with time. Circles: 5 g/l furfural, Squares: 10 g/l furfural and Triangles: 15 g/l furfural (initial concentrations).

An additional reason for observance of reduced amounts of furfural in the beginning of the reaction is that furfural may have polymerized to some extent, especially as it was

sterilized in the presence of glucose. Some of the furfural may have been converted into polymers and precipitated out of solution, rendering it hard to detect. With one of the controls used in the study (dosed with 30 g/l furfural in the absence of any yeast), just over 22% of the furfural was lost when the first sample was taken at  $t = 0.083$  hr. This presumed loss of furfural during sterilization is assumed to be dependent on the initial concentration of furfural employed, and has not been quantized or taken into account for estimation of the furfuryl alcohol yield.

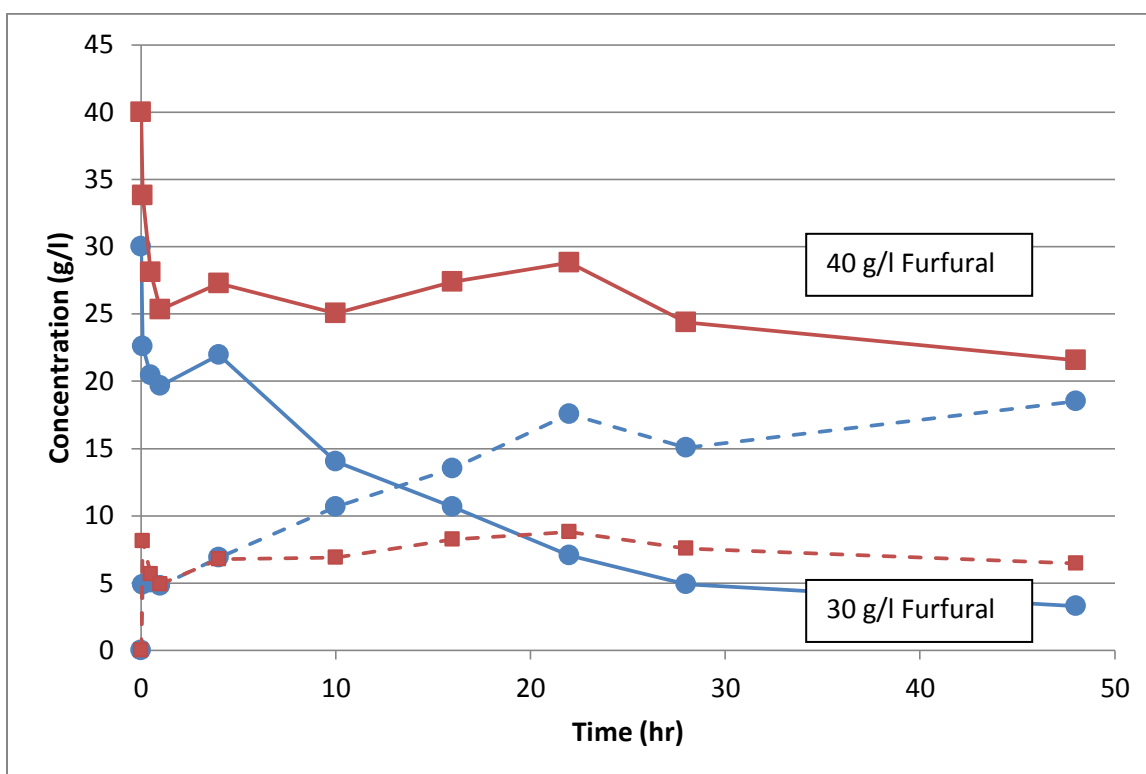


**Fig. 6.4:** Plot showing the conversion of furfural and detection of furfuryl alcohol at much higher furfural dosages of 30 g/l (Circles) and 40 g/l (Squares). Solid lines indicate concentration of furfural, while dashed lines indicate the concentration of furfuryl alcohol produced.

When the furfural dosage was 30 g/l, all of the furfural was not converted and ~10% could still be detected in solution, suggesting that a furfural uptake threshold for the yeast was crossed. This effect is shown in figure 6.4 where the furfural doses were 30 and 40 g/l.

Furfural conversion was not complete in both cases, with the effect observed to be more prominent in the latter. This leads to the inference that 30 g/l can be approximated as a threshold value for the tolerance of furfural by yeast, beyond which, complete uptake and conversion may not be possible (at least at the current organism loading of 10 g/l).

It was unclear as to the fate of the furfural that was not in solution, and whether it was being converted into other products via some other metabolism. The yield of furfuryl alcohol calculated was based on the initial amount of furfural put into the solution using equation 6.1:

$$FA \text{ Yield } (\%) = \left\{ \frac{[FA]_{final}}{[FF]_{init-soln}} \right\} \times 100 \quad (\text{eqn 6.1})$$

*Where*

*FA and FF are furfuryl alcohol, respectively*

*[FA]<sub>final</sub> denotes the final concentration (in M) of furfuryl alcohol obtained in solution*

*[FF]<sub>init-soln</sub> denotes the initial dosage (in M) of furfural*

The equation used underestimates the furfuryl alcohol yield, as the quantity is based on the initial amount of furfural put in. Any losses due to polymerization are not accounted

for, and neither is the fate of the furfural that may have been retained within the cells.

The potential yield for this process, provided better means of sterilization and more tolerant strains (with proper inoculation of a cultured strain) are employed, is presumed to be much higher.

The concentrations of furfural and furfuryl alcohol, and yields of the latter obtained at furfural dosages of 5, 10, 15, 30 and 40 g/l are shown in figure 6.5.

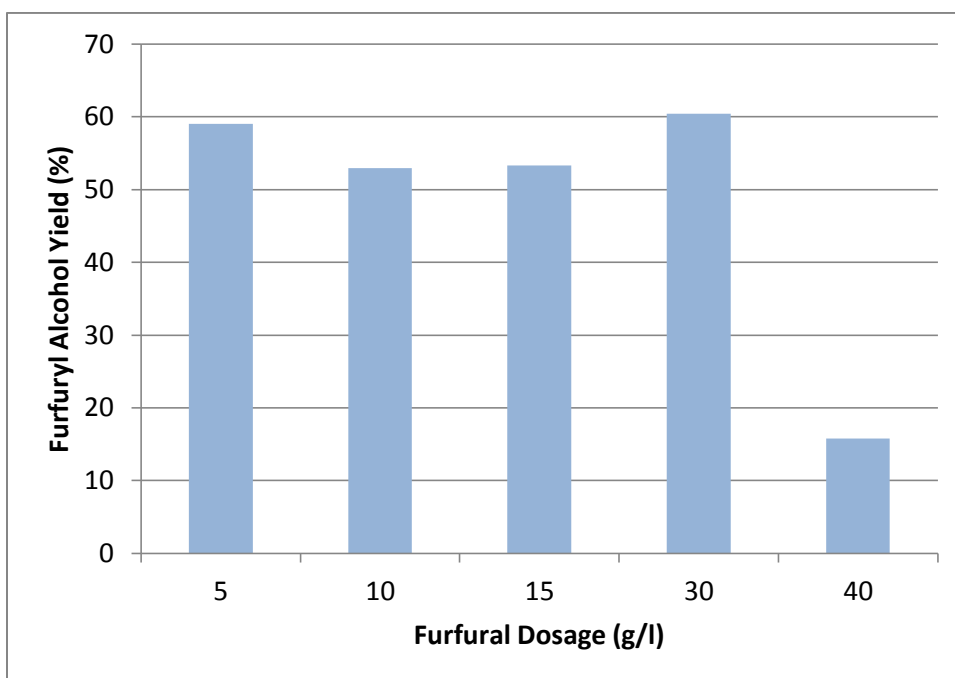


**Fig. 6.5:** Furfuryl alcohol yield obtained at different doses of furfural.

The results indicate that the furfural concentration does not have a significant effect on the yield of furfuryl alcohol obtained as long as the dosage was within the threshold of tolerance. As shown by the data, the furfuryl alcohol yield dropped from 60.5% to 15.8%

when the furfural dosage was increased from 30 to 40 g/l based on the furfural concentration detected initially (at time zero).

In light of the results obtained, it was decided the BRD product would not be concentrated, and it was attempted to be converted into furfuryl alcohol at its original concentration.

#### **6.4.2. Transformation of hybrid poplar BRD product in the presence of active dry yeast**

Active dry yeast was used to convert the aqueous furfural product of the BRD reaction of hybrid poplar hydrolysate. Samples were run in duplicates with the BRD product and pure furfural dosed at the same concentration as was in the former. Two controls (absence of yeast and absence of furfural) were used for comparison of the furfural-dosed samples.

The BRD product solution was prepared by mixing samples from four individual runs to provide an average furfural concentration of  $3.86 \pm 0.04$  g/l. Pure samples, for comparison, were also dosed at the same average concentration, and as before, the dry yeast concentration was 10 g/l. The fermentation was run for ten hours, with samples taken at set time intervals.

##### **6.4.2.1. Optical Density Results**

As with the previous experiments, the optical density of the yeast samples remained nearly constant with time, suggesting strictly anaerobic behavior. Figure 6.6 shows the variation of optical density with time for the control flask (no furfural added), the fermentation flask dosed with pure furfural, and the flask in which the fermentation was

carried out in the BRD product. The slight changes in the OD measurements can be attributed to the sensitivity of the instrument, and as before, no the data does not indicate any appreciable growth.

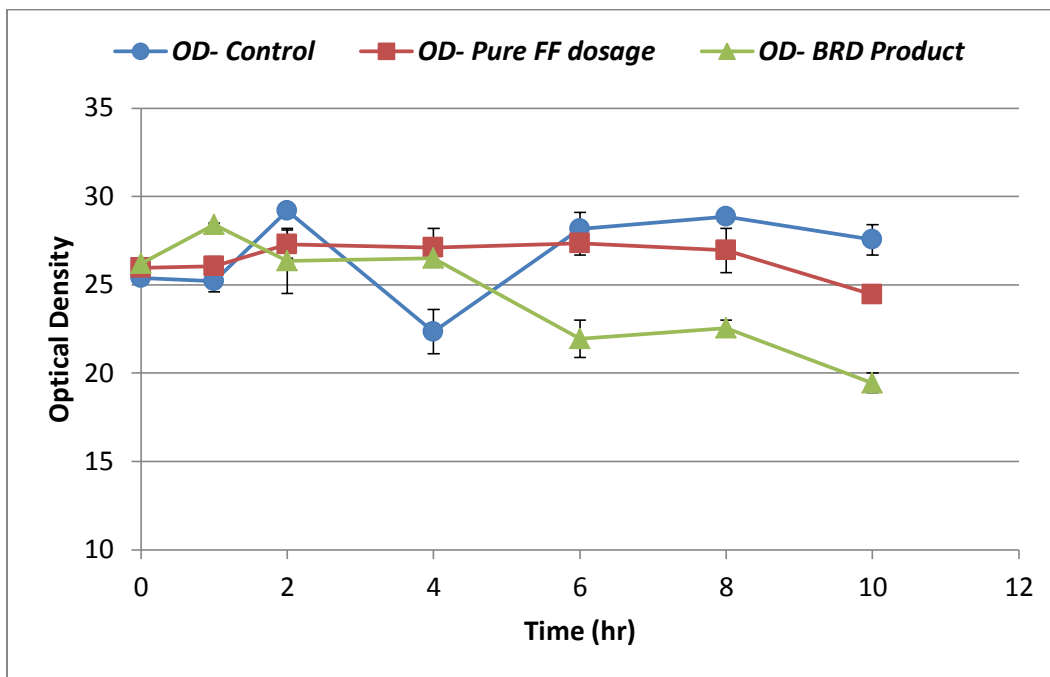


**Fig. 6.6:** Plot showing the optical density measured with time for the control with no furfural, one flask dosed with pure furfural, and flask containing the BRD product. Error bars shown depict the standard errors for duplicate measurements.

#### **6.4.2.2. Estimation of compounds formed**

Due to the lower concentration of furfural employed in this phase of experimentation, it was not possible to detect furfuryl alcohol using UV absorbance as was done previously. The furfuryl alcohol peak, with an absorption maximum at 220 nm, appeared to have been completely eclipsed by the presence of another UV-absorbing peak (probably ethanol). This necessitated use of HPL chromatography to detect compounds formed.

Due to the acidic eluent used (0.1 wt% phosphoric acid) in the analytical column that was maintained at 50 °C, it is presumed pure furfuryl alcohol formed condensed products and formed numerous small, contiguous peaks (figure 6.8). This meant that furfuryl alcohol could not be measured using this method. The polymerization of furfuryl alcohol in acidic conditions is thought to occur due to several condensation reactions and Diels-Alder cycloadditions<sup>167</sup>, and has been well documented<sup>168, 169</sup>.

Two other prominent peaks were observed during this analysis, eluting at 28.7 min and 32.4 min. Previous studies<sup>14</sup> had reported observing small amounts of furoic acid, pyruvate, acetate and acetaldehyde along with furfuryl alcohol, but most of the furfural was converted to the latter compound (~97%). A standard solution containing pure furoic acid revealed that the peak obtained at 32.4 min was indeed furoic acid.

Samples belonging to time zero and ten hours were run using HPL chromatography, and the results indicated that furoic acid and two unknown compounds were produced in small amounts. Most of the furfural uptake by the cells (~83%) in samples containing pure furfural occurred immediately (as indicated by its concentration in solution at  $t = 0.083$  hr). It was again assumed here that the time elapsed between inoculating the flasks with yeast and sampling was ~5 minutes. The percent conversion of furfural (between 0.083 and 10 hr) is shown in figure 6.7 for the controls, pure furfural-dosed samples, and the BRD product samples.

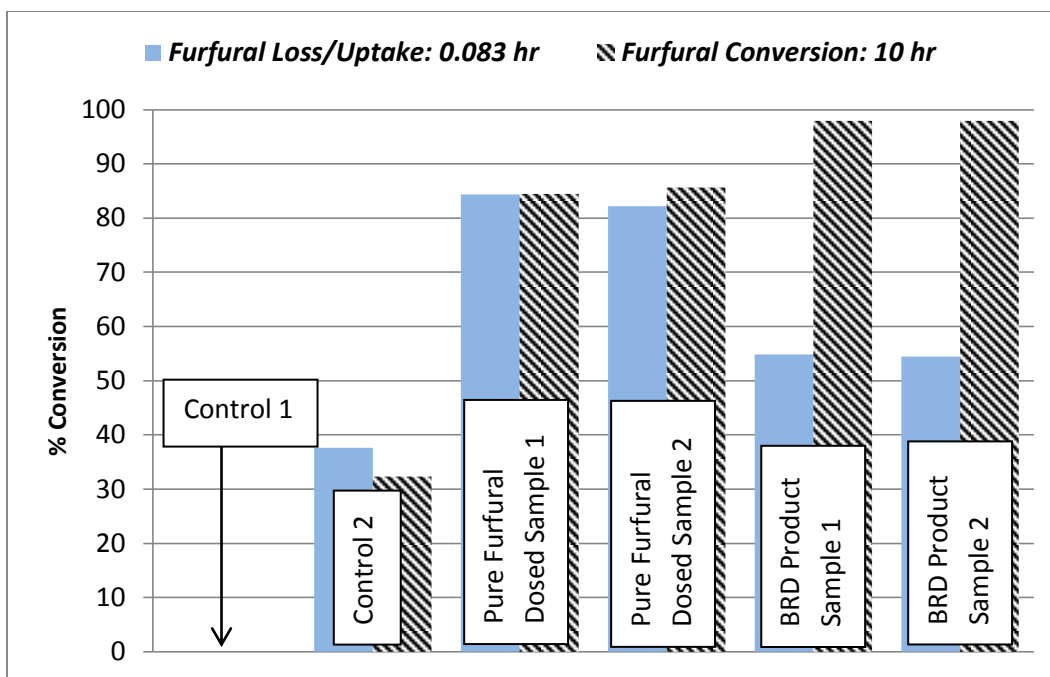


**Fig. 6.7:** Plot showing the conversion of furfural for the samples at 0.083 hr and at 10 hr when the reaction was finished. Samples dosed with pure furfural (Pure FF Dosage 1 and 2) and samples containing the BRD product (BRD Product 1 and 2) were run in duplicates; Control 1 contained no furfural (but was inoculated with 10 g/l yeast) and Control 2 contained no yeast but did contain furfural, with concentration equal to the other samples.

Uptake of furfural in the BRD samples was much slower, and more comprehensive towards the end of the reaction (~98% converted compared to ~85% using pure chemical). As before, no distinction can be made between furfural that was taken up by the yeast and any potential loss due to precipitation during sterilization.

The furfural uptake/conversion was inclusive of any losses that might have occurred during sterilization. This loss is evident from an apparent ‘uptake’ of furfural in Control 2 even though there was no yeast present, and the OD was consistently zero for the duration of the run. Between 32-37% of the initial furfural dosage of 3.86 g/l was lost,

presumably during sterilization, and was observed both before and after the end of the reaction.

Yields of furoic acid from samples dosed with pure furfural were essentially zero, as most of it disappeared by the end of the reaction. Furoic acid was produced in trace quantities from both the BRD samples, and was detected at yields of 3.81% and 3.37%, respectively, based on the initial concentration of furfural in the solution.

In addition to furoic acid, two other compounds were eluted at 28.7 and 56.2 min, whose identities are unknown at this point. For the purpose of this study, they have been referred to as compounds A (28.7 min) and B (56.2 min). In terms of peak areas of the BRD samples, the area occupied by compound A was similar to that of furoic acid at the start of the reaction, and was about twice the area of the furoic acid peaks by the end of the reaction (ten times and greater for the pure furfural samples). An example of these unidentified peaks is shown in figure 6.8, which is the ten-hour chromatogram for one of the BRD samples.

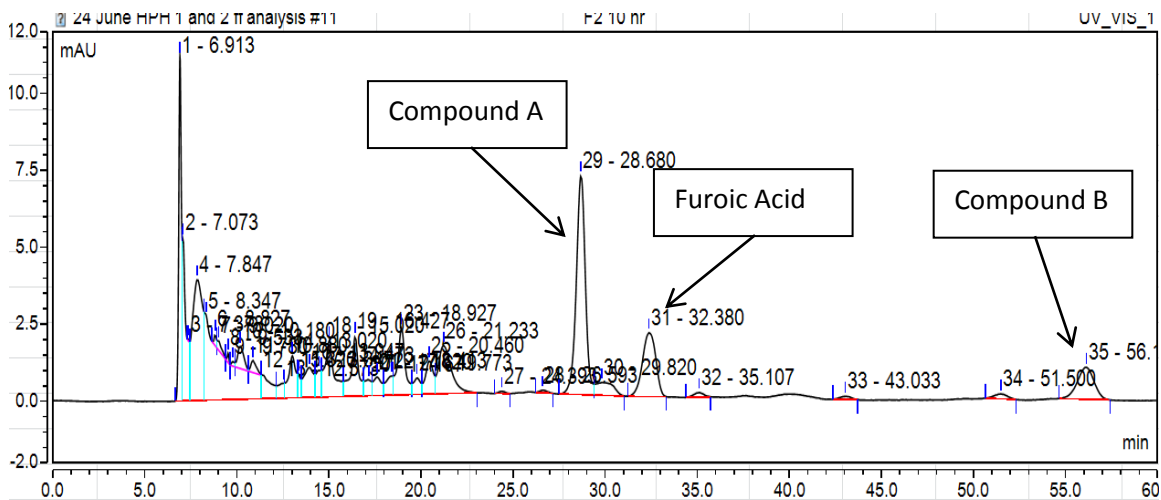


**Fig. 6.8:** Chromatograph showing the elution of peaks for the unknown compounds A and B, and for furoic acid for the 10 hour sample of a BRD product flask. Furfuryl alcohol is thought to elute as a set of contiguous peaks earlier than compound A based on observations with a solution of pure furfuryl alcohol.

Due to the significant furfural losses encountered during sterilization (over 30%), the yields of furfuryl alcohol (for the preliminary experiments) and those of furoic acid are under-predicted using the initial amount of furfural put into the solution.

## 6.5. Conclusions and next steps

Results from this section showed that *S cerevisiae* (commercial dry Bakers' yeast) were able to convert furfural into furfuryl alcohol, small amounts of furoic acid and other unknown chemicals. While it was not possible to estimate the concentration of furfuryl alcohol produced using the BRD product, results obtained from dosing with higher concentrations of furfural suggest that yields ranging from 50-60% of the theoretical were possible using this method. Possibly the most significant conclusion derived from these experiments is that this conversion was managed with yeast that was not designed for the

purpose of tolerating inhibitors such as furfural (even though the composition of the dry yeast is proprietary). In addition, optimization of this process to increase the yield of furfuryl alcohol will allow for the production and extraction of a high value product in a biorefinery setting. Since the yeast are capable of using both carbon sources (furfural and glucose), it is easy to envision dosing a cellulosic ethanol process with the BRD product to effect the conversion into furfuryl alcohol for its simultaneous production along with ethanol. Since furfuryl alcohol does not form an azeotropic mixture in aqueous solution as furfural does, it will be more economical to distill furfuryl alcohol following this transformation.

The most immediate need outlined by this phase of research lies in the understanding of the exact fate of furfural in solution. Observation of reduced furfural amounts in solution point out to both uptake and incomplete excretion by the yeast and possible polymerization with glucose during sterilization. This is thought to be the primary reason why near-quantitative yields of furfuryl alcohol were not realized in this process. Further research will also need to identify and quantize compounds A and B detected in this study. The exact amount of furfuryl alcohol produced will need to be quantified using an appropriate method. Researchers have commonly used HPL chromatography in a neutral eluent, with the detection performed using a Refractive Index Detector (RID). Performing this conversion using a common industrial strain of yeast will help better understand the biochemical pathways involved, as currently, the composition of the dry yeast used in this study is proprietary, and future experiments will need to use individual, cultured strains. An optimization designed to generate high yields of both furfuryl alcohol and

furoic acid will need to be performed so that a potential biorefinery based on this concept will be able to produce and separate both these chemicals and further diversify its product range.

Finally, following the optimization, an economic assessment for the whole process (the hydrolysis of biomass, BRD dehydration of hydrolysates and microbial transformation of furfural) needs to be made so that it can be compared to existing industrial methods of producing these furan-based chemicals. Research is needed on finding more conventional uses for furan-based chemicals, and as discussed in chapter 2, their potential for replacement of petroleum-derived chemicals for production of plastics, resins and adhesives is significant.

## Chapter 7-Conclusions and Future Work

### 7.1. Conclusions

Furfural could be produced in high yield from biomass and biomass hydrolysates using the BRD process for a variety of feedstock. Fractionation prior to dehydration allowed for the recovery of the cellulose fraction of biomass in a form that enabled potential applications towards pulping or cellulosic ethanol production. These solids were freed from some of the potential inhibitors that arise from the hemicellulose sugars during fermentation which impede microbial growth and activity. Furfural was also successfully transformed into its higher-value derivative furfuryl alcohol using commercial dry active Bakers' yeast, replacing energy-intensive hydrogenation reactions that require chromite-based catalysts and the issues of environmental toxicity associated with their use.

The BRD process of producing furfural presents a potentially cost-effective alternative to some of the approaches that have been proposed for improving the yield. The simplicity of its design allows for easy integration into a conventional furfural batch reactor abrogating the need for additional unit operations such as solvent recovery and catalyst separation needed for some of the other methods of producing furfural.

Research performed in this study has shown that the potential for a biorefinery based on the production of furan-based compounds is enormous, and merits further development.

The two processes described and employed as part of this research (BRD process for making furfural and microbial conversion into furfuryl alcohol) lend themselves well towards the concept of an integrated biorefinery. The BRD process is capable of producing furfural in high yields by exploiting the azeotropic nature of furfural-water

mixtures in a manner that is similar to the existing batch process with the exception of continuous furfural removal. Use of the microbial process to transform furfural into furfuryl alcohol offers the prospects of a truly green method that utilizes mild conditions and the potential of sourcing spent yeast from an ethanol production operation (possibly from fermentation of the water-extracted solids). To illustrate the vision of such a conceptual biorefinery, a simplified schematic incorporating hot-water extraction of biomass, the BRD process to produce furfural, and microbial conversion of furfural to produce furfuryl alcohol using yeast from the fermentation of the solids is shown in figure 7.1:

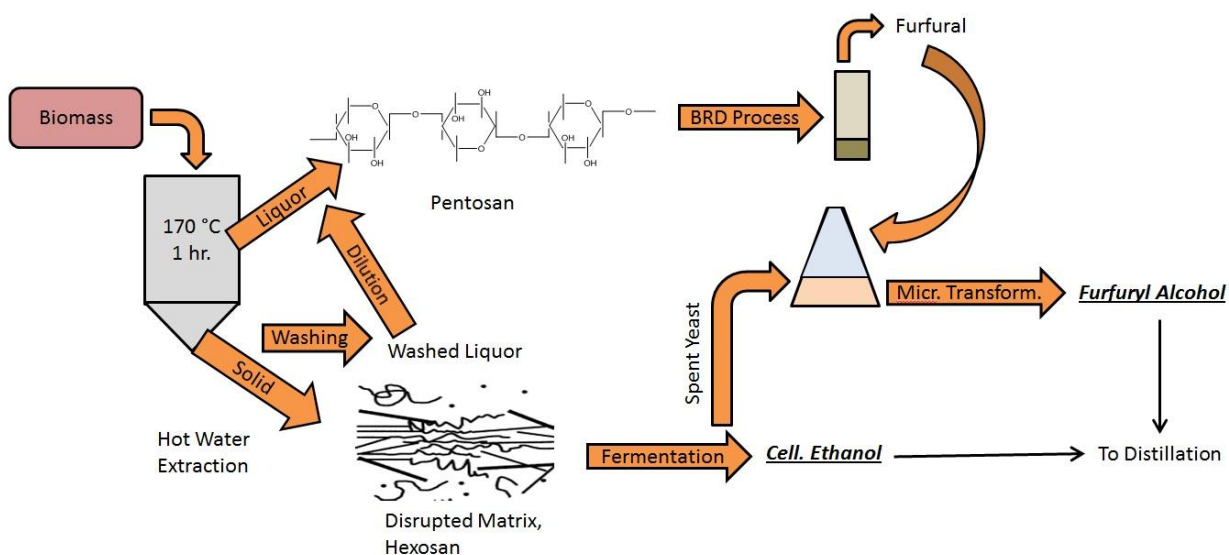


**Fig. 7.1:** Schematic of proposed biorefinery concept, based on hot-water extraction, utilizing the BRD process of making furfural in high yield and its conversion into furfuryl alcohol using recycled yeast derived from the co-production of cellulosic ethanol by fermentation of the solid fraction.

The concept is based on the fermentation of the solid fraction biomass following hot-water extraction (research on this aspect has not been performed in this study, but has been well-documented<sup>170-172</sup>). Negro et al<sup>173</sup> have shown that hydrothermal pretreatment techniques (both liquid hot water and steam explosion) are effective towards enhancing the enzymatic hydrolysis of the extracted solids (using poplar). In this regard, the water-extracted solids present a very suitable substrate for fermentation and production of cellulosic ethanol using the SSF (simultaneous saccharification and fermentation) configuration.

‘Spent yeast’ refers to yeast that has been obtained from recycling of the organisms from fermentation of the extracted solids. This yeast can be used as a low cost ‘catalyst’ at a high loading rate (as was done in the experiments in this study) to convert the BRD furfural product into furfuryl alcohol instead of culturing an expensive, inhibitor-resistant yeast strain. Recycling of yeast has been shown to be beneficial as it allows for adaptation of the organisms towards inhibitors<sup>174</sup>, so the yeast recycled from fermentation of the extracted solids should display more resistance to inhibitors. Researchers<sup>175, 176</sup> have used recycled yeast (*P. stipitis*) to produce ethanol from the fermentation red oak hydrolysates. It has been suggested<sup>177</sup> that the use of recycled yeast offers the benefits of adaptation and can aid fermentation (for galactose fermentation using several organisms in this particular study).

The furfuryl alcohol produced from the microbial conversion can then be distilled (more economical than the azeotropic distillation of furfural) to obtain a purified product, and the model biorefinery is thus capable of producing cellulosic ethanol and furfuryl alcohol

in separate streams, following liquid hot-water extraction. Production of the furan compounds will thus add value to an existing cellulosic ethanol plant and diversify the range of products that can be produced at such a facility.

## **7.2. Future research**

Certain issues exist with the processes explored in this study, and questions have been raised which need to be answered using more research in this area. Some of these questions and challenges are outlined underneath.

The furfural produced using the BRD product is extremely dilute, as obtaining high furfural yields requires that the pentosan content remain very dilute. This raises issues of scalability of the process, and future work needs to devise means of overcoming this by more efficient removal of furfural from the aqueous as it is being produced. It is felt that a continuous reactive distillation scheme where the hydrolysate is being fed into the reactor as the furfural is being removed at optimum flow-rates will overcome the problem faced by the batch BRD process.

The product of microbial conversion of the BRD furfural has not been characterized in this study, and any furfuryl alcohol that was produced was not identified or quantized due to the inability of available analytical instruments to do so. This would be the next immediate step to define the yield of furfuryl alcohol that can be obtained from such a conversion. Researchers<sup>14</sup> have used HPLC analytical techniques equipped with a neutral column and UV/ RI (refractive-index) detectors to quantize furfuryl alcohol. Based on the experiments with dosing pure furfural at much higher concentrations (5 g/l and beyond), it is anticipated that the furfuryl alcohol yield might be at least 52% and higher.

In the microbial conversion process, the true yield of furfuryl alcohol (with dosage of pure furfural) was not known as furfural losses occurred during sterilization. The next set of experiments will have to employ addition of furfural separately to the sterile reaction media to prevent these losses. Another question that has not been answered is the identity of the two additional compounds that were generated in significant amounts during the process along with furoic acid. Identification and quantification of these compounds will be essential to perform a carbon balance on the system and also helpful during optimization of the process to maximize yields of furfuryl alcohol.

Finally, the current study does not provide any energy or economic assessments. These will be critical when drawing comparisons to the existing batch process and several other methods of producing furfural. In addition, these will also be instrumental in evaluating the biorefinery concept proposed in this study, and favorable results will serve to prop up the idea and make it more attractive for development.

## References

1. NREL NREL: Biomass Research- What Is a Biorefinery?  
<http://www.nrel.gov/biomass/biorefinery.html>
2. Werpy, T.; Petersen, G.; Aden, A.; Bozell, J.; Holladay, J.; White, J.; Manheim, A., Top Value Added Chemicals From Biomass Volume I: Results of Screening for Potential Candidates from Sugars and Synthesis Gas. In Energy, U. S. D. o., Ed. Pacific Northwest National Laboratory and National Renewable Energy Laboratory: Oak Ridge, TN and Springfield, VA, 2004.
3. Bozell, J. J.; Petersen, G. R., Technology development for the production of biobased products from biorefinery carbohydrates-the US Department of Energy's "Top 10" revisited. *Green Chemistry* **2010**, *12*, (4), 539-554.
4. Sain, B.; Chaudhuri, A.; Borgohain, J.; Baruah, B.; Ghose, J., Furfural and Furfural-based Industrial Chemicals. *Journal of Scientific and Industrial Research* **1982**, 41.
5. Mamman, A. S.; Lee, J.-M.; Kim, Y.-C.; Hwang, I. T.; Park, N.-J.; Hwang, Y. K.; Chang, J.-S.; Hwang, J.-S., Furfural: Hemicellulose/xylose-derived biochemical. *Biofuels, Bioproducts and Biorefining* **2008**, *2*, (5), 438-454.
6. Zeitsch, K. J., *The Chemistry and Technology of Furfural and its Many By-Products*. 1 ed.; Elsevier: 2001.
7. W.J., M.; Collin, G.; Hoke, H.; K.J., Z., Furan and Derivatives. In *Ullmann's Encyclopedia of Industrial Chemistry*, 2001.
8. Xing, R.; Qi, W.; Huber, G. W., Production of furfural and carboxylic acids from waste aqueous hemicellulose solutions from the pulp and paper and cellulosic ethanol industries. *Energy & Environmental Science* **2011**, *4*, (6), 2193- 2205.
9. Foster, R. The production of furfural from concentrated solutions of xylose. Iowa State University, Ames, IA, 1932.
10. Lessard, J.; Morin, J.-F.; Wehrung, J.-F.; Magnin, D.; Chornet, E. In *High yield conversion of residual pentoses into furfural via zeolite catalysis and catalytic hydrogenation of furfural to 2-methylfuran*, Van Godewijckstraat 30, Dordrecht, 3311 GZ, Netherlands, 2010; Springer Netherlands: Van Godewijckstraat 30, Dordrecht, 3311 GZ, Netherlands, 2010; pp 1231-1234.
11. Weingarten, R.; Cho, J.; Conner, J., W.C.; Huber, G. W., Kinetics of furfural production by dehydration of xylose in a biphasic reactor with microwave heating. *Green Chemistry* **2010**, *12*, (8), 1423- 1429.
12. Marcotullio, G.; De Jong, W., Furfural formation from D-xylose: The use of different halides in dilute aqueous acidic solutions allows for exceptionally high yields. *Carbohydrate Research* **2011**, *346*, (11), 1291-1293.
13. Dong, H.; Bao, J., Metabolism: Biofuel via biodegradation. *Nat Chem Biol* **2010**, *6*, (5), 316-318.
14. Palmqvist, E.; Almeida, J. S.; Hahn-Hägerdal, B., Influence of furfural on anaerobic glycolytic kinetics of *Saccharomyces cerevisiae* in batch culture. *Biotechnology and Bioengineering* **1999**, *62*, (4), 447-454.
15. Palmqvist, E.; Hahn-Hägerdal, B., Fermentation of lignocellulosic hydrolysates. II: inhibitors and mechanisms of inhibition. *Bioresource Technology* **2000**, *74*, (1), 25-33.
16. Nichols, N. N.; Sharma, L. N.; Mowery, R. A.; Chambliss, C. K.; van Walsum, G. P.; Dien, B. S.; Iten, L. B., Fungal metabolism of fermentation inhibitors present in corn stover dilute acid hydrolysate. *Enzyme and Microbial Technology* **2008**, *42*, (7), 624-630.

17. EIA, International Energy Outlook 2011. In Energy, U. S. D. o., Ed. US Energy Information Administration: Washington DC, 2011.
18. China's GDP growth slows to 8.1 per cent - Xinhua. In 2012.
19. India's economic growth dips to lowest figure in nine years - PTI. In 2012.
20. IEA *Key World Energy Statistics*; International Energy Agency: Paris, France, 2010.
21. King, C. W., Energy intensity ratios as net energy measures of United States energy production and expenditures. *Environmental Research Letters* **2010**, 5, (4), 10.
22. Hamilton, J. D., Oil and the Macroeconomy since World War II. *Journal of Political Economy* **1983**, 91, (2), 228-248.
23. Turner, L., The Politics of the Energy Crisis. *International Affairs (Royal Institute of International Affairs 1944-)* **1974**, 50, (3), 404-415.
24. Kerr, R. A., The Next Oil Crisis Looms Large--and Perhaps Close. *Science* **1998**, 281, (5380), 1128-1131.
25. O'Neill, T., Curse of the Black Gold. *National Geographic* 2007, pp 88-117.
26. Vitousek, P. M., Beyond Global Warming: Ecology and Global Change. *Ecology* **1994**, 75, (7), 1861-1876.
27. Dickinson, R. E.; Cicerone, R. J., Future global warming from atmospheric trace gases. *Nature* **1986**, 319, (6049), 109-115.
28. Root, T. L.; Price, J. T.; Hall, K. R.; Schneider, S. H.; Rosenzweig, C.; Pounds, J. A., Fingerprints of global warming on wild animals and plants. *Nature* **2003**, 421, (6918), 57-60.
29. Thomas, C. D.; Cameron, A.; Green, R. E.; Bakkenes, M.; Beaumont, L. J.; Collingham, Y. C.; Erasmus, B. F. N.; de Siqueira, M. F.; Grainger, A.; Hannah, L.; Hughes, L.; Huntley, B.; van Jaarsveld, A. S.; Midgley, G. F.; Miles, L.; Ortega-Huerta, M. A.; Townsend Peterson, A.; Phillips, O. L.; Williams, S. E., Extinction risk from climate change. *Nature* **2004**, 427, (6970), 145-148.
30. Nicholls, R. J., Coastal megacities and climate change. *GeoJournal* **1995**, 37, (3), 369-379.
31. Nicklen, P., Vanishing Sea Ice. *National Geographic* 2007, pp 32-55.
32. Appenzeller, T., Big Thaw. *National Geographic* 2007, pp 56-71.
33. Holzman, D. C., Methane Found in Well Water Near Fracking Sites. *Environ Health Perspect* **2011**, 119, (7).
34. Drajem, M. Fracking Tied to Unusual Rise in Earthquakes in U.S.  
<http://www.bloomberg.com/news/2012-04-12/earthquake-outbreak-in-central-u-s-tied-to-drilling-wastewater.html>
35. Kerr, R. A., Learning How to NOT Make Your Own Earthquakes. *Science* **2012**, 335, (6075), 1436-1437.
36. Howarth, R.; Santoro, R.; Ingraffea, A., Methane and the greenhouse-gas footprint of natural gas from shale formations. *Climatic Change* **2011**, 106, (4), 679-690.
37. Perlack, R.; Wright, L.; Turhollow, A.; Graham, R.; Stokes, B.; Erbach, D., A bioenergy and bioproducts industry: The technical feasibility of a billion-ton annual supply. In Energy, U. D. o.; Agriculture, U. D. o., Eds. Oak Ridge National Laboratory: Oak Ridge, TN, 2005.
38. NREL Biomass Research-What is a Biorefinery?  
<http://www.nrel.gov/biomass/biorefinery.html> (June 24, 2012),
39. EERE Integrated Biorefineries.  
[http://www1.eere.energy.gov/biomass/integrated\\_biorefineries.html](http://www1.eere.energy.gov/biomass/integrated_biorefineries.html) (June 24, 2012),

40. Rentizelas, A. A.; Tolis, A. J.; Tatsiopoulos, I. P., Logistics issues of biomass: The storage problem and the multi-biomass supply chain. *Renewable and Sustainable Energy Reviews* **2009**, *13*, (4), 887-894.
41. EIA What are the products and uses of petroleum?  
<http://205.254.135.7/tools/faqs/faq.cfm?id=41&t=6> (June 24, 2012),
42. EIA How much oil is used to make plastic?  
<http://www.eia.gov/tools/faqs/faq.cfm?id=34&t=6> (June 24 2012),
43. Goldstein, I., Biomass Availability and Utility for Chemicals. In *Organic Chemicals from Biomass*, Goldstein, I., Ed. CRC Press: Boca Raton, FL, 1981; pp 2-7.
44. Montané, D.; Salvadó, J.; Torras, C.; Farriol, X., High-temperature dilute-acid hydrolysis of olive stones for furfural production. *Biomass and Bioenergy* **2002**, *22*, (4), 295-304.
45. Peters, F. N., Introduction - Furan Chemistry. *Industrial & Engineering Chemistry* **1948**, *40*, (2), 200-200.
46. Mansilla, H. D.; Baeza, J.; Urzúa, S.; Maturana, G.; Villaseñor, J.; Durán, N., Acid-catalysed hydrolysis of rice hull: Evaluation of furfural production. *Bioresource Technology* **1998**, *66*, (3), 189-193.
47. Kottke, R. H., Furan Derivatives. In *Kirk-Othmer Encyclopedia of Chemical Technology*, John Wiley & Sons, Inc.: 2000.
48. Kemp, J. L. C.; Hamilton, G. B.; Gross, H. H., Furfural as a Selective Solvent in Petroleum Refining. *Industrial & Engineering Chemistry* **1948**, *40*, (2), 220-227.
49. Rodriguez-Kabana, R.; Kloepper, J.; Weaver, C.; Robertson, D., Control of Plant Parasitic Nematodes with Furfural-A Naturally Occurring Fumigant. *Nematropica* **1993**, *23*, (1).
50. Miner, C. 1926.
51. Raeder, J.; Hungerford, C.; Chapman, N. *Seed treatment control of Rhizoctonia in Idaho*; Agricultural Experiment Station of the University of Idaho: Idaho, 1925.
52. Flor, H., Fungicidal Activity of Furfural. *Iowa State College Journal of Science* **1926**.
53. Canullo, G. H.; Rodríguez-kábana, R.; Kloepper, J. W., Changes in soil microflora associated with control of Sclerotium Rolfsii by Furfuraldehyde. *Biocontrol Science and Technology* **1992**, *2*, (2), 159-169.
54. Kokalis-Burelle, N., Effects of furfuralon nematode populations and galling on tomato and pepper. *Nematropica* **2007**, *37*, (2), 307-316.
55. Hurd, C. D.; Goldsby, A. R.; Osborne, E. N., FURAN REACTIONS. II. FURAN FROM FURFURAL. *Journal of the American Chemical Society* **1932**, *54*, (6), 2532-2536.
56. Wilson, C. L., 18. Reactions of furan compounds. Part V. Formation of furan from furfuraldehyde by the action of nickel or cobalt catalysts: importance of added hydrogen. *Journal of the Chemical Society (Resumed)* **1945**, 61-63.
57. Lejemble, P.; Gaset, A.; Kalck, P., From biomass to furan through decarbonylation of furfural under mild conditions. *Biomass* **1984**, *4*, (4), 263-274.
58. Singh, H.; Prasad, M.; Srivastava, R. D., Metal support interactions in the palladium-catalysed decomposition of furfural to furan. *Journal of Chemical Technology and Biotechnology* **1980**, *30*, (1), 293-296.
59. Kanetaka, J.; Asano, T.; Masamune, S., New Process for Production of Tetrahydrofuran. *Industrial & Engineering Chemistry* **1970**, *62*, (4), 24-32.
60. Gilbert, W. W.; Hoke, B. W. Process of hydrogenating maleic anhydride with a nickel or cobalt molybdate catalyst. 2772293, 1956.

61. Chamoulaud, G.; Floner, D.; Moinet, C.; Lamy, C.; Belgsir, E. M., Biomass conversion II: simultaneous electrosyntheses of furoic acid and furfuryl alcohol on modified graphite felt electrodes. *Electrochimica Acta* **2001**, 46, (18), 2757-2760.
62. Wojcik, B. H., Catalytic Hydrogenation of Furan Compounds. *Industrial & Engineering Chemistry* **1948**, 40, (2), 210-216.
63. Brown, H. D.; Hixon, R. M., Vapor Phase Hydrogenation of FurFural to FurFuryl Alcohol. *Industrial & Engineering Chemistry* **1949**, 41, (7), 1382-1385.
64. Sitthisa, S.; Sooknoi, T.; Ma, Y.; Balbuena, P. B.; Resasco, D. E., Kinetics and mechanism of hydrogenation of furfural on Cu/SiO<sub>2</sub> catalysts. *Journal of Catalysis* **2011**, 277, (1), 1-13.
65. Rao, R.; Dandekar, A.; Baker, R. T. K.; Vannice, M. A., Properties of Copper Chromite Catalysts in Hydrogenation Reactions. *Journal of Catalysis* **1997**, 171, (2), 406-419.
66. De Thomas, W. R.; Hort, E. V. Catalyst comprising Raney Nickel with adsorbed Molybdenum compound. 4,153,578, 1979.
67. Nagaraja, B. M.; Padmasri, A. H.; David Raju, B.; Rama Rao, K. S., Vapor phase selective hydrogenation of furfural to furfuryl alcohol over Cu–MgO coprecipitated catalysts. *Journal of Molecular Catalysis A: Chemical* **2007**, 265, (1–2), 90-97.
68. Himmel, M. E.; Ding, S.-Y.; Johnson, D. K.; Adney, W. S.; Nimlos, M. R.; Brady, J. W.; Foust, T. D., Biomass Recalcitrance: Engineering Plants and Enzymes for Biofuels Production. *Science* **2007**, 315, (5813), 804-807.
69. Villa, G. P.; Bartroli, R.; López, R.; Guerra, M.; Enrique, M.; Peñas, M.; Rodríguez, E.; Redondo, D.; Iglesias, I.; Díaz, M., Microbial transformation of furfural to furfuryl alcohol by *saccharomyces cerevisiae*. *Acta Biotechnologica* **1992**, 12, (6), 509-512.
70. Diaz De Villegas, M. E.; Villa, P.; Guerra, M.; Rodriguez, E.; Redondo, D.; Martinez, A., Conversion of furfural into furfuryl alcohol by *saccharomyces cerevisiae* 354. *Acta Biotechnologica* **1992**, 12, (4), 351-354.
71. Belay, N.; Boopathy, R.; Voskuilen, G., Anaerobic Transformation of Furfural by *Methanococcus deltae* (Delta)LH. *Applied and Environmental Microbiology* **1997**, 63, (5).
72. Gutiérrez, T.; Buszko, M.; Ingram, L.; Preston, J., Reduction of furfural to furfuryl alcohol by ethanologenic strains of bacteria and its effect on ethanol production from xylose. *Applied Biochemistry and Biotechnology* **2002**, 98-100, (1), 327-340.
73. Dunlop, A. P., Furfural Formation and Behavior. *Industrial & Engineering Chemistry* **1948**, 40, (2), 204-209.
74. Brownlee, H. J.; Miner, C. S., Industrial Development of Furfural. *Industrial & Engineering Chemistry* **1948**, 40, (2), 201-204.
75. Garrett, E. R.; Dvorchik, B. H., Kinetics and mechanisms of the acid degradation of the aldopentoses to furfural. *Journal of Pharmaceutical Sciences* **1969**, 58, (7), 813-820.
76. Los, J. M.; Simpson, L. B.; Wiesner, K., The Kinetics of Mutarotation of D-Glucose with Consideration of an Intermediate Free-aldehyde Form. *Journal of the American Chemical Society* **1956**, 78, (8), 1564-1568.
77. Bishop, C. T.; Cooper, F. P., GLYCOSIDATION OF SUGARS: II. METHANOLYSIS OF D-XYLOSE, D-ARABINOSE, D-LYXOSE, AND D-RIBOSE. *Canadian Journal of Chemistry* **1963**, 41, (11), 2743-2758.
78. Hurd, C. D.; Isenhour, L. L., PENTOSE REACTIONS. I. FURFURAL FORMATION. *Journal of the American Chemical Society* **1932**, 54, (1), 317-330.

79. Wolfrom, M. L.; Schuetz, R. D.; Cavalieri, L. F., Chemical Interactions of Amino Compounds and Sugars. III.1 The Conversion of D-Glucose to 5-(Hydroxymethyl)-2-furaldehyde. *Journal of the American Chemical Society* **1948**, 70, (2), 514-517.
80. Bonner, W. A.; Roth, M. R., The Conversion of D-Xylose-1-C<sup>14</sup> into 2-Furaldehyde- $\alpha$ -C<sup>14</sup>. *Journal of the American Chemical Society* **1959**, 81, (20), 5454-5456.
81. Feather, M. S.; Harris, D. W.; Nichols, S. B., Routes of conversion of D-xylose, hexuronic acids, and L-ascorbic acid to 2-furaldehyde. *The Journal of Organic Chemistry* **1972**, 37, (10), 1606-1608.
82. Nimlos, M. R.; Qian, X.; Davis, M.; Himmel, M. E.; Johnson, D. K., Energetics of Xylose Decomposition as Determined Using Quantum Mechanics Modeling. *The Journal of Physical Chemistry A* **2006**, 110, (42), 11824-11838.
83. Shafizadeh, F.; McGinnis, G. D.; Philpot, C. W., Thermal degradation of xylan and related model compounds. *Carbohydrate Research* **1972**, 25, (1), 23-33.
84. Antal Jr, M. J.; Leesomboon, T.; Mok, W. S.; Richards, G. N., Mechanism of formation of 2-furaldehyde from D-xylose. *Carbohydrate Research* **1991**, 217, 71-85.
85. Binder, J. B.; Blank, J. J.; Cefali, A. V.; Raines, R. T., Synthesis of furfural from xylose and xylan. *ChemSusChem* **2010**, 3, (11), 1268-1272.
86. Root, D. F.; Saeman, J. F.; Harris, J. F.; Neill, W. K., Kinetics of the Acid-Catalyzed Conversion of Xylose to Furfural. *Forest Products Journal* **1959**, 9, 158-165.
87. Hughes, E.; Acree, S., Quantitative formation of furfural from xylose. *Journal of Research of the National Bureau of Standards* **1938**, 21, 327-336.
88. Brownlee, H. Process for producing furfural. 2,140,572, 1938.
89. Gravitis, J.; Vedernikov, N.; Zandersons, J.; Kokorevics, A., Furfural and Levoglucosan Production from Deciduous Wood and Agricultural Wastes. In *Chemicals and Materials from Renewable Resources*, American Chemical Society: 2001; Vol. 784, pp 110-122.
90. Zeitsch, K. J. Process for the manufacture of furfural. 2004.
91. Zeitsch, K. J. Gaseous Acid Catalysis. 2007.
92. De Jong, W.; Marcotullio, G., Overview of Biorefineries based on Co-Production of Furfural, Existing Concepts and Novel Developments. *International Journal of Chemical Reactor Engineering* **2010**, 8.
93. Fitzpatrick Stephen, W., The Biofine Technology: A "Bio-Refinery" Concept Based on Thermochemical Conversion of Cellulosic Biomass. In *Feedstocks for the Future*, American Chemical Society: 2006; Vol. 921, pp 271-287.
94. Hayes, D. J.; Fitzpatrick, S.; Hayes, M. H. B.; Ross, J. R. H., The Biofine Process – Production of Levulinic Acid, Furfural, and Formic Acid from Lignocellulosic Feedstocks. In *Biorefineries-Industrial Processes and Products*, Wiley-VCH Verlag GmbH: 2005; pp 139-164.
95. Foyle, T.; Jennings, L.; Mulcahy, P., Compositional analysis of lignocellulosic materials: Evaluation of methods used for sugar analysis of waste paper and straw. *Bioresource Technology* **2007**, 98, (16), 3026-3036.
96. Sjostrom, E., *Wood Chemistry Fundamentals and Applications*. 1 ed.; Academic Press: 1981.
97. Rubin, E. M., Genomics of cellulosic biofuels. *Nature* **2008**, 454, (7206), 841-845.
98. Keshwani, D. R., Biomass Chemistry. In *Biomass to Renewable Energy Processes*, Cheng, J. J., Ed. CRC Press: Boca Raton, FL, 2010.

99. Klemm, D.; Philipp, B.; Heinze, T.; Heinze, U.; Wagenknecht, W., General Considerations on Structure and Reactivity of Cellulose: Section 2.1–2.1.4. In *Comprehensive Cellulose Chemistry*, Wiley-VCH Verlag GmbH & Co. KGaA: 1998; pp 9-29.
100. Okamura, K., Structure of cellulose. In *Wood and Cellulosic Chemistry*, Hon, D., Ed. Marcel Dekker Inc: 1991; pp 89-112.
101. Hon, D. N. S., Cellulose: a random walk along its historical path. *Cellulose* **1994**, 1, (1), 1-25.
102. Thygesen, A.; Oddershede, J.; Lilholt, H.; Thomsen, A. B.; Ståhl, K., On the determination of crystallinity and cellulose content in plant fibres. *Cellulose* **2005**, 12, (6), 563-576.
103. Klemm, D.; Heublein, B.; Fink, H.-P.; Bohn, A., Cellulose: Fascinating Biopolymer and Sustainable Raw Material. *Angewandte Chemie International Edition* **2005**, 44, (22), 3358-3393.
104. Fan, L.; Lee, Y.-H.; Beardmore, D., Major chemical and physical features of cellulosic materials as substrates for enzymatic hydrolysis  
Advances in Biochemical Engineering, Volume 14. In Springer Berlin / Heidelberg: 1980; Vol. 14, pp 101-117.
105. Li, Q.; Renneckar, S., Molecularly thin nanoparticles from cellulose: isolation of sub-microfibrillar structures. *Cellulose* **2009**, 16, (6), 1025-1032.
106. Saha, B., Hemicellulose bioconversion. *Journal of Industrial Microbiology & Biotechnology* **2003**, 30, (5), 279-291.
107. Whitney, S. E. C.; Gidley, M. J.; McQueen-Mason, S. J., Probing expansin action using cellulose/hemicellulose composites. *The Plant Journal* **2000**, 22, (4), 327-334.
108. Gírio, F. M.; Fonseca, C.; Carvalheiro, F.; Duarte, L. C.; Marques, S.; Bogel-Lukasik, R., Hemicelluloses for fuel ethanol: A review. *Bioresource Technology* **2010**, 101, (13), 4775-4800.
109. Timell, T. E., Wood Hemicelluloses: Part II. In *Advances in Carbohydrate Chemistry*, Melville, L. W., Ed. Academic Press: 1965; Vol. Volume 20, pp 409-483.
110. Whetten, R.; Sederoff, R., Lignin Biosynthesis. *The Plant Cell* **1995**, 7, 1001-1013.
111. Whetten, R.; Sederoff, R., Lignin Biosynthesis. *Plant Cell* **1995**, 7, (7), 1001-1013.
112. Suzuki, S.; Suzuki, Y.; Yamamoto, N.; Hattori, T.; Sakamoto, M.; Umezawa, T., High-throughput determination of thioglycolic acid lignin from rice. *Plant Biotechnology* **2009**, 26, (3), 337-340.
113. Sakakibara, A., Chemistry of Lignin. In *Wood and Cellulosic Chemistry*, Hon, D.; Shiraishi, N., Eds. Marcel Dekker Inc: New York, 1991; pp 113-175.
114. Yan, J. F.; Pla, F.; Kondo, R.; Dolk, M.; McCarthy, J. L., Lignin. 21. Depolymerization by bond cleavage reactions and degelation. *Macromolecules* **1984**, 17, (10), 2137-2142.
115. Baptista, C.; Robert, D.; Duarte, A. P., Effect of pulping conditions on lignin structure from maritime pine kraft pulps. *Chemical Engineering Journal* **2006**, 121, (2–3), 153-158.
116. Ralph, J. Lignin structure: recent developments.  
[http://www.dfrc.wisc.edu/DFRCWebPDFs/JR\\_Brazil99\\_Paper.pdf](http://www.dfrc.wisc.edu/DFRCWebPDFs/JR_Brazil99_Paper.pdf)
117. Helm, R. Lignin.  
<http://dwb4.unl.edu/Chem/CHEM869E/CHEM869ELinks/www.chem.vt.edu/chem-dept/helm/3434WOOD/notes1/lignin.html>
118. Kai, Y., Chemistry of Extractives. In *Wood and Cellulosic Chemistry*, Hon, D.; Shiraishi, N., Eds. Marcel Dekker Inc: New York, 1991; pp 215-255.
119. Burkhard, K. Terpenes. [http://www.chemie.fu-berlin.de/chemistry/oc/terpene/terpene\\_en.html](http://www.chemie.fu-berlin.de/chemistry/oc/terpene/terpene_en.html)

120. Pérez, J. A.; Ballesteros, I.; Ballesteros, M.; Sáez, F.; Negro, M. J.; Manzanares, P., Optimizing Liquid Hot Water pretreatment conditions to enhance sugar recovery from wheat straw for fuel-ethanol production. *Fuel* **2008**, *87*, (17–18), 3640-3647.
121. Mosier, N.; Wyman, C.; Dale, B.; Elander, R.; Lee, Y. Y.; Holtzapple, M.; Ladisch, M., Features of promising technologies for pretreatment of lignocellulosic biomass. *Bioresource Technology* **2005**, *96*, (6), 673-686.
122. Chandra, R.; Bura, R.; Mabee, W.; Berlin, A.; Pan, X.; Saddler, J., Substrate Pretreatment: The Key to Effective Enzymatic Hydrolysis of Lignocellulosics? Biofuels. In Olsson, L., Ed. Springer Berlin / Heidelberg: 2007; Vol. 108, pp 67-93.
123. Yu, Y.; Lou, X.; Wu, H., Some Recent Advances in Hydrolysis of Biomass in Hot-Compressed Water and Its Comparisons with Other Hydrolysis Methods†. *Energy & Fuels* **2007**, *22*, (1), 46-60.
124. Garrote, G.; Domínguez, H.; Parajó, J. C., Mild autohydrolysis: an environmentally friendly technology for xylooligosaccharide production from wood. *Journal of Chemical Technology & Biotechnology* **1999**, *74*, (11), 1101-1109.
125. Grethlein, H. E.; Converse, A. O., Common aspects of acid prehydrolysis and steam explosion for pretreating wood. *Bioresource Technology* **1991**, *36*, (1), 77-82.
126. Gratzl Josef, S.; Chen, C.-L., Chemistry of Pulping: Lignin Reactions. In *Lignin: Historical, Biological, and Materials Perspectives*, American Chemical Society: 1999; Vol. 742, pp 392-421.
127. Hendriks, A. T. W. M.; Zeeman, G., Pretreatments to enhance the digestibility of lignocellulosic biomass. *Bioresource Technology* **2009**, *100*, (1), 10-18.
128. Mok, W. S. L.; Antal, M. J., Uncatalyzed solvolysis of whole biomass hemicellulose by hot compressed liquid water. *Industrial & Engineering Chemistry Research* **1992**, *31*, (4), 1157-1161.
129. Tunc, M. S.; van Heiningen, A. R. P., Hemicellulose Extraction of Mixed Southern Hardwood with Water at 150 °C: Effect of Time. *Industrial & Engineering Chemistry Research* **2008**, *47*, (18), 7031-7037.
130. Zhu, J. Y.; Pan, X. J., Woody biomass pretreatment for cellulosic ethanol production: Technology and energy consumption evaluation. *Bioresource Technology* **2010**, *101*, (13), 4992-5002.
131. Wipperfurth, P. J. Optimizing the energy potential of lignocellulosic biomass. University of Wisconsin- Madison, Madison, Wisconsin, 2011.
132. ASTM, ASTM E1756-08 Standard Test Method for Determination of Total Solids in Biomass. In ASTM: 2008.
133. TAPPI, Moisture in pulp, paper and paperboard, Test Method T 412 om-11. In TAPPI: 2011.
134. Green, S. R.; Moehle, C. M., Media and Culture of Yeast. In *Current Protocols in Cell Biology*, John Wiley & Sons, Inc.: 2001.
135. Martinez, A.; Rodriguez, M. E.; York, S. W.; Preston, J. F.; Ingram, L. O., Use of UV absorbance to monitor furans in dilute acid hydrolysates of biomass. *Biotechnology Progress* **2000**, *16*, (4), 637-641.
136. Chi, C.; Zhang, Z.; Chang, H.-M.; Jameel, H., Determination of furfural and hydroxymethylfurfural formed from biomass under acidic conditions. *Journal of Wood Chemistry and Technology* **2009**, *29*, (4), 265-276.

137. Curtis, R. G.; Hatt, H. H., Equilibria in Furfural-Water Systems under Increased Pressure and the Influence of Added Salts upon the Mutual Solubilities of Furfural and Water. *Australian Journal of Chemistry* **1948**, 1, (2), 213-235.
138. Gadewar, S. B.; Malone, M. F.; Doherty, M. F., Selectivity Targets for Batch Reactive Distillation†. *Industrial & Engineering Chemistry Research* **2000**, 39, (6), 1565-1575.
139. Venimadhavan, G.; Malone, M. F.; Doherty, M. F., A novel distillate policy for batch reactive distillation with application to the production of butyl acetate. *Industrial and Engineering Chemistry Research* **1999**, 38, (3), 714-722.
140. Guo, Z.; Lee, J. W., Feasible products in batch reactive extractive distillation. *AIChE Journal* **2004**, 50, (7), 1484-1492.
141. Sun, Y.; Cheng, J., Hydrolysis of lignocellulosic materials for ethanol production: a review. *Bioresource Technology* **2002**, 83, (1), 1-11.
142. Baker, R. W. R.; Nissim, J. A., Expressions for Combining Standard Errors of Two Groups and for Sequential Standard Error. *Nature* **1963**, 198, (4884), 1020-1020.
143. Singh, A.; Das, K.; Sharma, D. K., Integrated process for production of xylose, furfural, and glucose from bagasse by two-step acid hydrolysis. *Industrial & Engineering Chemistry Product Research and Development* **1984**, 23, (2), 257-262.
144. Demirbaş, A., Relationships between lignin contents and heating values of biomass. *Energy Conversion and Management* **2001**, 42, (2), 183-188.
145. Pu, Y.; Treasure, T.; Gonzalez, R.; Venditti, R.; Jameel, H., Autohydrolysis pretreatment of mixed hardwoods to extract value prior to combustion. *BioResources* **2011**, 6, (4).
146. Oliva, J.; Sáez, F.; Ballesteros, I.; González, A.; Negro, M.; Manzanares, P.; Ballesteros, M., Effect of lignocellulosic degradation compounds from steam explosion pretreatment on ethanol fermentation by thermotolerant yeast &Kluyveromyces marxianus. *Applied Biochemistry and Biotechnology* **2003**, 105, (1), 141-153.
147. Alvira, P.; Tomás-Pejó, E.; Ballesteros, M.; Negro, M. J., Pretreatment technologies for an efficient bioethanol production process based on enzymatic hydrolysis: A review. *Bioresource Technology* **2010**, 101, (13), 4851-4861.
148. Martínez, J. M.; Reguant, J.; Montero, M. Á.; Montané, D.; Salvadó, J.; Farriol, X., Hydrolytic Pretreatment of Softwood and Almond Shells. Degree of Polymerization and Enzymatic Digestibility of the Cellulose Fraction. *Industrial & Engineering Chemistry Research* **1997**, 36, (3), 688-696.
149. Amidon, T. E.; Liu, S., Water-based woody biorefinery. *Biotechnology Advances* **2009**, 27, (5), 542-550.
150. Kadam, K.; Chin, C.; Brown, L., Flexible biorefinery for producing fermentation sugars, lignin and pulp from corn stover. *Journal of Industrial Microbiology & Biotechnology* **2008**, 35, (5), 331-341.
151. Sanchez, B.; Bautista, J., Effects of furfural and 5-hydroxymethylfurfural on the fermentation of *Saccharomyces cerevisiae* and biomass production from *Candida guilliermondii*. *Enzyme and Microbial Technology* **1988**, 10, (5), 315-318.
152. Brownlee, H. Process for producing furfural. 1938.
153. Riansa-ngawong, W.; Prasertsan, P., Optimization of furfural production from hemicellulose extracted from delignified palm pressed fiber using a two-stage process. *Carbohydrate Research* **2011**, 346, (1), 103-110.

154. Fireoved, R. L.; Mutharasan, R., Effect of Furfural and Ethanol on the Growth and Energetics of Yeast under Microaerobic Conditions. *Annals of the New York Academy of Sciences* **1986**, 469, (1), 433-446.
155. Nilsson, A.; Gorwa-Grauslund, M. F.; Hahn-Hagerdal, B.; Liden, G., Cofactor Dependence in Furan Reduction by *Saccharomyces cerevisiae* in Fermentation of Acid-Hydrolyzed Lignocellulose. *Applied and Environmental Microbiology* **2005**, 71, (12), 7866-7871.
156. Olsson, L.; Hahn-Hägerdal, B., Fermentation of lignocellulosic hydrolysates for ethanol production. *Enzyme and Microbial Technology* **1996**, 18, (5), 312-331.
157. Delgenes, J. P.; Moletta, R.; Navarro, J. M., Effects of lignocellulose degradation products on ethanol fermentations of glucose and xylose by *Saccharomyces cerevisiae*, *Zymomonas mobilis*, *Pichia stipitis*, and *Candida shehatae*. *Enzyme and Microbial Technology* **1996**, 19, (3), 220-225.
158. Weigert, B.; Klein, C.; Rizzi, M.; Lauterbach, C.; Dellweg, H., Xylose fermentation by yeasts. *Biotechnology Letters* **1988**, 10, (12), 895-900.
159. Banerjee, N.; Bhatnagar, R.; Viswanathan, L., Inhibition of glycolysis by furfural in *Saccharomyces cerevisiae*. *Applied Microbiology and Biotechnology* **1981**, 11, (4), 226-228.
160. Boyer, L. J.; Vega, J. L.; Klasson, K. T.; Clausen, E. C.; Gaddy, J. L., The effects of furfural on ethanol production by *saccharomyces cerevisiae* in batch culture. *Biomass and Bioenergy* **1992**, 3, (1), 41-48.
161. Horváth, I. S.; Taherzadeh, M. J.; Niklasson, C.; Lidén, G., Effects of furfural on anaerobic continuous cultivation of *Saccharomyces cerevisiae*. *Biotechnology and Bioengineering* **2001**, 75, (5), 540-549.
162. MacLeod, R.; Prosser, H.; Fikentscher, L.; Lanyi, J.; Mosher, H. S., Asymmetric Reductions. XII. Stereoselective Ketone Reductions by Fermenting Yeast\*. *Biochemistry* **1964**, 3, (6), 838-846.
163. Chen, S. L., Optimization of batch alcoholic fermentation of glucose syrup substrate. *Biotechnology and Bioengineering* **1981**, 23, (8), 1827-1836.
164. Stashenko, H.; Macku, C.; Shibamoto, T., Monitoring volatile chemicals formed from must during yeast fermentation. *Journal of Agricultural and Food Chemistry* **1992**, 40, (11), 2257-2259.
165. Lab, B. Media. <http://fbisson.ucdavis.edu/PDF/media.pdf> (March 2012),
166. Berry, D.; Brown, C., Physiology of yeast growth. In *Yeast Biotechnology*, Berry, D.; Russell, I.; Stewart, G., Eds. Allen & Unwin: London, 1987; pp 159-192.
167. Guigo, N.; Mija, A.; Vincent, L.; Sbirrazzuoli, N., Chemorheological analysis and model-free kinetics of acid catalysed furfuryl alcohol polymerization. *Physical Chemistry Chemical Physics* **2007**, 9, (39), 5359-5366.
168. Conley, R. T.; Metil, I., An investigation of the structure of furfuryl alcohol polycondensates with infrared spectroscopy. *Journal of Applied Polymer Science* **1963**, 7, (1), 37-52.
169. González, R.; Martínez, R.; Ortiz, P., Polymerization of furfuryl alcohol with trifluoroacetic acid: the influence of experimental conditions. *Die Makromolekulare Chemie* **1992**, 193, (1), 1-9.

170. Laser, M.; Schulman, D.; Allen, S. G.; Lichwa, J.; Antal Jr, M. J.; Lynd, L. R., A comparison of liquid hot water and steam pretreatments of sugar cane bagasse for bioconversion to ethanol. *Bioresource Technology* **2002**, 81, (1), 33-44.
171. van Walsum, G.; Allen, S.; Spencer, M.; Laser, M.; Antal, M.; Lynd, L., Conversion of lignocellulosics pretreated with liquid hot water to ethanol. *Applied Biochemistry and Biotechnology* **1996**, 57-58, (1), 157-170.
172. Kim, Y.; Mosier, N. S.; Ladisch, M. R., Enzymatic digestion of liquid hot water pretreated hybrid poplar. *Biotechnology Progress* **2009**, 25, (2), 340-348.
173. Negro, M.; Manzanares, P.; Ballesteros, I.; Oliva, J.; Cabañas, A.; Ballesteros, M., Hydrothermal pretreatment conditions to enhance ethanol production from poplar biomass. *Applied Biochemistry and Biotechnology* **2003**, 105, (1), 87-100.
174. Palmqvist, E.; Hahn-Hägerdal, B., Fermentation of lignocellulosic hydrolysates. I: inhibition and detoxification. *Bioresource Technology* **2000**, 74, (1), 17-24.
175. Tran, A. V.; Chambers, R. P., Red oak wood derived inhibitors in the ethanol fermentation of xylose by *Pichia stipitis*; CBS 5776. *Biotechnology Letters* **1985**, 7, (11), 841-845.
176. Tran, A. V.; Chambers, R. P., Ethanol fermentation of red oak acid prehydrolysate by the yeast *Pichia stipitis* CBS 5776. *Enzyme and Microbial Technology* **1986**, 8, (7), 439-444.
177. Lindén, T.; Hahn-Hägerdal, B., Fermentation of lignocellulose hydrolysates with yeasts and xylose isomerase. *Enzyme and Microbial Technology* **1989**, 11, (9), 583-589.

## Appendix A-Dehydration of xylose using different reactor schemes

### A1. Batch dehydration results using xylose as the model compound

Experiment	Temperature (°C)	Time (min)	Acid Conc (M)	Salt Conc (g/l)	CSF	Furfural Yield (mol%)
1	195	20	0.1	0	3.415994	36.01
2	175	21	0.3	0	3.325174	32.75
3	175	20	0.1	100	2.826721	58.11
4	195	20	0.3	100	3.893258	5.019
5	175	60	0.1	0	3.303842	37.08
6	195	60	0.3	0	4.370379	3.31
7	195	60	0.1	100	3.893115	8.50
8	175	60	0.3	100	3.781106	4.64
9	175	20	0.1	0	2.826721	41.42
10	195	60	0.3	100	4.370379	1.59
11	155	20	0.1	0	2.237447	22.01
12	155	20	0.1	100	2.237447	36.14
13	195	20	0.1	100	3.415994	14.33

### A2. BRD dehydration results using xylose as the model compound

#### A2.1. Initial Experiments

Experiment	Temperature (°C)	Acid conc (g/l)	Xylose Conc (g/l)	Valve Opening (degrees)	Collection Amount (g)	Furfural Yield (mol%)
1	190	10	1	60	200	70.25
2	190	20	1	60	235	69.8
3	200	20	1	60	180	67.99
4	190	10	0.5	45	200	67.07
5	170	10	0.5	45	200	70.96
6	170	20	0.5	45	200	78.29
7	170	20	0.5	33.75	200	66.0
8	150	30	0.5	45	200	70.35

Initial Experimentation to obtain optimum valve opening, xylose concentration and vapor phase extraction amount.

### A2.2. BRD Statistical Model

Experiment	Temperature (°C)	Acid Conc (%wt)	Furfural Yield (mol%)
1	150	1	43.01
2	170	1	71.9
3	150	3	64.76
4	170	3	70.79
5	150	2	60.06
6	170	2	67.63
7	160	1	60.96
8	160	3	70.90
9	160	2	74.31
10	150	0.5	33.01
11	170	0.5	68.39
12	<i>168.5</i>	<i>1.6</i>	<i>74</i>
13	<i>168.5</i>	<i>1.6</i>	<i>74.62</i>
14	<i>168.5</i>	<i>1.6</i>	<i>76.26</i>
<b>Average</b>			<b>74.96 ± 0.67</b>

BRD dehydration results using xylose pooled into MODDE 7.0.0.1 to generate the optimum reaction conditions (in italics), which was also used to predict the reproducibility of the model.

### A2.3. BRD Acid Injection

Experiment	Temperature (°C)	Acid Conc (%wt)	Xylose Conc (%wt)	Furfural Yield (%mol)
1	190	0.5	0.5	66.74
2	190	0.2	0.5	61.55
3	180	0.5	2	65.71
4	190	0.5	2	62.59
5	<i>168.5</i>	<i>1.6</i>	<i>0.5</i>	<i>68.56</i>
6	<i>168.5</i>	<i>1.6</i>	<i>0.5</i>	<i>70.07</i>

BRD dehydration results using xylose and an acid-injection system used to introduce sulfuric acid at high pressure (using N<sub>2</sub> gas) after the temperature ramp-up, to allow for higher reaction temperatures. Since the furfural yield did not exceed that obtained using the original BRD configuration, this method was not pursued.

## Appendix B-Characterization of hot-water hydrolysates

### B1. Hydrolysate sugar and furfural concentrations

Sample	Arabinose (g/l)	Galactose (g/l)	Glucose (g/l)	Xylose (g/l)	Mannose (g/l)	Furfural (g/l)
Pre-Hydrolysis						
HP L	0.214	0.169	0.115	1.444	0.08	0.234
MI L	0.91	0.187	0.648	3.387	0.077	0.411
SG L	0.743	0.295	0.505	2.033	0.113	0.787
CS L	0.472	0.357	0.304	1.929	0.129	0.503
HP WL	0.029	0.023	0.018	0.178	0	0.327
MI WL	0.277	0	0.133	0.630	0.015	0.103
SG WL	0.166	0.007	0.117	0.484	0	0.394
CS WL	0.122	0.043	0.057	0.535	0.014	0.19
Post-Hydrolysis						
HP L	0.285	0.636	1.456	12.521	1.746	1.405
MI L	1.259	0.662	1.966	17.528	0.262	1.125
SG L	1.46	1.097	2.872	16.16	0.459	2.089
CS L	1.146	1.274	3.423	14.27	0.411	1.136
HP WL	0.032	0.064	0.091	0.968	0.126	1.11
MI WL	0.221	0.089	0.206	2.287	0.039	0.414
SG WL	0.273	0.172	0.354	2.606	0.078	1.158
CS WL	0.251	0.286	0.576	2.74	0.096	0.526

Average of the sugar and furfural concentrations observed during triplicate analyses of the liquor and the wash liquor (HP is hybrid poplar, MI is miscanthus, SG is switchgrass and CS is corn stover; L and WL are for liquor and wash liquor, respectively).

### B2. Total Pentose and Total Hexose

Sample	TP (g/l)	TH (g/l)
HP L	13.98 ± 0.03	3.72 ± 0.2
HP WL	1.30 ± 0.22	0.28 ± 0.01
MI L	21.19 ± 0.21	2.98 ± 0.1
MI WL	3.23 ± 0.06	0.3 ± 0.02
SG L	19.13 ± 0.07	4.35 ± 0.07
SG WL	3.69 ± 0.24	0.59 ± 0.01
CS L	17.1 ± 0.26	5.14 ± 0.05
CS WL	3.82 ± 0.12	0.95 ± 0.01

Average of the Total Pentose (TP) and Total Hexose (TH) content (using equations 5.1 and 5.2) obtained in the liquor and wash liquor, with standard error; abbreviations are the same as used before.

## Appendix C-Optical Density of Bakers' yeast during fermentation

### C1. Optical density of control samples- fermentation in YPD lacking furfural

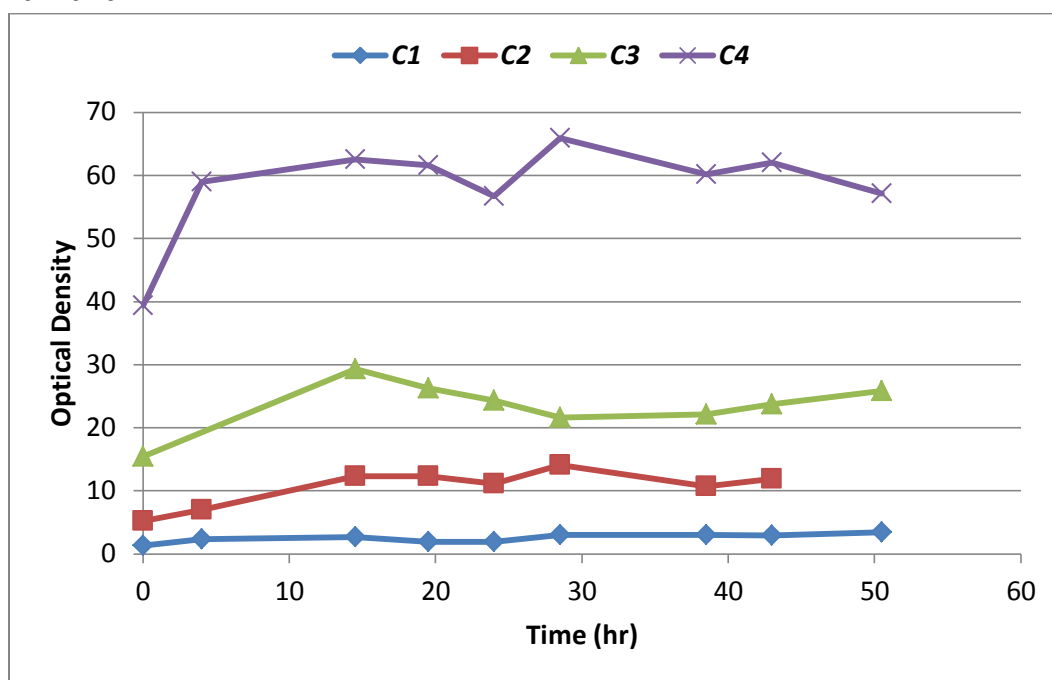


Figure showing four the optical density of Red Star active dry bakers' yeast during fermentation of four different control samples based on the concentration of cells added at time zero; C1=1, C2=5, C3=10 and C4=15 g/l initial yeast concentration.

## C2. Optical density of yeast- fermentation of BRD product

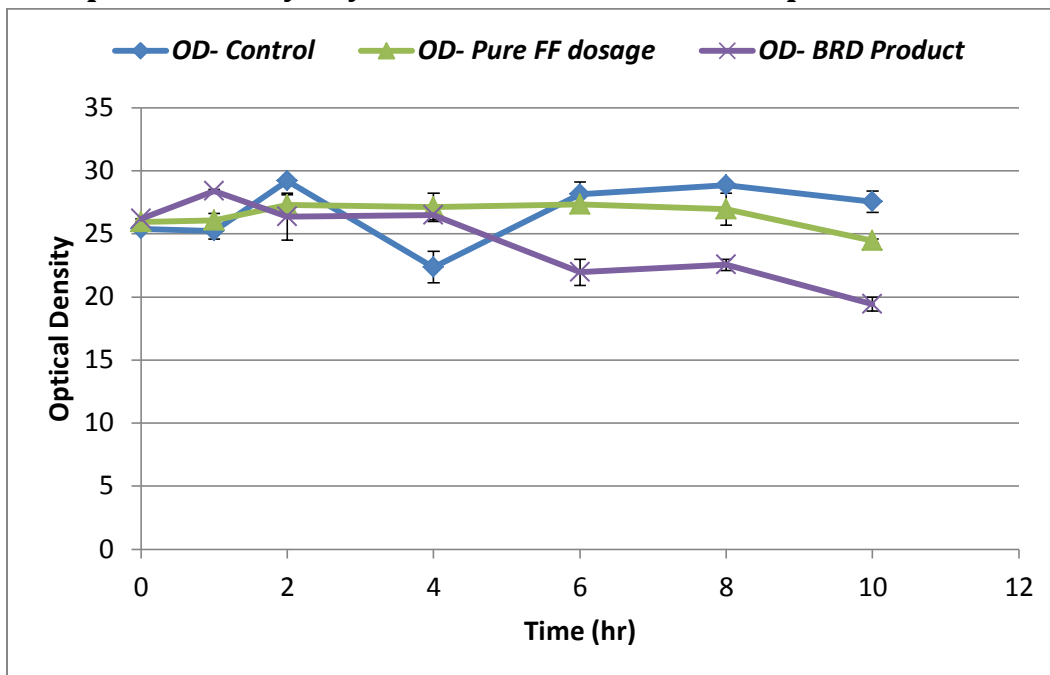


Figure showing the optical density of the control sample (no furfural added), duplicate samples dosed using pure furfural at 3.86 g/l (prior to sterilization) and duplicate samples containing the hybrid poplar hydrolysate BRD product (standard error bars from duplicate analysis).